Development of Aspartic Acid Modified Waste Battery Electrode for Simultaneous Determination of Vitamin C, Paracetamol and Caffeine

by

Md. Hasanuzzaman

A thesis submitted in partial fulfillment of the requirements for the degree of
Master of Science in Chemistry

Khulna University of Engineering & Technology
Khulna 9203, Bangladesh

July 2018

Declaration

This is to certify that the thesis work entitled “Development of Aspartic Acid Modified Waste Battery Electrode for Simultaneous Determination of Vitamin C, Paracetamol and Caffeine” has been carried out by Md. Hasanuzzaman in the Department of Chemistry, Khulna University of Engineering & Technology, Khulna, Bangladesh. The above thesis work has not been submitted anywhere for the award of any degree or diploma.

Signature of Supervisor

Signature of Candidate

Approval

This is to certify that the thesis work submitted by Md. Hasanuzzaman entitled "Development of Aspartic Acid Modified Waste Battery Electrode for Simultaneous Determination of Vitamin C, Paracetamol and Caffeine" has been approved by the board of examiners for the partial fulfillment of the requirements for the Degree of M.Sc in the Department of Chemistry, Khulna University of Engineering & Technology, Khulna, Bangladesh in May, 2018.

BOARD OF EXAMINERS

1. _____
   Prof. Dr. Md. Abdul Motin — Chairman (Supervisor)
   Department of Chemistry
   Khulna University of Engineering & Technology

2. _____
   Head — Member
   Department of Chemistry
   Khulna University of Engineering & Technology

3. _____
   Prof. Dr. Md. Mizanur Rahman Badal — Member
   Department of Chemistry
   Khulna University of Engineering & Technology

4. _____
   Prof. Dr. M. Rostom Ali — Member (External)
   Department of Applied Chemistry&
   Chemical Engineering
   Rajshahi University

Acknowledgements

The author is extremely indebted to the Almightily Allah for the successful completion of the research work and the preparation of this dissertation.

The author expresses his deepest sense of gratitude and indebtedness to his respective and honorable supervisor **Dr. Md. Abdul Motin**, Professor, Department of Chemistry, Khulna University of Engineering & Technology, Khulna for providing me the opportunity of working under his kind supervision. He had helped me at each and every point of the thesis work with his dedication, comments, suggestions and guidance which put me on the right path to fulfill the requirement, without which this situation was impossible to overcome. I learnt a lot of things from him, not only the academic knowledge, but also the way of research. This will be precious wealth in all my future academic life. Our communication is always flexible and efficient. He also friendly supported me a lot in my daily life which I am truly comprehended.

I would like to thank **Prof. Dr. Mohammad Hasan Morshed**, Head, Department of Chemistry, KUET and the staff of the department for their continuous support during my thesis work.

Again the author bestows thanks to his respective teacher **Md. Abdul Hafiz Mia**, Assistant Professor, Department of Chemistry, KUET, Khulna for his lucid cooperation and necessary advice during the period of study. I am indeed grateful to all my dear teachers of the Department of Chemistry, KUET.

The author wishes to offer deepest appreciation to all his friends and well-wishers especially **Md. Bulbul Chowdhuri** for his continuous support and help.

The author feels proud to express his sincere appreciation and indebtedness to his parents, family members who always blessed, inspired and sacrificed a lot in the long process of building his academic career which can never be repaid.

Md. Hasanuzzaman

Abstract

Vitamin C (VC) is regarded as the most important water soluble antioxidant in human plasma. Paracetamol (PA) and Caffeine (CA) are important analgesic and antipyretic agents. The fixed combination of VC, PA and CA is widely used for the treatment of common diseases such as headache, cold, fever, muscle aches, arthritis, toothaches etc. A modified waste battery (WB) electrode sensor has been developed using Aspartic acid (APA) as a trifunctional electrochemical sensor for simultaneous detection of VC, PA and CA. Cyclic voltammetry (CV), differential pulse voltammetry (DPV) and UV-Vis spectroscopy were used as detection techniques.

In this study, battery electrode and pencil graphite (PG) electrode were prepared from waste battery and pencil respectively. Then waste battery (WB), pencil graphite (PG), glassy carbon (GC), gold (Au) and platinum (Pt) electrodes were used as the working electrodes for the determination of VC, PA and CA. These electrodes were modified with APA by applying continuous potential cycle for 15 scans at a range of -0.3 to 1.8 V at 100 mVs^{-1}. A ternary solution of VC, PA and CA was prepared and the CV and DPV were taken at the modified (WB, PG, GC, Au and Pt) electrodes. It is observed that the performances of modified WB and GC electrodes are better than that of the modified PG, Au, Pt electrodes. But the GC electrode is more costly than WB electrode.

The influence of pH has been studied by varying pH from 3 to 9. The detection was mostly favorable at pH 7. The effect of different scan rates has been discussed and the variation of peak current was plotted with the square root of scan rate. The peak current increases with the increase of square root of scan rates. The nearly proportionality of the peak current suggests that the peak current of the reactant at each redox reaction is controlled by diffusion process with some chemical complications.

The effects of bare and modified WB electrode on single, binary and ternary solution of VC, PA and CA have been studied carefully. CVs of the single solution of VC, PA and CA at bare WB electrode show the oxidation peaks at 0.27V, 0.51V and 1.44V respectively. But at modified WB electrode, they exhibit the oxidation peaks at 0.18V, 0.42V and 1.40V. At bare WB electrode, the ternary mixture of VC, PA and CA reveal two oxidation peaks at 0.49V and 1.44V. But the APA modified WB electrode shows three separated and well defined oxidation peaks at 0.18V, 0.42V and 1.40V. The peak intensity of APA modified

electrode was higher than that of the bare WB electrode. Similar behavior has been observed in the DPV technique.

Quantitative analysis of VC, PA and CA has been carried out by DPV using APA modified WB electrode in a single, binary and ternary solution. In every cases, the peak currents of VC, PA and CA increased linearly with the increasing of their concentrations over the range of 1.0 mM to 5.0 mM. The APA modified WB electrode showed good selectivity as well as strong anti-interference activity for the determination of VC, PA and CA in binary and ternary mixture with excellent result. The limit of detection (LoD) has been calculated by signal-to-noise (S/N=3) ratio. In simultaneous detection, the LoDs for VC, PA and CA are 0.20 μmol L^{-1}, 0.16 μmol L^{-1} and 0.33 μmol L^{-1} respectively at APA modified WB electrode. The sensitivities of VC, PA and CA are 54.4 μA/mM/cm^2, 99.9 μA/mM/cm^2 and 151.7 μA/mM/cm^2 respectively at APA modified WB electrode.

APA modified WB electrode has been successfully used for the quantitative determination of VC, PA and CA in some commercial tablets of different pharmaceutical companies in Bangladesh. The results have been valided by UV-Vis spectroscopic method. The amount of VC, PA and CA in some well-established pharmaceutical (Square, ACI, Beximco, Glaxopharma, ACME, Opsonin, Aristopharma, Incepta etc) tablet samples have been found approximately same compared to the labeled value. But in some pharmaceutical companies (IBN Sina, Kemico, Shubatech, Novelta, Eskayef etc), the amount of VC, PA and CA have been found less compared to the labeled value in the tablets.

Contents

LIST OF TABLES

LIST OF FIGURES

CHAPTER I

Introduction

1.1 General

Electrochemistry deals with the chemical response of an electrode/electrolyte system to an electrical stimulation. The electrochemical studies can appraise entire behavior of species including concentration, kinetics and reaction mechanisms [1]. Electroanalytical chemistry is an important branch of electrochemistry that utilizes the relationship between chemical phenomena that involves oxidation-reduction and charge-transfer reactions and the electrical properties that escort these strategies for analytical determinations [2]. Techniques concerned with the interaction between electricity and chemistry that consist of the measurements of electrical quantities such as current, potential, or charge and their relationship to chemical parameters are known as electroanalytical techniques [3]. These techniques have introduced the most promising methods with vast range of applications including industrial, food and water quality control, clinical and biomedical analysis, environmental monitoring along with research development [4-6]. Electrochemistry has many advantages that make it an appealing choice for biomedical and pharmaceutical analysis since it has always provided analytical techniques characterized with instrumental simplicity, moderate cost and portability. Additional applications of electrochemistry comprise the determination of electrode reaction mechanisms and redox properties of biomolecules and drugs which can provide insights into their metabolic fate and pharmaceutical activity [7].

Voltammetric sensors examine the concentration effect of the detecting species on the current-potential characteristics of the reduction or oxidation reaction involved. The mass transfer rate of the detecting species in the reaction on to the electrode surface and the kinetics of the faradic or charge transfer reaction at the electrode surface directly affect the current potential characteristics. The electrode reaction kinetics and the mass transfer processes contribute to the rate of the faradic process in an electrochemical cell. This provides the basis for the operation of the voltammetric sensor. The construction of the

voltammetric sensors is very robust that makes it suitable in different areas of industrial applications. The voltammetric electronic tongue (taste sensor) has very promising features as a general tool for wet-end control, hence, been used successfully for the evaluation of pharmaceutical samples [8]. It has also been used to follow the rinsing process in washing machines, dishing and cleaning processes [9]. Other important industrial applications of voltammetric tongues consist of their use as a monitoring device in drinking water production plants, dairy industry and for the detection of microbial activity [10].

Quantification of common drugs is important for pharmaceutical industry, and studies on doping agents is needed to keep a check on the doping cases in competitive games. Current technologies rely on well-equipped central laboratories for molecular diagnosis which are expensive and time consuming and often cause delay in medical treatments. Hence, still there is an expanding demand of design small, fast, less expensive and simple sensors for molecular analysis. Electrochemical quantification of variety of biomolecules, medicines and doping agents using electrodes modified with different modifier substances lead to worldwide explosion of research interest due to promising advantages that they offer. The modified sensors have been found to show consistently good results with high sensitivity and selectivity. Hence, an endeavor has been made in the present investigation to develop simple, selective and sensitive electroanalytical methods for qualitative and quantitative analysis of biologically important compounds and drugs using modified electrodes [11]. The foremost aim of the present investigation is to assess the utility of voltammetric methods using various electrodes and surface active agents for the determination of pharmaceuticals with low running cost, high speed and sensitivity.

1.2 Electroanalytical Techniques

Electroanalytical techniques encompasses a group of quantitative analytical methods that are based upon the electrical properties of a solution of the analyte when it is made a part of an electrochemical cell. These techniques are capable of producing exceptionally low detection limits and wealth of characterization information describing electrochemical addressable systems [12-13]. Electroanalytical techniques are powerful and versatile analytical techniques that offer high sensitivity, accuracy and precision as well as a large linear dynamic range. Electroanalytical measurements offer a number of important benefits:

(a) specificity
(b) selectivity resulting from the choice of electrode material
(c) high sensitivity and low detection limit
(d) possibility of furnishing results in real time or close to real time
(e) application of miniature sensors where other sensors may not be useful.

The principal criterion for electroanalytical measurements is that the species, which is desired to be measured, should react directly (or indirectly through coupled reaction) at or be adsorbed onto the electrode. Electroanalytical measurements can only be carried out in situations in which the medium between the two electrodes making up the electrical circuit is sufficiently conducting.

1.3 Classification of Electroanalytical Techniques

Electroanalytical techniques can be greatly classified into three types. They are:

1. Potentiometry
2. Coulometry
3. Voltammetry/Amperometry

1.3.1 Potentiometry

Potentiometric methods of analysis are based on measuring the potential of electrochemical cell without drawing appreciable current. In potentiometry the measuring set up always consists of two electrodes: the measuring electrode, also known as the indicator electrode and the reference electrode. When placed in a solution together they produce a certain potential [13]. The equilibrium potential of the indicator electrode is measured against a selected reference electrode under a high impedence voltmeter. By judicious choice of electrode material, the selectivity of one particular ion can be increased, in some cases with very minimal interferences in the measured potential from other ions. Such electrodes are known as ion selective electrodes [14-15].

1.3.2 Coulometry

Coulometry is an Electroanalytical method which involves the measurement of the quantity of electricity (in columbs) needed to convert the analyte quantitatively to a different oxidation state. Like gravimetric methods, coulometry has the advantage that the proportionality constant between the measured quantity (charge in columbs) and the mass of analyte can be computed from known physical constants: thus, calibration or standardization is not usually necessary. Coulometric methods are often as accurate as gravimetric or volumetric procedures and they are usually faster and more convenient than gravimetric methods [13].

1.3.3 Voltammetry/Amperometry

Voltammetry is an electroanalytical technique in which the current-potential behavior at an electrode surface is measured. The potential is varied in some systematic manner to cause oxidation or reduction of the electroactive chemical species at the electrode. The resultant current is proportional to the concentration of the electrochemical species [16].
A three electrode system is used, which includes a working electrode, at which the oxidation or reduction process of interest occurs, a reference electrode, such as the SCE (Standard calomel Reference Electrode) or silver-silver chloride electrode and an auxiliary or counter electrode, which carries the bulk of the current (instead of reference electrode). The three electrodes are connected to the power source, which is specially designed circuit for precise control of the potential applied to the working electrode and often called a potentiostat [17].

1.4 Sensors

A sensor can be defined as something which senses a particular analyte or a substance. It is a device which measures a physical quantity and converts it into a signal which can be read by an observer or instrument. Sensors are designed to detect and respond to an analyte in the gaseous, liquid or solid state [18]. Sensors can be broadly classified into physical sensor and chemical sensor.
Physical sensors are sensitive to such physical responses as temperature, pressure, magnetic field, force etc and do not have a chemical interface.

A chemical sensor is a device which responds to a particular analyte in a selective way through a chemical reaction and can be used for the qualitative and quantitative determination of the analyte [19]. A useful definition for a chemical sensor is a small device that as a result of a chemical interaction or process between the analyte and sensor device, transforms chemical or biochemical information of a quantitative or qualitative type into an analytical useful signal.

1.5 Types of chemical sensors

Chemical sensors are categorized into the following groups according to the transducer type-

1.5.1 Optical sensor

In optical sensors there is a spectroscopic measurement associated with the chemical reaction. Optical sensors are often referred to as 'optodes' and the use of optical fibers is a common feature. Absorbance, reflectance and luminescence measurements are used in the different types of optical sensors.

1.5.2 Mass sensitive sensor

These make use of the piezoelectric effect, include devices such as the surface acoustic wave (SAW) sensor and are particularly useful as gas sensors. They rely on a change in mass on the surface of an oscillating crystal which shifts the frequency of oscillation. The extent of the frequency shift is a measure of the amount of material adsorbed on the surface.

1.5.3 Heat sensitive sensor

The heat of a chemical reaction involving the analyte is monitored with transducers such as thermistor or a Platinum thermometer. They are often called calorimetric sensors.
Compared to optical, mass and thermal sensors, electrochemical sensors are especially attractive because of their remarkable detectability, experimental simplicity and low cost. They have a leading position among the presently available sensors that have reached the commercial stage and which have found a vast range of important applications in the fields of clinical, industrial, environmental and agricultural analysis [20].

1.5.4 Electrochemical sensor

Electrochemical sensors are the devices, which are composed of an active sensing material with a signal transducer. The role of these two important components in sensors is to transmit the signal without any amplification from a selective compound or from a change in a reaction. These devices produce any one of the signals as electrical, thermal or optical output signals which could be converted into digital signals for further processing. One of the ways of classifying sensors is done based on these output signals. Among these, electrochemical sensors have more advantage over the others because; in these, the electrodes can sense the materials which are present within the host without doing any damage to the host system.

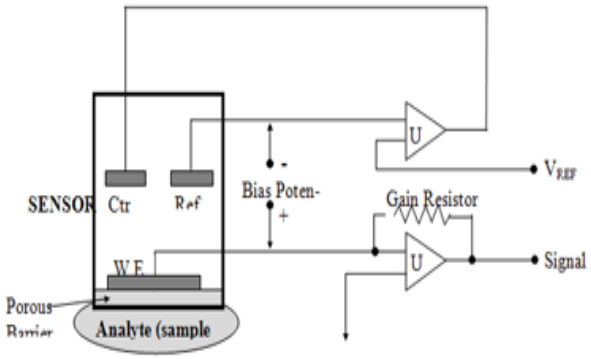

Figure 1.1: Mechanism of electrochemical sensor

1.6 Chemically modified electrodes (CMEs)

An active area of research in electrochemistry is the development of electrodes produced by chemical modification of various conductive substrates. Such electrodes have been tailored to accomplish a broad range of functions. Modifications include applying irreversibly adsorbing substances with desired functionalities, covalent bonding of components to the surface and coating the working electrode with polymer films or films of other substances. One of the most important properties of CMEs is their ability to catalyze the oxidation or reduction of solute species that exhibits high over voltages at unmodified surfaces. Thus CMEs play an important role in reducing the high overvoltage required for the voltammetric determination of analyte without its major interferences [21].

Recently, the field of modified electrodes has become incredibly popular with large number of applications in industry, quality control of drugs and food, determination of pharmaceutical dosage forms and environmental monitoring. Desirable characteristics for modified electrodes in voltammetric experiments comprise the diminution in the overpotential of the analyte under investigation, increased stability of the electrode response coupled with increments in peak heights facilitating lower detection limits and increased specificity compared to the bare electrode. Modified electrodes can benefit analytical applications by various ways which incorporate acceleration of electron transfer reactions, preferential accumulations or selective membrane permeation. Such steps can impart higher selectivity, sensitivity and stability to electrochemical devices and these analytical applications and improvements have been extensively reviewed [22-23]. Many other important applications including controlled release of drugs, electro-synthesis and corrosion protection are also benefited from the rational design of electrode surfaces.

1.7 General methods of modification of electrodes

The concept of chemically modified electrodes (CMEs) is one of the exciting developments in the field of electroanalytical chemistry. Many different strategies have been employed for the modification of the electrode surface. The motivations behind the modifications of the electrode surface are: (i) improved electrocatalysis, (ii) freedom from surface fouling and (iii) prevention of undesirable reactions competing kinetically with the desired electrode process [24]. The increasing demand for it has led to the development of a rapid, simple and non-separation method for the simultaneous determination of compounds where the CMEs have emerged as an efficient and versatile approach, and have attracted considerable attention over the past decades due to its advantages in terms of reduced costs, automatic and fast analysis, high sensitivity and selectivity [25-26]. There are numerous techniques that may be used to modify electrode surfaces. Among various CMEs, polymer-modified electrodes (PMEs) are promising approach to determination. Some modification processes are-

Covalent Bonding: A method that uses chemical agents to create a covalent bond between one or more monomolecular layers of the chemical modifier and the electrode surface. The common agents to use in this method include organosilanes and cyanuric chloride [27].

Drop-Dry Coating (or solvent evaporation): A few drops of the polymer, modifier or catalyst solution are dropped onto the electrode surface and left to stand to allow the solvent to dry out [28].

Dry-Dip Coating: The electrode is immersed in a solution of the polymer, modifier or catalyst for a period sufficient for spontaneous film formation to occur by adsorption. The electrode is then removed from solution and the solvent is allowed to dry out [29].

Composite: The chemical modifier is simply mixed with an electrode matrix material, as in the case of an electron-transfer mediator (electrocatalyst) combined with the carbon particles (plus binder) of a carbon paste electrode. Alternatively, intercalation matrices such as certain Langmuir-Blodgett films, zeolites, clays and molecular sieves can be used to contain the modifier [30].

Spin-Coating (or Spin-Casting): it is also called spin casting; a droplet of a dilute solution of the polymer is applied to the surface of a rotating electrode. Excess solution is spun off the surface and the remaining thin polymer film is allowed to dry. Multiple layers are applied in the same way until the desired thickness is obtained. This procedure typically produces pinhole-free thin films for example; oxide xerogel film electrodes prepared by spin-coating a viscous gel on an indium oxide substrate [31].

Electrodeposition: In this technique the electrode is immersed in a concentrated solution ($\sim 10^{-3}$ $molL^{-1}$) of the polymer, modifier or catalyst followed by repetitive voltammetry scans. The first and second scans are similar, subsequent scans decrease with the peak current. For example, electrochemical deposition of poly (o-toluidine) on activated carbon fiber [32].

Electropolymerization: A solution of monomer is oxidized or reduced to an activated form that polymerizes to form a polymer film directly on the electrode surface. This procedure results in few pinholes since polymerization would be accentuated at exposed (pinhole) sites at the electrode surface. Unless the polymer film itself is redox active, electrode passivation occurs and further film growth is prevented.

In this technique the electrode is immersed in a polymer, modifier or catalyst solution and layers of the electropolimerized material builds on the electrode surface. Generally, the peak current increases with each voltammetry scan such that there is a noticeable difference between the first and final scans indicating the presence of the polymerized material. For example, electropolymerization of aniline on platinum electrode perturbations.

1.8 Simultaneous Detection

Simultaneous detection of analytes is an interesting subject in electroanalytical chemistry. The increasing demand for it has led to the development of a rapid, simple and nonseparation method for the simultaneous detection of analytes where the chemically modified electrodes (CMEs) have emerged as an efficient and versatile approach and have attracted considerable attention over the past decades due to its advantages in terms of reduced costs, automatic and fast analysis, high sensitivity and selectivity [33-35]. Measurement of multiple analytes in a mixture by using a single technique can be termed as simultaneous determination.

In this work, Vitamin-C (VC) (Ascorbic acid), Paracetamol (PA) and Caffeine (CA) were determined simultaneously by Aspartic acid (APA) modified electrodes. These compounds (VC and PA) go through redox reaction on the electrode surface within the same potential range which causes an overlapping oxidation peak at bare electrode. The electro activeness of such compounds depends upon the pH of the medium, nature of the electrode and active moiety present in their structures. In this research work Cyclic voltammetry (CV), Differential pulse voltammetry (DPV) techniques have used to simultaneous detection of VC, PA and CA.

1.9 Prospect of Modified Electrodes in Simultaneous Detection of VC, PA and CA

Electrochemical detection of VC, PA and CA by modified electrode sensor is a preferred method, because they are electrochemically active [36] and they have basic structures that might be electrochemically oxidized at a gold, platinum or carbon electrodes [37-39]. But so many difficulties were existed to simultaneously determine VC, PA and CA. The major difficulty is that the voltammetric peaks corresponding to oxidation/reduction of VC and PA are, in many cases, highly overlapped [40]. At bare Waste battery electrode and other

available electrodes VC, PA and CA are detectable quantitatively if they are investigated individually. But when investigated simultaneously one in presence of other, in spite of giving corresponding peaks they give a broad overlapped peak resulting from all the drugs. This is why modification of electrode is necessary to get corresponding, non-overlapped peaks. Recently, an enormous amount of research has been devoted to the development of new chemically modified electrodes for monitoring VC, PA and CA. Among various chemically modified electrodes, polymer-modified electrodes (PMEs) are promising approach to detect VC, PA and CA. Polymer-modified electrodes prepared by electropolymerization have received extensive interest in the detection of analytes because of their selectivity, sensitivity and homogeneity in electrochemical deposition, strong adherence to electrode surface and chemical stability of the films. Selectivity of PMEs as a sensor can be attained by different mechanisms such as size exclusion, ion exchange, hydrophobicity interaction and electrostatic interaction [41-45].

1.10 Vitamin C (Ascorbic acid)

Vitamin C is a water-soluble vitamin, meaning that our body doesn't store it. We have to get what you need from food, including citrus fruits, broccoli, and tomatoes. Vitamin C is needed for the growth and repair of tissues in all parts of your body. It helps the body make collagen, an important protein used to make skin, cartilage, tendons, ligaments, and blood vessels. Vitamin C is needed for healing wounds, and for repairing and maintaining bones and teeth. It also helps the body to absorb iron. Vitamin C is an antioxidant, along with vitamin E, beta-carotene, and many other plant-based nutrients. Antioxidants block some of the damage caused by free radicals, substances that damage DNA. The buildup of free radicals over time may contribute to the aging process and the development of health conditions such as cancer, heart disease, and arthritis [46-48].

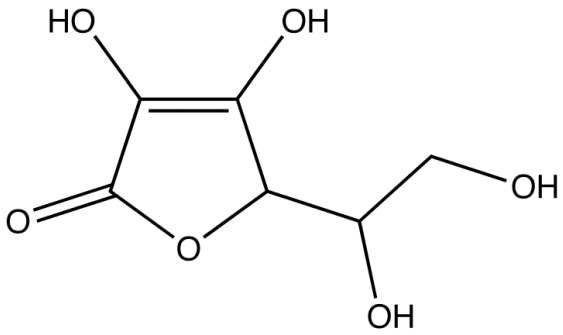

Figure 1.2: Vitamin-C (Ascorbic acid)

1.10.1 Uses of Vitamin-C

Ascorbic acid (Vitamin C) plays an important role in the body. Vitamin C is used to prevent or treat low levels of vitamin C in people who do not get enough of the vitamin from their diets. Most people who eat a normal diet do not need extra ascorbic acid. Low levels of vitamin C can result in a condition called scurvy. Scurvy may cause symptoms such as rash, muscle weakness, joint pain, tiredness, or tooth loss. It is needed to maintain the health of skin, cartilage, teeth, bone, and blood vessels. It is also used to protect body cells from damage. Vitamin C is also important for bones and connective tissues, muscles, and blood vessels. Vitamin C helps the body to absorb iron, which is needed for red blood cell production. It is known as an antioxidant [49].

1.11 Paracetamol

Paracetamol (PA) known as acetaminophen or N-acetyl-p-amino or N-(4-hydroxyphenyl) phenol is a mild analgesic, antipyretic agent and also a non-steroidal anti-inflammatory drug [50]. Paracetamol is part of the class of drugs known as "aniline analgesics"; it is the only such drug still in use today [51]. It is not considered as nonsteroidal anti-inflammatory drugs (NSAIDs) because it does not exhibit significant anti-inflammatory activity (it is a weak Cyclooxygenase (COX) inhibitor) [52-53]. This is despite the evidence that paracetamol and NSAIDs have some similar pharmacological activity [54].

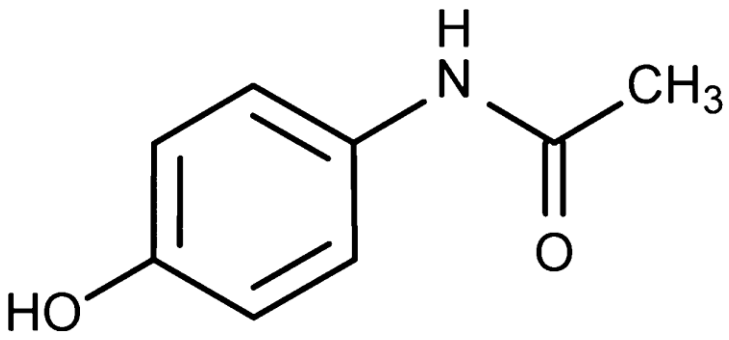

Figure 1.3: Paracetamol

1.11.1 Uses of Paracetamol

Paracetamol is a medicine used to treat pain and fever. It is typically used for mild to moderate pain. There is poor evidence for fever relief in children. It is often sold in combination with other ingredients such as in many cold medications [55-56]. In combination with opioid pain medication, paracetamol is used for more severe pain such as cancer pain and after surgery [57]. It is typically used either by mouth or rectally but is also available intravenously. Effects last between two and four hours [58].

1.12 Caffeine

Caffeine is a bitter, white crystalline purine, a methylxanthine alkaloid, and is chemically related to the adenine and guanine bases of deoxyribonucleic acid (DNA) and ribonucleic acid (RNA). It is found in the seeds, nuts, or leaves of a number of plants native to South America and East Asia and confers on them several survival and reproductive benefits. The most well-known source of caffeine is the coffee bean, a misnomer for the seed of *Coffea* plants. Beverages containing caffeine are ingested to relieve or prevent drowsiness and to improve performance. To make these drinks, caffeine is extracted by steeping the plant product in water, a process called infusion. Caffeine-containing drinks, such as coffee, tea, and cola are very popular [59].

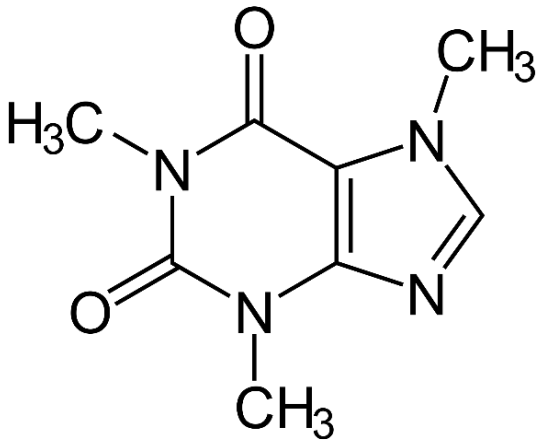

Figure 1.4: Caffeine

1.12.1 Uses of Caffeine

Caffeine is a central nervous system (CNS) stimulant of the methyl xanthine class. It is the world's most widely consumed psychoactive drug. Unlike many other psychoactive substances, it is legal and unregulated in nearly all parts of the world. There are several known mechanisms of action to explain the effects of caffeine. The most prominent is that it reversibly blocks the action of adenosine on its receptor and consequently prevents the onset of drowsiness induced by adenosine. Caffeine also stimulates certain portions of the autonomic nervous system [60].

1.13 Aspartic acid (APA)

Aspartic acid also known as aspartate, is an α-amino acid which is molecular formula is $C_4H_7NO_4$ and chemical name is 2-Aminobutanedioic acid. Similar to all other amino acids it contains an amino group and a carboxylic acid. Its α-amino group is in the protonated $–NH_3^+$ form under physiological conditions, while its α-carboxylic acid group is deprotonated $–COO^–$ under physiological conditions. Aspartic acid has an acidic side chain (CH_2COOH) which reacts with other amino acids, enzymes and proteins in the body [61]. Under physiological conditions (pH 7.4) in proteins the side chain usually occurs as the negatively charged aspartate form, $–COO^–$. The overall molecule is neutral in nature due to the presence of opposite charges. It is a non-essential amino acid in humans, meaning the body can synthesize it as needed. D-Aspartate is one of two D-amino acids commonly found in mammals [62].

Aspartic acids, L-isomer is one of the 22 proteinogenic amino acids, i.e., the building blocks of proteins. Aspartic acid is classified as acidic, with a pK_a of 3.9, however in a peptide this is highly dependent on the local environment (as with all amino acids), and could be as high as 14.

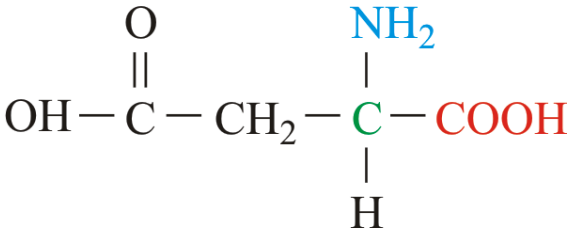

Figure 1.5: Aspartic acid

1.13.1 Uses of Aspartic acid

Aspartic acid, also known as L-aspartate, is thought to help promote a robust metabolism, and is sometimes used to treat fatigue and depression. Aspartic acid plays an important role in the citric acid cycle, or Krebs cycle, during which other amino acids and biochemicals, such as asparagine, arginine, lysine, methionine, threonine, and isoleucine, are synthesized. Aspartic acid moves the coenzyme nicotinamide adenine dinucleotide (NADH) molecules from the main body of the cell to its mitochondria, where it is used to generate adenosine triphosphate (ATP), and the fuel that powers all cellular activity. In short, the more NADH a cell has, the more chemical fuel it produces, and the more energy you have to get through your day. In addition, this amino acid helps transport minerals needed to form healthy RNA and DNA to the cells, and strengthens the immune system by promoting increased production of immunoglobulins and antibodies (immune system proteins). Aspartic acid keeps your mind sharp by increasing concentrations of NADH in the brain, which is thought to boost the production of neurotransmitters and chemicals needed for normal mental functioning. Aspartic acid is a good material as a component in theranostics. When used as a biomaterial in the composite of hydroxyapatite aspartic acid increases the efficiency of bone tissue regeneration. Additionally, it can serve as a material for creating smart hydrogels [63].

1.14 Waste battery electrode (WBE)

The electrochemical reactivity of the working electrode (where the reaction of interest occurs) has significant impact on the function of electrochemical sensors. Currently, the glassy carbon electrode (GCE) is the most commonly employed working electrode material due to the ability of carbon to react with diverse classes of analyte. In the field of the detection of the amount of different pharmaceutical tablets, GCEs have been widely used. However, despite their widespread, GCEs are prone to electrode fouling, are relatively costly (approximately **$**190 to **$**1200 each, depending on the exact specifications and supplier).
Numerous modifications and novel electrode materials have been proposed to overcome the limitations of traditional glassy carbon based sensors including metallization, derivatization and doping. In particular, however, interest has turned to the development of waste battery electrode (WBE), due to their disposability, simplicity and low cost [64-65].

1.15 Electrical double layer

Electroanalytical studies are centered on electrode, which is considered as a probe in the electrolyte. An electrode can only donate or accept electrons from a species that is present in a layer of solution that is immediately adjacent to the electrode. Thus, this layer may have a composition that differs significantly from that of the bulk of the solution. Let us consider the structure of the solution immediately adjacent to that electrode. Immediately after impressing the potential, there will be a momentary surge of current, which rapidly decays to zero if no reactive species is present at the surface of the electrode. This current is a charging current that creates an excess of negative charge at the surface of the two electrodes. As a consequence of ionic mobility, however, the layers of solution immediately adjacent to the electrodes acquire an opposing charge. This effect is illustrated in Figure 1.5. The surface of the metal electrode is shown as having an excess of positive charge as a consequence of an applied positive potential. The charged solution layer consists of two parts: (1) a compact inner layer (d_0 to d_1), in which the potential decreases linearly with distance from the electrode surface and (2) a diffuse layer (d_1 to d_2), in which the decrease is exponential. This assemblage of charge at the electrode surface and in the solution adjacent to the surface is termed as electrical double layer.

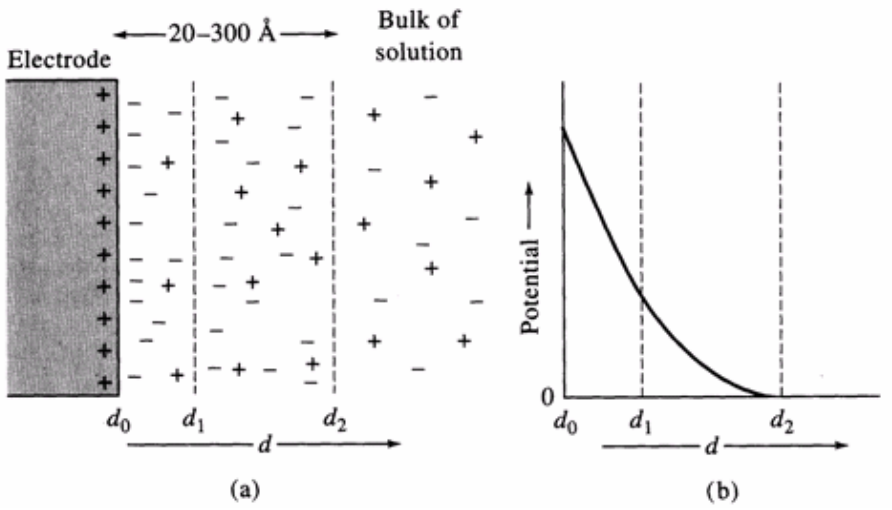

Figure 1.6: Electrical double layer formed at electrode surface as a result of an applied potential

1.16 Faradaic and nonfaradaic currents

Two types of processes can conduct currents across an electrode/solution interface. One involves a direct transfer of electrons via an oxidation reaction at one electrode and a reduction reaction at the other. Processes of this type are called faradaic processes because they are governed by Faraday's law, which states that the amount of chemical reaction at an electrode is proportional to the current; the resulting currents are called faradaic currents. Under some conditions a cell will exhibit a range of potentials where faradaic processes are precluded at one or both of the electrodes for thermodynamic or kinetic reasons. Here, conduction of continuous alternating currents can still take place. With such currents, reversal of the charge relationship occurs with each half cycle, as first negative and then positive ions are attracted alternately to the electrode surface. Thus, each electrode surface behaves as one plate of a capacitor, the capacitance of which may be large. The capacitive current increases with frequency and with electrode area; by controlling these variables, it is possible to arrange conditions such that essentially all the alternating current in a cell is carried across the electrode interface by this nonfaradaic process [66].

Current in voltammetric experiment is a measure of the rate of the electrode process. When an electrode is placed in an electrolyte solution, different processes may occur. Steps involved in an electrode reaction are (Figure 1.7**)**.

1) Mass transfer of species between bulk solution and the electrode surface.
2) Heterogeneous electron transfer at the electrode/solution interface.
3) Chemical reactions, either preceding or following electron transfer.
4) Surface reactions such as adsorption, desorption and electrodeposition-dissolution [67].

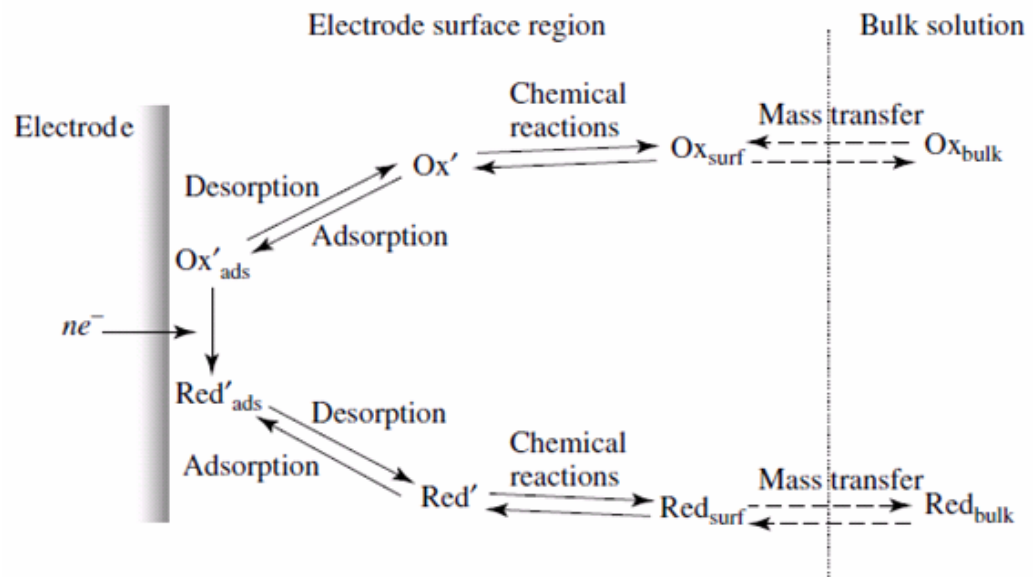

Figure 1.7: Typical steps involved in an electrode reaction

1.17 Mass transfer process in voltammetry

The movement of the electro-active substance through solution is referred as mass transfer at the electrode surface. In electrochemical systems, there are different types of mass transfer system by which a substance may be transferred to the electrode surface from bulk solution. Depended on the experimental conditions, any of these or more than one might be operating in a given experiment system.

A reacting species may be brought to an electrode surface by three types of mass transfer processes [68]. These are,

- Migration
- Diffusion
- Convection

1.17.1 Migration

Migration refers to movement of a charge particle in a potential field. It occurs by the movement of ions through a solution as a result of electrostatic attraction between the ions and the electrodes. In general, most electrochemical experiment it is unwanted but can be eliminated by the addition of a large excess of supporting electrolytes. In the electrolysis solution, ions will move towards the charged electrode that means cations to the cathode and

anions to the anode. This motion of charged particle through solution, induced by the charges on the electrodes is called migration [69]. This charge movement constitutes a current. This current is called migration current. Migration is the movement of charged species due to a potential gradient. In voltammetric experiments, migration is undesirable but can be eliminated by the addition of a large excess of supporting electrolytes in the electrolysis solution. The effect of migration is applied zero by a factor of fifty to hundred ions excess of an inert supporting electrolyte such as KCl, KNO_3 etc.

1.17.2 Diffusion

The movement of a substance through solution by random thermal motion is known as diffusion. Whereas a concentration gradient exists in a solution, that is the concentration of a substance, is not uniform throughout the solution. There is a driving force for diffusion of the substance from regions of high concentration to regions of lower concentration [70]. The one kind of mode of mass transfer is diffusion to an electrode surface in an electrochemical cell. The rate of diffusion is directly proportional to the concentration difference. When the potential is applied, the cations are reduced at the electrode surface and the concentration is decreased at the surface film. Hence a concentration gradient is produced. Finally, the result is that the rates of diffusion current become larger.

1.17.3 Convection

By mechanical way reactants can also be transferred to or from an electrode. Thus forced convection is the movement of a substance through solution by stirring or agitation. This will tend to decrease the thickness of the diffuse layer at an electrode surface and thus decrease concentration polarization. Natural convection resulting from temperature or density differences also contributes to the transport of species to and from the electrode [71]. At the same time a type of current is produced. This current is called convection current. Removing the stirring and heating can eliminate this current. Convection is a far more efficient means of mass transport than diffusion. These three kinds of mass transfer processes are shown in Figure 1.8.

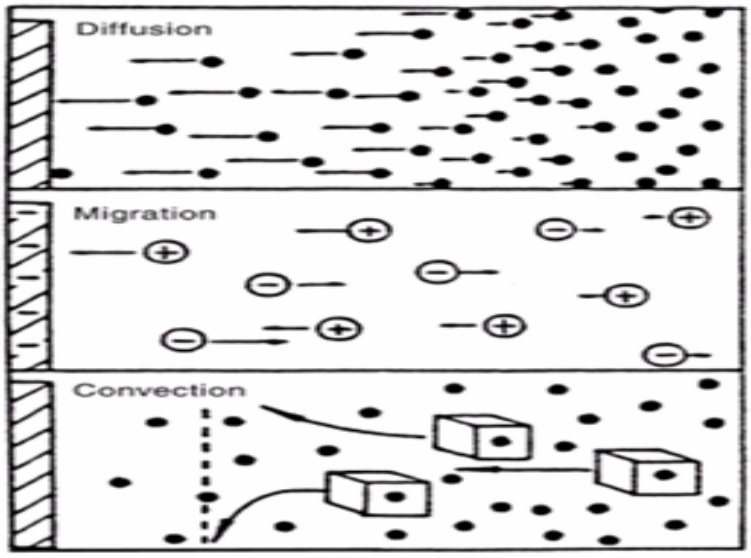

Figure 1.8: Modes of mass transfer

In this research work, various electrochemical techniques such as cyclic voltammetry (CV), differential pulse voltammetry (DPV) along with UV-visible Spectrophotometry were used for the qualitative and quantitative determination of VC, PA and CA.

1.18 Cyclic Voltammetry (CV)

Cyclic Voltammetry (CV) is perhaps the most effective and versatile electroanalytical technique available for the mechanistic study of redox systems. It enables the electrode potential to be rapidly scanned in search of redox couples. Once located, a couple can then be characterized from the potentials of peaks on the cyclic voltammogram and from changes caused by variation of the scan rate. CV is often the first experiment performed in an electrochemical study. CV consists of imposing an excitation potential nature on an electrode immersed in an unstirred solution and measuring the current and its potential ranges varies from a few millivolts to hundreds of millivolts per second in a cycle. This variation of anodic and cathodic current with imposed potential is termed as voltammogram [72].

The technique involves under the diffusion controlled mass transfer condition at a stationary electrode utilizing symmetrical triangular scan rate ranging from $1mVs^{-1}$ to hundreds millivolts per second.

1.18.1 Uses of CV

The cyclic voltammetric technique reveals information about the following important phenomena:

i) reversibility of a reaction and a very rapid means of analysis of various systems

ii) direct investigation of reactive intermediate

iii) investigation of stepwise electrochemical and chemical reaction

iv) redox characteristic of oxidizing-reducing couple [73].

1.19 Differential Pulse Voltammetry (DPV)

Differential Pulse Voltammetry (DPV) or Differential Pulse Polarography (DPP) is often used to make electrochemical measurements. It can be considered as a derivative of linear sweep voltammetry or staircase voltammetry, with a series of regular voltage pulses superimposed on the potential linear sweep or stair steps [74]. The current is measured immediately before each potential change, and the current difference is plotted as a function of potential. By sampling the current just before the potential is changed, the effect of the charging current can be decreased.

1.19.1 Uses of DPV

DPV is a very important analytical tool for quantitative determination in trace level. This technique can be used to study the redox properties of extremely small amounts of chemicals because of the following two features [75]:

i) In these measurements, the effect of the charging current can be minimized, so high sensitivity is achieved.

ii) Faradaic current is extracted, so electrode reactions can be analyzed more precisely.

1.20 Aim of this research

- Preparation of cost effective electrode sensor
- To develop Aspartic acid modified WB, GC, Au, Pt and PG electrodes
- To recognize the most favorable condition (such as pH and scan rate) for the separation of VC, PA and CA
- To determine the quantity of VC, PA and CA in known sample and tablet samples of some Bangladeshi pharmaceutical industry.

CHAPTER II

Literature Review

Many analytical techniques have been described for simultaneous determination of VC, PA and CA, such as spectrophotometry, high-performance liquid chromatography and electrochemical methods. Among them, electrochemical method based on modified electrode sensor has attracted more attention for their high sensitivity, simplicity, reproducibility, on site monitoring and low cost. Some literatures have been reviewed and are summarized below:

Khoshhesab, Z. M. *et al*., 2015, prepared nanocomposite based on CuO nanoparticles/graphene nanosheets and used as a new electrode material for the simultaneous determination of acetaminophen, caffeine and ascorbic acid. CuO nanoparticles were supported on graphene nanosheets by a simple method. This nanostructure was characterized by different techniques including scanning electron microscopy, X-ray diffraction, energy dispersive X-ray spectroscopy and Fourier transform infrared spectroscopy. The high electrochemical activity, fast electron transfer rate, high surface area and good antifouling properties of the synthesized nanostructure enhanced the oxidation peak currents and reduced the peak potentials of acetaminophen, caffeine and ascorbic acid at the surface of the proposed sensor. Simultaneous determination of analytes was explored using differential pulse voltammetry. A linear range of 0.025–5.3 μmol L^{-1} was achieved for acetaminophen, caffeine and ascorbic acid with detection limits of 0.008, 0.010 and 0.011 μmol L^{-1}, respectively. Finally, the proposed method was used for their determination in blood serum, urine and pharmaceutical samples [76].

Tefera, M. *et al*., 2016, prepared Poly(4-amino-3-hydroxynaphthalene sulfonic acid)-modified glassy carbon electrode (poly(AHNSA)/GCE) for simultaneous determination of caffeine and paracetamol using square-wave voltammetry. The method was used to study

the effects of pH and scan rate on the voltammetric response of caffeine and paracetamol. Linear calibration curves in the range of 10–125 μM were obtained for both caffeine and paracetamol in acetate buffer solution of pH 4.5 with a correlation coefficient of 0.9989 and 0.9986, respectively. The calculated detection limits (S/N = 3) were 0.79 μM for caffeine and 0.45 μM for paracetamol. The method was successfully applied for the quantitative determination of caffeine and paracetamol in Coca-Cola, Pepsi-Cola and tea samples [77].

Chitravathi, S. *et al*., 2016, fabricated poly(Nile blue) modified glassy carbon electrode (PNBMGCE) by electropolymerisation of Nile blue (NB) monomer using cyclic voltammetry (CV) and was used for the determination of paracetamol (ACOP), tramadol (TRA) and caffeine (CAF). The electrochemical investigations showed that PNB — film formed on the surface of glassy carbon electrode (GCE) improved the electroactive surface area and displayed a remarkable increase in the peak current and a substantial decrease in over potential of ACOP, TRA and CAF when compared to bare GCE. The dependence of peak current and potential on pH, sweep rate and concentration were also investigated at the surface of PNBMGCE. It showed good sensitivity and selectivity in a wide linear range from 2.0×10^{-7} to 1.62×10^{-5} M, 1.0×10^{-6} to 3.1×10^{-4} M and 8.0×10^{-7} to 2.0×10^{-5} M, with detection limits of 0.08, 0.5 and 0.1 μM, for ACOP, TRA and CAF, respectively. The PNBMGCE was also successfully applied for the determination of ACOP, TRA and CAF in pharmaceutical dosage forms [78].

Sadok, I. *et al*., 2016, developed a sensitive and selective voltammetric method of simultaneous or separated detection of paracetamol and caffeine at a non-toxic bismuth particles Nafion covered boron-doped diamond electrode. The bismuth particles were deposited by an in situ method at Nafion covered boron-doped diamond electrode from 0.1 mol L^{-1} sulphuric acid solution containing metal ions and different concentrations of paracetamol and caffeine. The obtained oxidation peaks of paracetamol and caffeine appear at 0.78 and 1.44 V (vs. Ag/AgCl), respectively. The obtained detection limits for paracetamol and caffeine were 2.62×10^{-8} and 1.14×10^{-9} mol L^{-1} respectively. The proposed voltammetric method was applied in simultaneous determination of paracetamol and caffeine in pharmaceutical and individual detection of caffeine in beverages (energy drinks, cola beverages, tea and coffee) and weight loss supplements [79].

Kalambate, P. K. *et al*., 2016, studied the fabrication and application of electrochemical sensor for simultaneous determination of paracetamol (PCT), cetirizine (CTZ) and

phenylephrine (PHE) based on carbon paste electrode modified with multiwalled carbon nanotube-platinum nanoparticles (MWCNT-PtNPs) nanocomposite. The electrochemical oxidation of PCT, CTZ and PHE has been investigated by application of said electrode using cyclic voltammetry (CV), adsorptive stripping differential pulse voltammetry (AdSDPV) and electrochemical impedance spectroscopy (EIS). Under optimized experimental conditions PCT, CTZ and PHE gave linear response over the linear ranges 3.51×10^{-7}–5.61×10^{-5} M, 1.9×10^{-7}–1.93×10^{-4} M and 2.9×10^{-7}–5.69×10^{-5} M for PCT, CTZ and PHE, respectively. The detection limits were found to be 2.79×10^{-8} M, 5.86×10^{-8} M and 2.83×10^{-8} M for PCT, CTZ and PHE respectively. The method described is highly sensitive and has been applied for the simultaneous determination of PCT, CTZ and PHE in commercially available pharmaceutical formulations, blood serum and urine samples. A good recovery level obtained for real samples suggests practical utility of the MWCNT-PtNPs-CPE as an effective and reliable electrochemical sensor for simultaneous determination of PCT, CTZ and PHE [80].

Kalambate, P. K. *et al*., 2015, electrochemically reduced Graphene oxide and hexachloroplatinic acid on a glassy carbon electrode (GCE) surface so as to form a graphene (Gr)–platinum nanoparticles (PtNP) composite. This nano composite was then coated with nafion (NAF) film so as to form NAF/PtNP/Gr/GCE. In this work, an electrochemical method based on adsorptive stripping square wave voltammetry (AdSSWV) employing NAF/PtNP/Gr/GCE has been proposed for the subnanomolar determination of paracetamol (PCT) and domperidone (DOM) simultaneously. The electrochemical performance of PCT and DOM on modified electrode was investigated by cyclic voltammetry, electrochemical impedance spectroscopy, and chronocoulometry. Under the optimized conditions, the method allowed simultaneous determination of PCT and DOM in the linear working range of 8.2×10^{-6}–1.6×10^{-9} M with detection limits ($3 \times$ SD/s) of 1.06×10^{-10} and 4.37×10^{-10} M for PCT and DOM respectively. The practical analytical utilities of the modified electrode were demonstrated by the determination of PCT and DOM in pharmaceutical formulations, human urine, and blood serum samples [81].

Bouabi, Y. E. *et al*., 2016, developed and evaluated a novel analytical approach for the quantitative analysis of paracetamol (PCT). The anodic peak currents of paracetamol on the CS–CPE were about 200 fold higher than that of the unmodified electrodes. The influence of various parameters on the CS–CPE was investigated. Under the optimized working

conditions, the oxidation peak current is linear to the paracetamol concentration in the ranges of 1.0×10^{-3}–4.0×10^{-4} mol L^{-1} and 2.0×10^{-4}–8.0×10^{-7} mol L^{-1} with a detection limit of 5.08×10^{-7} mol L^{-1}. The repeatability of the method expressed as relative standard deviation (RSD) is 1.73% (n = 8). Possible interferences were tested and evaluated in 1.0×10^{-4} mol L^{-1} paracetamol in the presence of inorganic ions, dopamine, ibuprofen, ascorbic acid and uric acid. The proposed method was successfully applied to PCT determination in natural waters, tablets and urine samples [82].

Bouabi, Y. E. *et al*., 2016, modified a carbon paste electrode with fluoroapatite (FAP–CPE) for examined to catalyze the electrochemical reduction of paracetamol (PCT). The electrochemical behavior of PCT has been investigated and the optimum experimental conditions were achieved. Moreover, a good linear relationship was achievable over the concentration range from 4.0×10^{-8} mol/L to 1.0×10^{-3} mol/L using square wave voltammetry (SWV). The detection limit (S/N = 3) was also calculated and a low value of 1.25×10^{-8} mol/L was obtained with 210 s of accumulation time. The effect of coexisting of interferent compounds such as ascorbic acid (AA), citric acid (CA) and a binary mixture with dopamine (DA) was also investigated. The proposed method was successfully applied to PCT determination in natural waters, tablets and urine samples with the results agreeing with independently verified HPLC [83].

Daneshvar, L. *et al*., 2016, fabricated a carbon ionic liquid paste electrode (CILPE) based on butyl-3-methylimidazolium bis (trifluoromethylsulfonyl) imide ([bmim] NTF2) and further modified with graphene/multiwall carbon nanotube (GR/MWCNT) hybrid composite. The modified electrode (GR/MWCNT/CILPE) was used for measurement of carbamazepine (CBZ) in the presence of paracetamol (PA) with an excellent electrochemical catalytic behavior. The application of the electrode was investigated by cyclic voltammetry and differential pulse voltammetry. The oxidation peak currents of CBZ and PA were linear at the ranges of 1–60 μM and 2–80 μM, respectively. Also, the detection limits for CBZ and PA were 0.233 μM and 0.262 μM, respectively. The proposed sensor was successfully applied for the determination of CBZ and PA in tablet and urine samples [84].

Majidi, M. R. *et al*., 2016, used ionic liquid as 1-allyl-3-methylimidazolium tetraflouroborate ([AMIM][BF_4]) for surface modification of carbon-ceramic electrode. This modified electrode was used for simultaneous electrochemical determination of dopamine (DA) and acetaminophen (AP). Because of effective separation of oxidation peak potentials

of DA and AP on modified electrode, simultaneous determination of them was possible. Operational parameters such as amount of IL volume, solution pH, scan rate; which affected the analytical performance of modified electrode were optimized. The calibration curves for DA and AP were linear in the range of 0.1–20 μM and 0.1–20 μM with the detection limit (S/N = 3) of 68 nM and 63 nM, respectively. The present electrode was successfully applied for the determination of DA and AP in some commercial pharmaceutical samples, human blood serum, and urine samples with satisfactory results [85].

Afrasiabi *et al*., 2015, demonstrated that simultaneous determination of ascorbic acid (AA), uric acid (UA) and acetaminophen (ACT) can be performed on a novel single walled carbon nanotubes (SWCNTs), chitosan (CHIT) and MCM-41 composite modified glassy carbon electrode (SWCNTs-CHIT-MCM-41/GCE). The electro-oxidations of AA, UA and ACT were investigated by using differential pulse voltammetry (DPV), chronoamperometry (CA) and electrochemical impedance spectroscopy (EIS) methods. Under optimum conditions application of DPV method showed that the linear relationship between oxidation peak current and concentration of AA, UA and ACT were 1-160 μM, 0.1-24 μM and 0.1-21 μM with detection limits of 0.41, 0.04 and 0.03 μM, respectively [86].

Karimi-Maleh, H. *et al*., 2014, studied the electrooxidation of isoproterenol (ISPT), acetaminophen (AC) and tryptophan (Trp) and their mixture using an 8,9-dihydroxy-7-methyl-12H-benzothiazolo[2,3-b]quinazolin-12-one modified multiwall carbon nanotubes paste electrode (DMBQ-MCNTPE). The novel sensor exhibited potent and persistent electron mediating behavior followed by well separated oxidation peaks towards ISPT, AC and Trp with activation over-potential. The peak currents were linearly dependent on ISPT, AC and Trp concentrations using square wave voltammetry (SWV) method in the range of 0.04–400, 5.0–500, and 10.0–800 μmol L^{-1}, with detection limits of 0.009, 1.0, and 4.0 μmol L^{-1}, respectively. The modified electrode was used for the determination of ISPT, AC and Trp in biological and pharmaceutical samples [87].

Mazloum-Ardakani, M. *et al*., 2011, described a new electrochemical sensor for the determination of norepinephrine (NE), acetaminophen (AC) and tryptophan (Trp). The sensor is based on carbon paste electrode (CPE) modified with 3, 4-dihydroxybenzaldehyde-2,4-dinitrophenylhydrazone (DDP) and takes the advantages of carbon nanotubes (CNTs), which makes the modified electrode highly sensitive for the electrochemical detection of

these compounds. Under the optimum pH of 7.0, the oxidation of NE occurs at a potential about 215 mV less positive than that of the unmodified CPE. Differential pulse voltammetry (DPV) of NE at the modified electrode exhibited two linear dynamic ranges with a detection limit (3σ) of 77 ± 2 nM. DPV was used for simultaneous determination of NE, AC and Trp at the modified electrode, and quantitation of NE in some real samples by the standard addition method [88].

Liu, B. *et al*., 2016, have been fabricated transition metal oxides decorated graphene (GR) for simultaneous determination of dopamine (DA), acetaminophen (AC) and tryptophan (Trp) using square wave voltammetry. Electro-deposition is a facile preparation strategy for the synthesis of nickel oxide (NiO) and copper oxide (CuO) nanoparticles. GR can be modified by using citric acid to produce more functional groups, which is conducive to the deposition of dispersed metal particles. Moreover, the electrochemical performances of the composite film were investigated by cyclic voltammetry and electrochemical impedance spectroscopy. The modified electrode exhibited that the linear response ranges for detecting DA, AC and Trp were 0.5–20 μM, 4–400 μM and 0.3–40 μM respectively, and the detection limits were 0.17 μM, 1.33 μM and 0.1 μM (S/N=3). Under optimal conditions, the sensor displayed high sensitivity, excellent stability and satisfactory results in real samples analysis [89].

Tavana, T. *et al*., 2012, fabricated a novel ionic liquid modified carbon nanotubes paste electrode (IL/CNTPE) by using hydrophilic ionic liquid 1-methyl-3-butylimidazolium bromide [MBIDZ] Br as a new binder. Electrochemical behavior of epinephrine (EP) at the IL/CNTPE had been investigated in pH 7.0 phosphate buffer solution (PBS) by cyclic voltammetry (CV), electrochemical impedance spectroscopy (EIS), chronoamperometry (CA) and differential pulse voltammetry (DPV). Detection limit of EP and AC was found to be 0.09 and 0.5 μM respectively. The proposed sensor was successfully applied for the determination of EP and AC in human urine, pharmaceutical, and serum samples [90].

Keyvanfard, M. *et al*., 2013, modified a carbon-paste electrode with multiwall carbon nanotubes (MWCNTs) and used for the sensitive and selective voltammetric determination of ascorbic acid (AA) in the presence of 3,4-dihydroxycinnamic acid (3,4-DHCA) as mediator. The mediated oxidation of AA at the modified electrode was investigated by cyclic voltammetry (CV), chronoamperommetry and electrochemical impedance spectroscopy

(EIS). Using square wave voltammetry (SWV), a highly selective and simultaneous determination of AA, acetaminophen (AC) and tryptophan (Trp) has been explored at the modified electrode. In the mixture containing AA, AC and Trp, the three compounds can well separate from each other with potential differences of 200, 330 and 530 mV between AA and AC, AC and Trp and AA and Trp, respectively, which was large enough to determine AA, AC and Trp individually and simultaneously [91].

Mazloum-Ardakani, M. *et al*., 2012, prepared an electrochemical sensor by modification of carbon paste electrode with a nanostructured mesoporous material. The electrooxidation of norepinephrine (NE), paracetamol (AC) and folic acid (FA) was studied at this electrode by cyclic voltammetry (CV) and differential pulse voltammetry (DPV). CV experiments showed that the oxidation overpotential of these substances decreased and their oxidation current increased sharply at the modified electrode rather than bare carbon paste electrode. The overlapped DPV peaks of NE, AC and FA has been resolved into three separated peaks by the electrochemical sensor. DPV peak currents increased linearly with concentration over the range of 7.0×10^{-8} to 2.0×10^{-3}, 5.0×10^{-7} to 2.2×10^{-3} and 5.0×10^{-6} to 2.0×10^{-3} M for NE, AC, and FA, respectively. Also, the proposed electrochemical sensor was used for the determination of these substances in some real samples [92].

Beitollahi, H. *et al*., 2012, developed a new electrochemical sensor for the simultaneous determination of dopamine (DA), acetaminophen (AC), folic acid (FA) and N-acetylcysteine (NAC). The sensor is based on carbon-paste electrode (CPE) modified with 5-amino-3′,4′-dimethyl -biphenyl-2-ol (5ADB) and takes the advantages of carbon nanotubes (CNTs), which makes the modified electrode highly sensitive for the electrochemical detection of these compounds. Under the optimum pH of 7.0, the oxidation of DA occurs at a potential about 170 mV less positive than that of the unmodified CPE. Also, square wave voltammetry was used for the simultaneous determination of DA, AC, FA and NAC at the modified electrode [93].

Beitollahi, H. *et al*., 2012, modified a carbon paste electrode with carbon nanotubes and 5-amino-3′, 4′-dimethyl-biphenyl-2-ol (5ADB) and used to prepare a novel electrochemical sensor. The objective of this novel electrode modification was to seek new electrochemical performances for the detection of isoproterenol (IP) in the presence of acetaminophen (AC) and N-acetylcysteine (NAC). The peak potentials recorded in a phosphate buffer solution

(PBS) of pH 7.0 were 265, 445 and 950 mV vs. Ag/AgCl/KCl (3.0 M) for IP, AC and NAC, respectively. The response of catalytic current with IP concentration showed a linear relation in the range from 4.0×10^{-7} to 9.0×10^{-4} M with a detection limit of 2.0×10^{-7} M [94].

Taei, M. *et al*., 2017, developed a poly-Trypan Blue modified glassy carbon electrode for simultaneous determination of ascorbic acid (AA), noradrenaline (NA), acetaminophen (AC) and tryptophan (Try). Bare glassy carbon electrode (GCE) has limitations for resolving the oxidation currents of these compounds. Poly-Trypan Blue modified electrode not only separates the voltammetric signals of AA, NA, AC and Try with potential differences of 150, 170, and 280 mV between AA–NA, NA-AC, and AC–Try, but it can also enhance the oxidation currents of AA, NA, AC and Try by 11.0, 7.0, 1.4, and 3.8 times, respectively, compared to bare electrode. The detection limits of AA, NA, AC and Try were also calculated as 0.10, 0.06, 0.10 and 0.80 μmol L^{-1}, respectively. Finally, the fabricated sensor was satisfactorily used for the simultaneous determination of these molecules in pharmaceutical and human biological samples [95].

Adhikari, B. *et al*., 2015, reported on a high-performance electrochemical sensor for the sensitive detection of acetaminophen based on graphene, which was simultaneously electrochemically reduced and deposited onto a glassy carbon electrode (GCE). An extremely low detection limit of 2.13 nM and a wide linear detection range of from 5.0 nM to 800 μM were achieved via the combination of the amperometric technique and DPV. The developed electrochemical sensor was further employed for the determination of acetaminophen in human serum, with excellent recovery, ranging from 96.08% to103.2%. The fabricated electrochemical sensor also demonstrated high selectivity, stability and reproducibility. The wide linear detection range obtained in this study for the detection of acetaminophen showed strong potential as a promising sensing technique for pharmaceuticals, in terms of quality control and in clinical laboratories for acetaminophen as relates to the determination of hepatotoxicity [96].

Raoof, J.B. *et al*., 2014, investigated simultaneous voltammetric determination of Noradrenaline (NA), Acetaminophen (AC), Xanthine (XN) and Caffeine (CF) at a flavonoid nanostructured sensor. The construction of modified electrode was performed through the electrodeposition of luteolin on a functionalized multi-wall carbon nanotube immobilized on the surface of a glassy carbon electrode (Lt/fMWCNT/MGCE). The

Lt/fMWCNT/MGCE offered substantially lower overpotential for electro-oxidation of NA, AC, XN and CF in phosphate buffer solution (pH 7.0) compared with Lt/GCE, fMWCNT/GCE and bare GCE. Differential pulse voltammogram peak currents of NA, AC, XN and CF increased linearly with their concentration at the ranges of 0.7–100.0 μM, 0.9–80.0 μM, 1.0–70.0 μM and 10.0–110.0 μM, respectively, and the detection limits for NA, AC, XN and CF were sequentially 0.53 μM, 0.78 μM, 0.65 μM and 3.54 μM. Furthermore, this electrochemical sensor was successfully implemented for the determination of NA in pharmaceutical samples using standard addition method and the obtained results were found to be satisfactory [97].

Afkhami, A. *et al*., 2014, developed an effective electrochemical sensor for the rapid and simultaneous determination of tramadol and acetaminophen based on carbon paste electrode (CPE) modified with $NiFe_2O_4$/graphene nanoparticles. The peak currents of square wave voltammetry of tramadol and acetaminophen increased linearly with their concentration in the range of 0.01–9 μmol L^{-1}. The detection limit for their determination was found to be 0.0036 and 0.0030 μmol L^{-1}, respectively. The results show that the combination of graphene and $NiFe_2O_4$ nanoparticles causes a dramatic enhancement in the sensitivity of the sensor. The fabricated sensor exhibited high sensitivity and good stability, and would be valuable for the clinical assay of tramadol and acetaminophen [98].

Beitollahi, H. *et al*., 2011, prepared a carbon-paste electrode modified with 2, 7-bis (ferrocenyl ethyl) fluoren-9-one (2, 7-BF) and carbon nanotubes (CNTs) for the sensitive and selective voltammetric determination of *N*-acetylcysteine (NAC). The mediated oxidation of NAC at the modified electrode was investigated by cyclic voltammetry (CV). Differential pulse voltammetry (DPV) of NAC at the modified electrode exhibited two linear dynamic ranges with a detection limit (3σ) of 52.0 nmol L^{-1}. DPV was used for simultaneous determination of NAC and acetaminophen (AC) at the modified electrode, and quantitation of NAC and AC in some real samples by the standard addition method [99].

Liu, X. *et al*., 2017, developed a novel electrochemical sensor based on FeS/rGO nanosheets modified glassy carbon electrode (GCE). It has been proved that the resultant FeS/rGO/GCE sensor is very suitable for the individual and simultaneous measurement of dopamine (DA) and acetaminophen (AC) and delivers excellent anti-interference ability to ascorbic acid (AA) and uric acid (UA). Under optimum conditions with differential pulse voltammetry method, a broad linear response versus the concentrations of DA and AC has been observed

in the ranges of 2.0 to 250.0 μM and 5.0 to 300.0 μM, respectively. The detection limits for DA and AC are 0.098 μM and 0.18 μM, respectively. Furthermore, the sensor has been successfully utilized in real samples and satisfactory results have been achieved [100].

Taei, M. *et al*., 2014, constructed a novel Au-nanoparticles/poly-(2-amino-2-hydroxymethyl-propane-1,3-diol) film modified glassy carbon electrode (AuNPs/poly(trisamine)/GCE) for the simultaneous determination of norepinephrine (NE), acetaminophen (AC) and L-tyrosine (Tyr) by differential pulse voltammetry. The separation of the oxidation peak potentials for NE–AC and AC–Tyr were about 160 mV and 240 mV, respectively. The calibration curves for NE, AC and Tyr were obtained in the range of 1.3–230.1 μmol L^{-1}, 1.90–188.0 μmol L^{-1}, and 3.9–61.8 μmol L^{-1}, respectively. The detection limits (S/N = 3) were 0.07 μmol L^{-1}, 0.1 μmol L^{-1} and 0.9 μmol L^{-1}, for NE, AC and Tyr, respectively. The diffusion coefficient and the catalytic rate constant for the oxidation reaction of NE at AuNPs/poly (trisamine)/GCE were calculated as 1.55 (±0.2) × 10^{-6} cm^2 s^{-1} and 2.28 (±0.17) × 10^3 mol^{-1} L s^{-1}, respectively. Finally, AuNPs/poly(trisamine)/GCE was satisfactorily used for the determination of NE, AC, and Tyr in pharmaceutical and biological samples [101].

Madrakian, T. *et al*., 2015, developed an electrochemical magneto Au nanoparticles/carbon paste electrodes (MAuNP/CPE) which is used for the determination of acetaminophen (AC) in real samples. For investigation of the performance of AuNPs@Fe_3O_4 and MAuNPs/CPE, cyclic voltammetry and DPV were used. Under the optimized conditions, the anodic peak current was linear to the concentration of AC in the range of 0.1 to 70.0 μmol L^{-1} with the detection limit of 4.5 × 10^{-2} μmol L^{-1}. This method was also successfully used to detect the concentration of AC in pharmaceutical formulations and human serum samples. In addition, the proposed magneto sensor exhibited good reproducibility, long-term stability and fast current response [102].

BEITOLLAHI, H. *et al*., 2013, prepared a carbon paste electrode (CPE) modified with carbon nanotubes and 5-amino-3′,4′-dimethyl- biphenyl-2-ol (5ADB). Under the optimum pH of 7.0, the oxidation of ascorbic acid (AA) on the modified CPE occurs at a potential about 280 mV less positive than that on the unmodified CPE. AA, acetaminophen (AC), and tryptophan (TRP) were detected simultaneously using the modified CPE. The peak potentials recorded using the modified CPE in phosphate-buffered solution at pH 7.0 were

265, 465, and 780 mV for AA, AC, and TRP, respectively. The modified CPE was successfully used to determine the concentrations of AA, AC, and TRP in real samples [103].

Ensafi, A.A. *et al*., 2015, prepared a porous silicon/palladium nanostructure and used as a new electrode material for the simultaneous determination of acetaminophen (ACT) and codeine (COD). The high electrochemical activity, fast electron transfer rate, high surface area and good antifouling properties of this nanostructure enhanced the oxidation peak currents and reduced the peak potentials of ACT and COD at the surface of the proposed sensor. Simultaneous determination of ACT and COD was explored using differential pulse voltammetry. A linear range of 1.0–700.0 μmol L^{-1} was achieved for ACT and COD with detection limits of 0.4 and 0.3 μmol L^{-1}, respectively. Finally, the proposed method was used for the determination of ACT and COD in blood serum, urine and pharmaceutical compounds [104].

Chen, X. *et al*., 2012, reported a high performance electrochemical sensor for the detection of acetaminophen (APAP) at the single-walled carbon nanotube (SWCNT)–graphene nanosheet (GNS) hybrid film modified electrode. The electrochemical behavior of APAP at the SWCNT–GNS modified glassy carbon (GC) electrode was investigated by cyclic voltammetry. The results showed significantly enhanced electrochemical reactivity and voltammetric response of APAP. The electrochemical sensor based on the hybrid modified electrode exhibited excellent analytical performance for APAP detection in neutral solution with a low detection limit of 38 nM and a wide linear range of 0.05–64.5 μM. Moreover, the SWCNT–GNS/GC electrode also showed good selectivity and stability. The high performances of the novel APAP sensor are mainly attributed to high surface area and multi-modal pore structure of the SWCNT–GNS hybrid, which provide an increased sensing area and effective mass transportation pathway [105].

Kong, J. *et al*., 2014, fabricated a multi-walled carbon nanotubes (MWNTs) bridged mesocellular graphene foam (MGF) nanocomposite (MWNTs/MGF) modified glassy carbon electrode and successfully used for simultaneous determination of ascorbic acid (AA), dopamine (DA), uric acid (UA) and tryptophan (TRP). Comparing with pure MGF, MWNTs or MWNTs/GS (graphene sheets), MWNTs/MGF displayed higher catalytic activity and selectivity toward the oxidation of AA, DA, UA and TRP. Under the optimal conditions, MWCNs/MGF/GCE can simultaneously detect AA, DA, UA and TRP with high selectivity and sensitivity. The detection limits were 18.28 μmol L^{-1}, 0.06 μmol L^{-1},

0.93 µmol L^{-1} and 0.87 µmol L^{-1}, respectively. Moreover, the modified electrode exhibited excellent stability and reproducibility [106].

Mazloum-Ardakani, M. *et al*., 2010, investigated the electrochemical behavior of vitamin C (ascorbic acid or AA) on the surface of a carbon-paste electrode modified with TiO_2 nanoparticles and 2,2′-(1,2 butanediylbis(nitriloethylidyne))-bis-hydroquinone (BBNBH). The prepared modified electrode showed an efficient catalytic role in the electrochemical oxidation of AA, leading to remarkable decrease in oxidation overpotential and enhancement of the kinetics of the electrode reaction. This modified electrode exhibits well-separated oxidation peaks for AA and uric acid (UA). The modified electrode is successfully applied for the accurate determination of AA in pharmaceutical preparations [107].

Tadayon, F. *et al*., 2016, employed an Au-Pd/reduced graphene oxide composite as a novel electrode material for the sensitive and simultaneous determination of ascorbic acid, acetaminophen and tyrosine. The electrochemical response characteristics of the modified electrode toward the analytes were investigated by differential pulse voltammetry and cyclic voltammetry. The experimental conditions for simultaneous determination of these species have been established. Ternary mixtures of analytes can be determined in the ranges of 0.03–9.50 µM. Under optimal conditions, the limits of detection were 15.7, 7.6 and 11.1 nM for ascorbic acid, acetaminophen, and tyrosine, respectively. The method was applied successfully to determine the analytes in urine, serum and pharmaceutical samples simultaneously [108].

Karuppiah, C. *et al*., 2016, reported a rapid and sensitive detection of the acetaminophen based on the bare (unmodified) screen printed carbon electrode (BSPCE) and its electrochemistry was studied in various pHs. From the observed results, the mechanism of the electro-oxidation of acetaminophen was derived for various pHs. However, it is stable in intermediate pHs due to the dimerization of acetaminophen. Moreover, the BSPCE determined the acetaminophen with the linear concentration ranging from 0.05 to 190 µM and the lower detection limit of 0.013 µM. Besides that it reveals the good recoveries towards the pharmaceutical samples and shows the excellent selectivity, sensitivity and stability. To the best of our knowledge, this is the better performance compare to the previously reported unmodified acetaminophen sensors [109].

Song, J. *et al*., 2011, prepared the graphite oxide (GO) via the chemical oxidation of natural graphite powder, and then used to modify the surface of glassy carbon electrode (GCE). The electrochemical behavior of acetaminophen was examined. In 0.01 mol L^{-1} HCl, an irreversible oxidation peak is observed for acetaminophen, and the peak current remarkably increases at the GO film-modified GCE. The influences of supporting electrolyte, amount of GO suspension, accumulation potential and time were studied on the oxidation peak current of acetaminophen. As a result, a new electrochemical method was developed for the detection of acetaminophen. The linear range is from 25 μg L^{-1} to 4 mg L^{-1}, and the limit of detection is 6 μg L^{-1} based on three signal–noise ratio. Finally, it was successfully used to detect acetaminophen in tablets [110].

Swain, S. *et al*., 2017, developed a rapid, an accurate and precise Ultra Performance Liquid Chromatography (UPLC) method and validated for simultaneous estimation of paracetamol and caffeine in its capsule dosage form (325 mg and 30 mg) by selecting chromatographic parameters. The UPLC method was developed using 2.1 × 50 mm, reverse phase C_{18} column (Acquity UPLC ethylene bridge hybrid (BEH) C_{18} 1.7 μm) with mobile phases containing 0.1% w/v H_3PO_4 and 100% v/v buffer as mobile phase A and methanol: Acetonitrile (50:50) as mobile phase B and water: acetonitrile: H_3PO_4 (80:20:0.1) as diluent and the run considered as an isocratic elution. Flow rate was 0.5 ml/min with PDA detection at (λ_{max}) 275 nm for paracetamol and caffeine and the injection volume was set at 2 μL with run time 7 min. The method was validated by using various validation parameters like accuracy, precision, linearity and specificity. These results show the method could find practical application as a quality control tool for analysis of the drug in its capsule dosage forms in pharmaceutical industries. The developed validated method and stability testing of new dosage forms as per ICH-Q2 (R1) and ICH-Q1C guidelines applicable for the analysis of bulk drug and in its capsules dosage form [111].

2.1 Objectives of this Thesis

VC, PA and CA are three important pharmaceutical tablets. PA known as acetaminophen or N-acetyl-p-amino or N-(4-hydroxyphenyl) phenol is a mild analgesic, antipyretic agent and also a non-steroidal anti-inflammatory drug. Vitamin-C known as L-ascorbic acid is mostly

abundant in citrus foods. Caffeine is the common name for trimethylxanthine or 1,3,7-trimethylxanthine is an active alkaloid component and used for asthma, gallbladder disease, shortness of breath in newborns and low blood pressure [112]. PA and VC are often combined with CA in pharmaceutical formulations to improve the pharmacological value of these preparations. The simultaneous detection of VC, PA and CA is highly desirable due to their coexistence.

From the literature, it is seen that most of the work for the simultaneous detection has been done by modified glassy carbon electrode. In most of the cases glassy carbon is modified by graphene, carbon nano tube and some other reagents which are very costly and the processes are also very difficult. For simultaneous detection ultra-performance liquid chromatography (UPLC) has a great effect. But the UPLC technique is very difficult and it needs very much specialization to make it and use it. Some work have been done by carbon paste electrode but the fabrication of carbon paste electrode strenuous. The carbon paste is made by ionic liquid which is also expensive and rare to purchase. The electrodes have been used such as glassy carbon, diamond etc which are commercial and also expensive. Therefore it is very important to develop a new facile and cheap method capable of determination of medicinal compounds which may applicable to the pharmaceuticals to quantify the formulated tablets of VC, PA and CA individually or in a combined tablet. Waste battery is very cheap and available material that was used in this work. Aspartic acid has choose as the sensing material because, Aspartic acid is a promising material regarding its low cost and availability, high sensitivity and selectivity. The modification process of waste battery electrode with Aspartic acid is easy compared with the carbon paste electrodes. Considering all these facts objectives of this research work are-

i) to prepare a new electrode from waste battery,
ii) to develop APA modified WB, GC, Au, Pt and PG electrodes based on the best sensitivity and detection limit,
iii) to develop a cheap method for separation and determination qualitatively and quantitatively of VC, PA and CA,
iv) to recognize the most favorable condition (such as pH and scan rate) for the separation of VC, PA and CA,
v) to determine the quantity of PA, VC and CA in known sample and tablet samples of some Bangladeshi Pharmaceutical industry.

CHAPTER III

Experimental

Simultaneous detection of vitamin-C (VC), paracetamol (PA) and caffeine (CA) in buffer solution at various pH has been investigated using cyclic voltammetry (CV), Differential pulse voltammetry (DPV) at Waste battery (WB), Glassy carbon (GC), Gold (Au), Platinum (Pt) and Pencil graphite (PG) electrode. The selectivity and sensitivity of electrode reactions have been improved be modifying the electrodes with Aspartic acid. Differential Pulse Voltammetry (DPV) have been employed for the quantitative estimation of VC, PA and CA. Determination of VC, PA and CA in tablet samples using APA modified WB electrode have been compared with the UV-Vis spectroscopic methods. Instrumentation is given details in the following sections and the source of different chemicals, instruments and methods are briefly given below.

3.1 Chemicals

Analytical grade chemicals and solvents have been used in electrochemical synthesis and analytical work. The used chemicals were-

Sl. No.	Chemicals	Molecular formula	Molar mass	Reported purity	Producer
1.	Ascorbic Acid	$C_6H_8O_6$	176.12	99%	Loba Chemie Pvt. Ltd., India
2.	Paracetamol	$C_8H_9NO_2$	151.16	99%	Loba Chemie Pvt. Ltd., India
3.	Caffeine	$C_8H_{10}N_4O_2$	133.10	99%	Qualikem Pvt. Ltd., India
4.	Aspartic Acid	$C_4H_7NO_4$	45.08	99.5%	E-Merck, Germany
6.	Glacial Acetic Acid	CH_3COOH	60.05	99.5%	Loba Chemie Pvt. Ltd., India
7.	Sodium Acetate	$CH_3COONa.3H_2O$	136.08	99%	MerkSpecialities Pvt. Ltd., India

Sl. No.	Chemicals	Molecular formula	Molar mass	Reported purity	Producer
8.	Potasium Chloride	KCl	74.60	99.5%	E-Merck, Germany
9.	Sodium Di hydrogen Orthophosphate	$NaH_2PO_4.2H_2O$	156.01	98-100%	Loba Chemie Pvt. Ltd., India
10.	Di-sodium Hydrogen Orthophosphate	$Na_2HPO_4.2H_2O$	177.99	97-100%	Thermo Fisher Scientific India Pvt. Ltd.
11.	Sodium Hydroxide	NaOH	40.0	97%	E-Merck, Germany
12.	Sodium Bicarbonate	$NaHCO_3$	84.0	99%	E-Merck, Germany

3.2 Equipments

During this research work the following instruments were used-

- The electrochemical studies (CV, DPV) were performed with a computer controlled potentiostats/ galvanostats (µstat 400, Drop Sens, Spain)
- A Pyrex glass micro cell with teflon cap
- Waste battery (WB)/ Pencil graphite (PG) as working electrode
- Commercial Glassy carbon (GC)/ Gold (Au)/ Platinum (Pt) as working electrode (BASi, USA)
- Ag/AgCl as reference electrode (BASi, USA)
- Liquid micro size (0.05µm) polishing alumina (BAS Inc. Japan)
- Pt wire as counter electrode (Local market, Dhaka, Bangladesh)
- A HR 200 electronic balance with an accuracy of ± 0.0001g was used for weighting and
- A pH meter (pH meter, Hanna Instruments, Italy) was employed for maintaining the pH of the solutions.
- The UV-Vis spectroscopic analysis was performed by a computer controlled spectrophotometer (Thermo Scientific, USA).

3.3 Cyclic voltammetry (CV)

There are many well developed electro-analytical techniques are used for the study of electrochemical reactions. Among these we have selected the CV technique to study and analyze the redox reactions occurring at the polarizable electrode surface. This technique provides suitable information to understand the mechanism of electron transfer reaction of the compounds as well as the nature of adsorption of reactants or products on the electrode surface. CV is often the first experiment performed in an electrochemical study. CV consists of imposing an excitation potential nature on an electrode immersed in an unstirred solution and measuring the current and its potential ranges varies from a few millivolts to hundreds of millivolts per second in a cycle. This variation of anodic and cathodic current with imposed potential is termed as voltammogram [113].

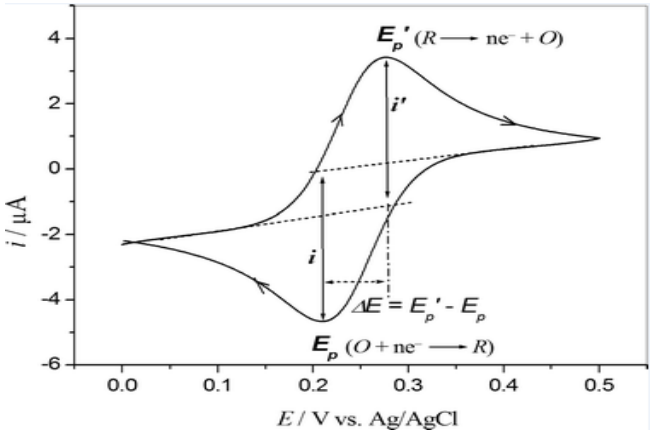

Figure 3.1: The expected response of a reversible redox couple during a single potential cycle

This technique is based on varying the applied potential at a working electrode in both forward and reverse directions while monitoring the current. Simply stated, in the forward scan, the reaction is $O + e^- \rightarrow R$, R is electrochemically generated as indicated by the cathodic current. In the reverse scan, $R \rightarrow O + e^-$, R is oxidized back to O as indicated by the anodic current. The CV is capable of rapidly generating a new species during the forward scan and then probing its fate on the reverse scan. This is a very important aspect of the technique [114].

In CV the current function can be measured as a function of scan rate. The potential of the working electrode is controlled vs a reference electrode such as Ag/AgCl electrode. The

electrode potential is ramped linearly to a more negative potential and then ramped is reversed back to the starting voltage. The forward scan produces a current peak for any analyte that can be reduced through the range of potential scan. The current will increase as the current reaches to the reduction potential of the analyte [115].

The current at the working electrode is monitored as a triangular excitation potential is applied to the electrode. The resulting voltammogram can be analyzed for fundamental information regarding the redox reaction. The potential at the working electrode is controlled vs a reference electrode, Ag/AgCl (standard NaCl) electrode. The excitation signal varies linearly with time. First scan positively and then the potential is scanned in reverse, causing a negative scan back to the original potential to complete the cycle. Signal on multiple cycles can be used on the scan surface. A cyclic voltammogram is plot of response current at working electrode to the applied excitation potential.

3.4 Important features of CV

An electrochemical system containing species 'O' capable of being reversibly reduced to 'R' at the electrode is given by,

$$O + ne^- = R \quad \ldots\ldots\ldots\ldots\ldots\ldots\ldots\ldots 3.1$$

Nernst equation for the system is

$$E = E^0 + \frac{0.059}{n} \log \frac{C_0^s}{C_R^s} \quad \ldots\ldots\ldots\ldots\ldots\ldots\ldots\ldots 3.2$$

Where,

E = Potential applied to the electrode

E^0 = Standard reduction potential of the couple versus reference electrode

n = Number of electrons in Equation (3.1)

C_0^s = Surface concentration of species 'O'

C_R^s = Surface concentration of species 'R'

A redox couple that changes electrons rapidly with the working electrode is termed as electrochemically reverse couple. The relation gives the peak current i_{pc}

$$i_{pc} = 0.4463\ nFA\ (D\alpha)^{1/2}C \quad \ldots\ldots\ldots\ldots\ldots\ldots 3.3$$

$$\alpha = \left(\frac{nFv}{RT}\right) = \left(\frac{nv}{0.026}\right)$$

Where,

i_{pc} = peak current in amperes

F= Faraday`s constant (approximately 96500)

A = Area of the working electrode in cm^2

v= Scan rate in volt/ sec

C= Concentration of the bulk species in mol/L

D= Diffusion coefficient in cm^2 /sec

In terms of adjustable parameters, the peak current is given by the Randless- Sevcik equation,

$$i_{pc} = 2.69\times10^5\times n^{3/2}AD^{1/2}Cv^{1/2} \quad \ldots\ldots\ldots\ldots\ldots\ldots\ldots 3.4$$

The peak potential E_p for reversible process is related to the half wave potential $E_{1/2}$, by the expression,

$$E_{pc} = E_{1/2} - 1.11\left(\frac{RT}{nF}\right), \quad \text{at } 25^0\text{C} \ldots\ldots\ldots\ldots\ldots\ldots 3.5$$

$$E_{pc} = E_{1/2} - \left(\frac{0.0285RT}{n}\right) \ldots\ldots\ldots\ldots\ldots\ldots\ldots\ldots 3.6$$

The relation relates the half wave potential to the standard electrode potential

$$E_{1/2} = E^0 - \frac{RT}{nF}\ln\frac{f_{red}}{f_{ox}}\left(\frac{D_{ox}}{D_{ox}}\right)^{1/2}$$

$$E_{1/2} = E^0 - \frac{RT}{nF}\ln\left(\frac{D_{ox}}{D_{red}}\right)^{1/2} \ldots\ldots\ldots\ldots\ldots\ldots\ldots 3.7$$

Assuming that the activity coefficient f_{ox} and f_{red} are equal for the oxidized and reduced species involved in the electrochemical reaction.

From Equation (3.6), we have,

$$E_{pa} - E_{pc} = 2.22\left(\frac{RT}{nF}\right) \qquad \text{at } 25^0\text{C} \ldots\ldots\ldots\ldots\ldots 3.8$$

$$\text{or } E_{pa} - E_{pc} = \left(\frac{0.059}{n}\right) \qquad \text{at } 25^0\text{C} \ldots\ldots\ldots\ldots\ldots 3.9$$

This is a good criterion for the reversibility of electrode process. The value of i_{pa} should be close for a simple reversible couple,

$$i_{pa}/i_{pc} = 1 \ldots\ldots\ldots\ldots\ldots\ldots\ldots\ldots \quad \ldots 3.10$$

And such a system $E_{1/2}$ can be given by,

$$E_{1/2} = \frac{E_{pa} + E_{pc}}{2} \ldots\ldots\ldots\ldots\ldots\ldots\ldots 3.11$$

For irreversible processes (those with sluggish electron exchange), the individual peaks are reduced in size and widely separated, Totally irreversible systems are characterized by a shift of the peak potential with the scan rate [116];

$$E_p = E^0\text{-}(RT/\alpha n_a F)[0.78\text{-}\ln(k^0/(D)^{1/2}) + \ln(\alpha n_a F\alpha/RT)^{1/2}] \ldots\ldots\ldots 3.12$$

Where α is the transfer coefficient and n_a is the number of electrons involved in the charge transfer step. Thus E_p occurs at potentials higher than E^0, with the over potential related to k^0 (standard rate constant) andα. Independent of the value k^0, such peak displacement can be compensated by an appropriate change of the scan rate. The peak potential and the half-peak potential (at 25^0 C) will differ by 48/ αn mV. Hence, the voltammogram becomes more drawn-out as αn decreases.

The peak current, given by

$$i_p = (2.99\times10^5)n(\alpha n_a)^{1/2}ACD^{1/2}v^{1/2} \ldots\ldots\ldots\ldots 3.13$$

is still proportional to the bulk concentration , but will be lower in height (depending upon the value of α) . Assuming α = 0.5, the ratio of the reversible–to–irreversible current peaks is 1.27 (i.e. the peak current for the irreversible process is about 80% of the peak for a reversible one). For quasi-reversible systems (with $10^{-1}>k^0>10^{-5}$ cm/s) the current is controlled by both the charge transfer and mass transport [117]. The shape of the cyclic voltammogram is a function of the ratio k^0 $(\pi vnFD/RT)^{1/2}$. As the ratio increases, the process approaches the reversible case. For small values of it, the system exhibits an irreversible behavior. Overall, the voltammograms of a quasi-reversible system are more drawn out and exhibit a larger separation in peak potential compared to a reversible system.

Unlike the reversible process in which the current is purely mass transport controlled, currents due to quasi-reversible process are controlled by a mixture of mass transport and charge transfer kinetics [118, 119]. The process occurs when the relative rate of electron transfer with respect to that of mass transport is insufficient to maintain Nernst equilibrium at the electrode surface.

3.5 Pulse methods

The basis of all pulse techniques is the difference in the rate of decay of the charging and the faradaic currents following a potential step (or pulse). The charging current decays considerably faster than the faradaic current. A step in the applied potential or current represents an instantaneous alteration of the electrochemical system. Analysis of the evolution of the system after perturbation permits deductions about electrode reactions and their rates to be made. The potential step is the base of pulse voltammetry. After applying a pulse of potential, the capacitive current dies away faster than the faradic one and the current is measured at the end of the pulse. This type of sampling has the advantage of increased sensitivity and better characteristics for analytical applications. At solid electrodes there is an additional advantage of discrimination against blocking of the electrode reaction by adsorption [120]. Three of these pulse techniques are widely used.

- Normal Pulse Voltammetry (NPV)
- Differential Pulse Voltammetry (DPV)
- Square Wave Voltammetry (SWV)

In this research work differential pulse voltammetry was used for the quantitative determination of VC, PA and CA.

3.6 Differential pulse voltammetry (DPV)

Differential pulse voltammetry (DPV) is a technique in which potential is applied after certain period of time and measures the resulting faradic current as a function of applied potential either in oxidation or reduction. It is designed to minimize background charging currents. The waveform in DPV is a sequence of pulses, where a baseline potential is held for a specified period of time prior to the application of a potential pulse. Current is sampled just prior to the application of the potential pulse. The potential is then stepped by a small amount (typically < 100 mV) and current is sampled again at the end of the pulse. The potential of the working electrode is then stepped back by a lesser value than during the forward pulse such that baseline potential of each pulse is incremented throughout the sequence.

By contrast, in normal pulse voltammetry the current resulting from a series of ever larger potential pulse is compared with the current at a constant 'baseline' voltage. Another type of pulse voltammetry is square wave voltammetry, which can be considered a special type of differential pulse voltammetry in which equal time is spent at the potential of the ramped baseline and potential of the superimposed pulse. The potential wave form for differential pulse voltammetry (DPV) is shown in figure 3.2. The potential wave form consists of small pulses (of constant amplitude) superimposed upon a staircase wave form [121]. Unlike NPV, the current is sampled twice in each pulse Period (once before the pulse, and at the end of the pulse), and the difference between these two current values is recorded and displayed.

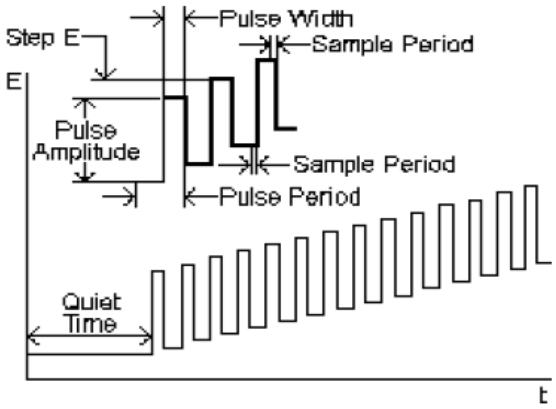

Figure 3.2: Excitation signal and potential wave form for differential pulse voltammetry

The important parameters for pulse techniques are as follows:

- Pulse amplitude is the height of the potential pulse. This may or may not be constant depending upon the technique.
- Pulse width is the duration of the potential pulse.
- Sample period is the time at the end of the pulse during which the current is measured.
- For some pulse techniques, the pulse period or drop time must also be specified. This parameter defines the time required for one potential cycle, and is particularly significant for polarography (i.e., pulse experiments using a mercury drop electrode), where this time corresponds to the lifetime of each drop (i.e., a new drop is dispensed at the start of the drop time, and is knocked off once the current has been measured

at the end of the drop time - note that the end of the drop time coincides with the end of the pulse width).

3.7 Important features of DPV

Differential pulse voltammetry has following important features in this work:

i) Current is sampled just prior to the application of the potential pulse.

ii) DPV help to improve the sensitivity of the detection and the resolution of the voltammogram.

3.8 Computer controlled potentiostats (for CV and DPV experiment)

Potentiostats/ Galvanostats (μStat 400, DropSens, Spain) is the main instrument for voltammetry which has been applied to the desired potential to the electrochemical cell (i.e. between a working electrode and a reference electrode), and a current-to-voltage converter which measures the resulting current and the data acquisition system produces the resulting voltammogram.

Figure 3.3: The computer controlled potentiostat (μStat 400, DropSens)

3.9 Electrochemical cell

An electrochemical cell is a device capable of either generating electrical energy from chemical reactions or facilitating chemical reactions through the introduction of electrical energy [122]. A typical electrochemical cell consists of the sample dissolved in a solvent, an ionic electrolyte, and three (or sometimes two) electrodes (Figure 3.4). These are reference electrode (RE), working electrode (WE), and counter electrode (CE) (also called the secondary or auxiliary electrode). The applied potential is measured against the RE, while the CE closes the electrical circuit for the current to flow. The experiments are performed by a potentiostat that effectively controls the voltage between the RE and WE, while measuring the current through the CE (the WE is connected to the ground). Cells (sample holders) come in a variety of sizes, shapes, and materials. The type used depends on the amount and type of sample, the technique, and the analytical data to be obtained. The material of the cell (glass, Teflon, polyethylene) is selected to minimize reaction with the sample. In this investigation three electrodes electrochemical cell has been used. It has advantages over two electrodes cell because of using 3rd electrode. It reduces the solvent resistance and ensures that no electron transfer through the reference electrode.

Figure 3.4: The three electrode system consisting of a working electrode, a reference electrode and a counter electrode.

3.10 Electrodes

An electrode by definition is a point where current enters and leaves the electrolyte. When the current leaves the electrodes it is known as the cathode and when the current enters it is known as the anode. Electrodes are vital components of electrochemical cells. They transport produced electrons from one half-cell to another, which produce an electrical charge. This charge is based off a standard electrode system (SHE) with a reference potential of 0 volts and serves as a medium for any cell potential calculation [123].

An electrolytic cell consists three types of electrodes. They are-

1. Working electrode (WE)
2. References electrode (RE)
3. Counter electrode (CE)

3.10.1 Working electrode (WE)

The working electrode (WE) represents the most important component of an electrochemical cell. It is at the interface between the WE and the solution that electron transfers of greatest interest occur. The selection of a working electrode material is critical to experimental success. Several important factors should be considered. Firstly, the material should exhibit favorable redox behavior with the analyte, ideally fast, reproducible electron transfer without electrode fouling. Secondly, the potential window over which the electrode performs in a given electrolyte solution should be as wide as possible to allow for the greatest degree of analyte characterization. Additional considerations include the cost of the material, its ability to be machined or formed into useful geometries, the ease of surface renewal following a measurement, and toxicity. The most commonly used working electrode materials are platinum, gold, carbon, and mercury [124]. In this research waste battery electrode (WBE) also made and used as a working electrode (Figure 3.5).

Figure 3.5: WB working electrode

3.10.2 References electrode (RE)

The purpose of the RE is to provide a stable, reproducible voltage to which the WE of an electrochemical cell. Ideally, if a small current is passed through the electrode, the potential change is negligible, and in any case, returns to the initial value when the current ceases. In addition, the potential value should not vary with time and should be reproducible from electrode to electrode. Usually Ag|AgCl electrode used as references electrode. We measure the potential of working electrode with respect the reference electrode. The redox process for this electrode is:

$$AgCl + e^- \Leftrightarrow Ag + Cl^-$$

This electrode consists of a silver wire, coated with silver chloride, which is immersed in a solution containing chloride ions.

3.10.3 Counter electrode (CE)

Modern three and four electrode potentiostats use a feedback circuit to prevent this from happening, but this feedback circuit requires that an additional auxiliary electrode be introduced into the electrochemical cell. This auxiliary (or counter) electrode provides an alternate route for the current to follow, so that only a very small current flows through the reference electrode. The auxiliary electrode can be made from just about any material using any desired electrode geometry. Design choices are usually based on finding a material that is chemically inert in the particular test solution being studied, and it is generally a good idea for the auxiliary electrode to have a large surface area. In most cases, a coil of platinum wire is used, but stainless steel, copper or aluminium wire may work in non- corrosive solutions where metal cation interference is not a concern. If the electrochemical cell is made of metal, then the cell itself might be used as the auxiliary. Because current flows at the auxiliary electrode, electrochemical processes will also occur there. If the working electrode is reducing something, then the auxiliary electrode must oxidize something, and vice versa [125].

3.11 Electrodes used in research

Three types of electrodes are used in this research:

i) Working electrodes are Waste battery (WB), Pencil graphite (PG), Glassy carbon (GC) electrode with 3.0 mm diameter disc, Gold (Au) & Platinum (Pt) electrode with 1.6 mm diameter disc

ii) Ag/AgCl (standard NaCl) electrode used as reference electrode from BASi, USA

iii) Counter electrode is a Pt wire

The working electrode is an electrode on which the reaction of interest is occurring. The reference electrode is a half-cell having a known electrode potential and it keeps the potential between itself and the working electrode. The counter electrode is employed to allow for accurate measurements to be made between the working and reference electrodes.

3.12 Preparation of Waste battery electrode (WBE)

At first the waste battery was collected. Then the outer part of the battery was separated and the inner rod of the battery was removed. The rod was polished by sandpaper for giving a precise electrode shape. Then one part of the new shaped rod was painted by nail polish and end tip of the rod was left free or unpainted for using as electrode surface. Then this end tip was polished by rubbing it on a smooth offset white paper. The resultant end tip of the rod surface would look like a shiny black mirror. Other part of the rod (unpainted part) was used to warp it with a copper wire. The copper wire was used to make the connection with the potentiostat. Steps of making WBE has been shown in figure 3.6.

b

c

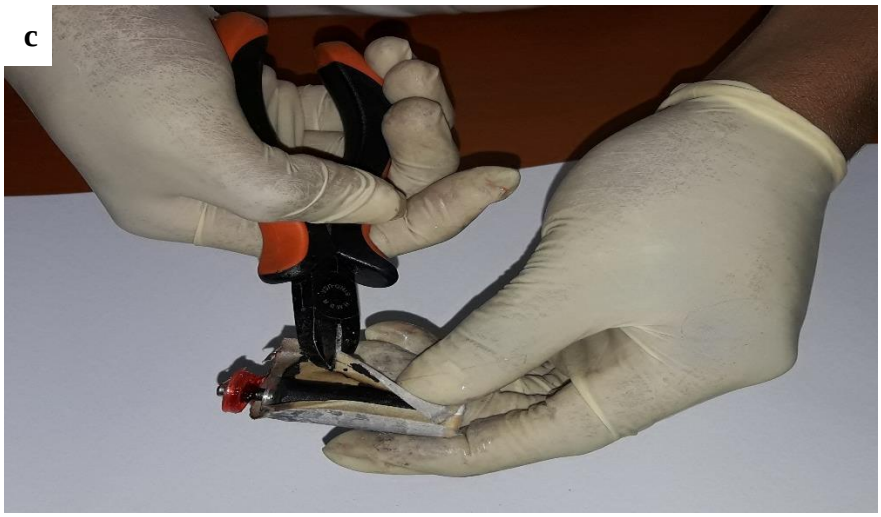

d

e

f

g

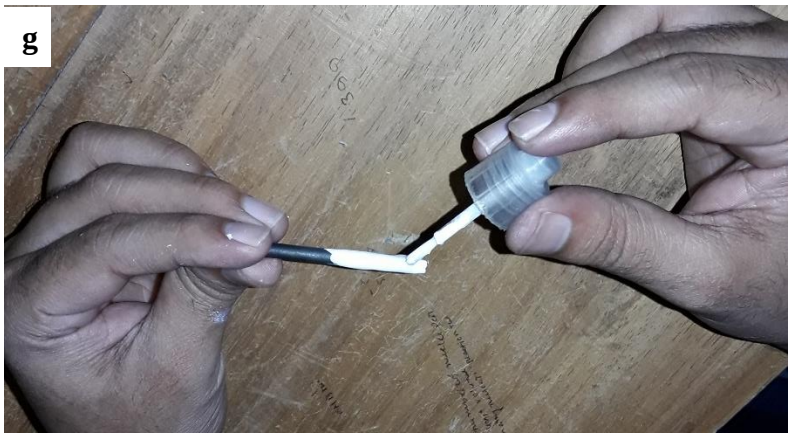

h

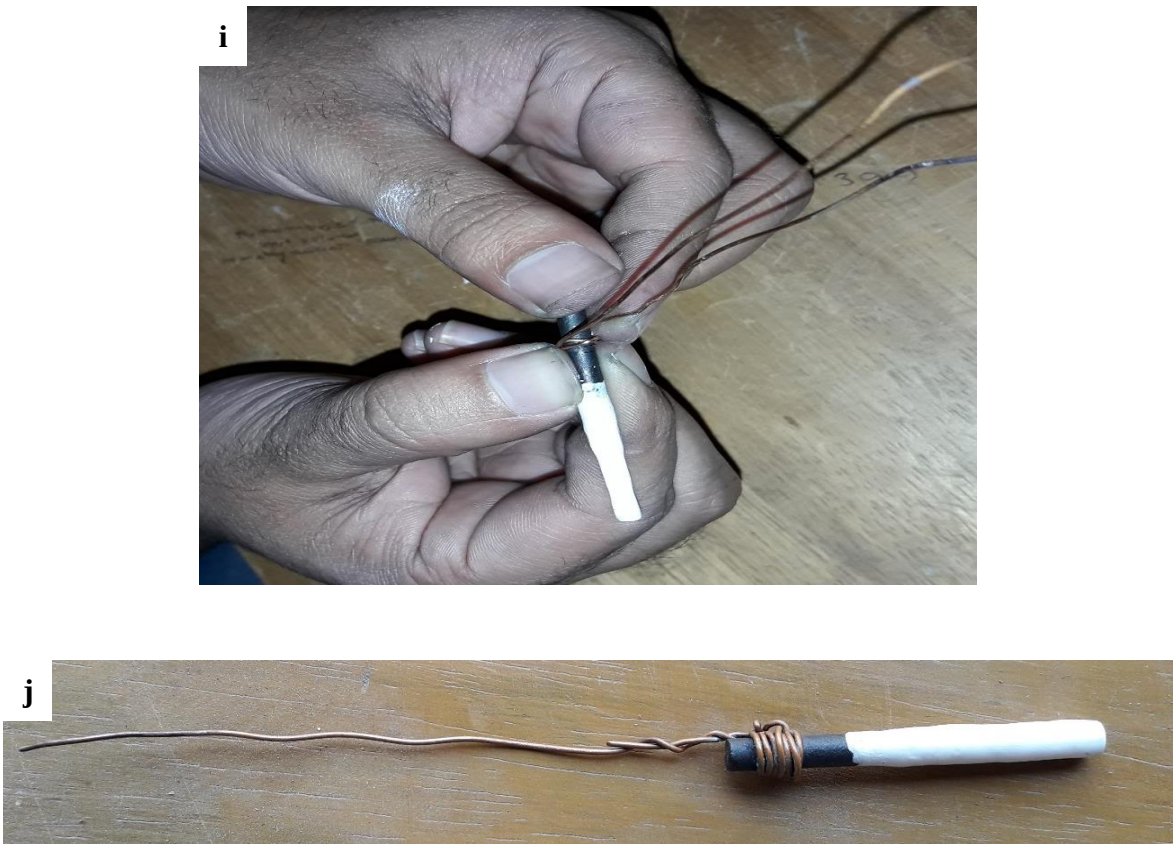

Figure 3.6: Different steps (a, b, c, d, e, f, g, h, i and j) of waste battery electrode (WBE) preparation

3.13 Preparation of modified electrodes

In this study, Waste battery (WB) and Pencil graphite (PG) electrodes are prepared and Glassy carbon (GC), Gold (Au) and Platinum (Pt) electrodes purchase from the BASi, USA are used as working electrode. The electrode was polished with 0.05µm alumina powder on a wet polishing cloth. For doing so a part of the cloth was made wet with deionized water and alumina powder was sprinkled over it. Then the electrode was polished by softly pressing the electrode against the polishing surface at least 10 minutes before modify. But for WB and PG electrode, at first the bare WBE and PGE were polished on a paper then polished with 0.05µm alumina powder on a wet polishing cloth. Then the electrodes were rinsed with distilled water. Aspartic acid (APA) was weighted and kept in phosphate buffer solution (pH 7). Then it was placed on a magnetic stirrer and stirred for 30 minutes at room temperature. After that the electrochemical cell was made ready by connecting electrodes to the computer controlled potentiostate as shown Figure 3.3. Bare electrode was modified with

APA by using Cycling Voltammetry (CV) technique. The potential was cycled for 15 scans at a range of -0.3V to +1.8 and cycled for 10 scans to activate in phosphate buffer solution of pH 7.0. Then the modified electrode was dried by nitrogen gas for 10 minutes. Then a thin layer of APA was appeared on the surface of the electrode.

Bare WB electrode

APA modified WB electrode

Figure 3.7: Bare and APA modified WB electrode

3.14 Supporting electrolyte

The supporting electrolyte is an inert soluble ionic salt added to the solvent; generally in 10-fold or 100-fold excess over the concentration of the species being studied. The inertness meant here is the ability to avoid oxidation or reduction at the indicating or reference electrode during the course of the electrochemical measurements.

There are three functions of the supporting electrolyte. First, it carries most of the ionic current of the cell since its concentration is much larger than that of the other species in solution. Thus it serves to complete the circuit of the electrochemical cell and keep the cell resistance at a low value. Second, it maintains a constant ionic strength. This is necessary because the structure of the inter phase region should not change significantly if a reaction occurs there. A stable structure is created on the electrolyte side by adding a high concentration of an inert salt. Third, migration current observed is reduced by the presence

of large excess of ions that are not electrochemically active at the potentials in use, because they can carry an ionic current without permitting its conversion into electronic, and hence net or measured, current at the electrodes.

3.15 Preparation of buffer solutions

Preparation of different kinds of buffer solution is discussed below:

Acetate Buffer Solution: To prepare acetate buffer (pH 3.0-5.0) solution definite amount of sodium acetate was dissolved in 0.5M acetic acid in a volumetric flask and the pH was measured with pH meter (Figure 3.7). The pH of the buffer solution was adjusted by further addition of acetic acid and / or sodium acetate.

Phosphate Buffer Solution: Phosphate buffer solution (pH 6.0-8.0) was prepared by mixing a solution of 0.5M sodium dihydrogenortho-phosphate ($NaH_2PO_4.2H_2O$) with a solution of 0.5M disodium hydrogen ortho-phosphate ($Na_2HPO_4.2H_2O$). The pH of the prepared solution was measured with pH meter (Figure 3.7).

Bicarbonate Buffer Solution: To prepare hydroxide buffer (pH 9.0-11.0) solution definite amount of sodium hydroxide was dissolved in 0.5M sodium bicarbonate in a volumetric flask. The pH of the prepared solution was measured with pH meter (Figure 3.7).

Figure 3.8: pH meter

3.16 Electrode polishing

Materials may be adsorbed to the surface of a working electrode after each experiment. Then the current response will degrade and the electrode surface needs to clean. In this case, the cleaning required is light polishing with 0.05µm alumina powder. At first the WB electrode is grazed on the paper. Then a few drops of polish are placed on a polishing pad and the electrode is held vertically and the polish rubbed on in a figure-eight pattern for a period of 30 seconds to a few minutes depending upon the condition of the electrode surface. After polishing the electrode surface is rinsed thoroughly with deionized water.

3.17 Preparation of solutions

All standard solutions of VC, PA and CA of different concentrations (1mM to 5mM) were prepared in 50ml 0.5M phosphate buffer solution at pH 7. Tablet samples are dissolved in 50 ml 0.5M PBS (pH 7) with continues stirring by magnetic stirrer.

3.18 Removing dissolved oxygen from solution

Dissolved oxygen can interfere with observed current response so it is needed to remove it. Experimental solution was indolent by purging for at least 5-10 minutes with 99.99% pure and dry nitrogen gas (BOC, Bangladesh). By this way, traces of dissolved oxygen were removed from the solution.

3.19 Experimental procedure

The electrochemical cell filled with solution 50mL of the experimental solution and the Teflon cap was placed on the cell. The working electrode together with reference electrode and counter electrode was inserted through the holes. The electrodes were sufficiently immersed. The solution system is deoxygenated by purging the nitrogen gas for about 10 minutes. The solution has been kept quiet for 10 seconds. After determination the potential window the voltammogram was taken at various scan rates, pH and concentrations from the Drop View Software.

Figure 3.9: Experimental setup (Software controlled Potentiostat (μstat 400))

3.20 UV-Visible Spectrophotometry

In spectrometric analysis a source of radiation is used that extends into the ultraviolet region of the spectrum. The instrument employed for this purpose is a spectrophotometer. An optical spectrometer is an instrument possessing an optical system which can produce dispersion of incident electromagnetic radiation and with which measurements can be made of the quantity of transmitted radiation at selected wavelength of the spectral range. A photometer is a device for measuring the intensity of transmitted radiation. When combined in the spectrophotometer the spectrometer and photometer are employed conjointly to produce a signal corresponding to the difference between the transmitted radiation of a reference material and that of a sample of selected wavelengths.

The essential parts of spectrophotometer are:

1. A source of radiant energy
2. A monochromator
3. Glass or silica cells for holding the solvent and for the solution under test
4. A device to receive of measure the beam or beam of radiant energy passing through the solvent or solution.

Lambert law states that when monochromatic light passes through a transparent medium, the rate of decrease in intensity with the thickness of the medium is proportional to the intensity of light [126]. This is equivalent to stating that the intensity of the emitted light decrease exponentially as the thickness of the absorbing medium increase arithmetically, or that any layer of given thickness of the medium absorbs the same fraction of the light incident upon it.

Beer studied the effect of concentration of the colored constituent in solution upon the light transmission. He found the same relation between transmission and concentration as Lambert had discovered between transmission and thickness of the layer. By combining both of the theories the final expression can be written as,

$$A = \log \frac{I_0}{I_t} = acl$$

Here, I_o = intensity of the incident light; I_t = intensity of the transmitted light; A = Absorbance of the medium; l = dimensions of the cell, c = concentration of the solution.

Figure 3.10: UV-visible spectrophotometer

A computer controlled spectrophotometer (Thermo Scientific, USA) was used for UV-Vis experiment in a pair of quartz cells.

3.21 Standard deviation

In probability and statistics, the standard deviation of a probability distribution, random variable or population or multiset of values is a measure of the spread of its values. It is usually denoted with the letter σ (lower case sigma). It is defined as the square root of the variance.

To understand standard deviation, keep in mind that variance is the average of the squared differences between data points and the mean. Variance is tabulated in units squared. Standard deviation being the square root of that quantity, therefore measures the spread of data about the mean, measured in the same units as the data.

Said more formally, the standard deviation is the root mean square (RMS) deviation of values from their arithmetic mean. For example, in the population {4, 8}, the mean is 6 and the deviations from mean are {-2, 2}. Those deviations squared are {4, 4} the average of which (the variance) is 4. Therefore, the standard deviation is 2. In this case 100% of the values in the population are at one standard deviation of the mean.

The standard deviation is the most common measure of statistical dispersion, measuring how widely spread the values in a data set are. If the data points are close to the mean, then the standard deviation is small. As well, if many data points are far from the mean, then the standard deviation is large. If all the data values are equal, then the standard deviation is zero [127].

3.22 Recovery percentage

Recovery percentage is an indication of a measurement that indicates the accuracy of a measurement or quantitative determination. The percentage of the recovered amount with response to amount taken is termed as recovery percentage as below-

$$\%\ of\ Recovery = \frac{amount\ found}{total\ amount\ taken} \times 100$$

CHAPTER IV

Results and Discussion

Cyclic voltammetry (CV) and differential pulse voltammetry (DPV) techniques were used to investigate the electrochemical behavior of Vitamin-C (VC), Paracetamol (PA) and Caffeine (CA) in presence of buffer solution by using bare and modified Waste battery (WB), Glassy carbon (GC), Gold (Au), Platinum (Pt) and Pencil graphite (PG) electrodes. In concordance with the experiment we have abstracted precious information considering electrochemical oxidations of VC, PA and CA which has been disputed elaborately in following section. DPV and UV-Vis spectroscopy were used to all quantitative estimation of VC, PA and CA in this work.

4.1 Electrochemical behavior of VC, PA and CA at bare electrodes

4.1.1 Electrochemical behavior of VC, PA and CA at bare WB electrode

Cyclic voltammogram (CV) of the ternary solution of VC, PA and CA at bare WB electrode in Phosphate buffer solution (PBS) (pH 7) is shown in Fig. 4.1. It shows two anodic peaks at 0.51 V and 1.48 V at 0.1 V/s. It indicates that the bare WB electrode is unable to separate the individual oxidation peaks of VC, PA and CA by using cyclic voltammetry technique.

Differential pulse voltammogram (DPV) of the ternary solution of VC, PA and CA at bare WB electrode in PBS (pH 7) is shown in Fig. 4.2. It shows two peaks at 0.48 V and 1.44 V where three electroactive compounds present in the solution. It also indicates that the bare WB electrode is unable to separate the individual oxidation peaks of VC, PA and CA by using differential pulse voltammetry technique.

4.1.2 Electrochemical behavior of VC, PA and CA at bare GC electrode

Cyclic voltammogram (CV) of the ternary solution of VC, PA and CA at bare GC electrode in Phosphate buffer solution (PBS) (pH 7) is shown in Fig. 4.3. It shows two anodic peaks at 0.53 V and 1.53 V at 0.1 V/s. It indicates that the bare GC electrode is unable to separate the individual oxidation peaks of VC, PA and CA by using cyclic voltammetry technique.

Differential pulse voltammogram (DPV) of the ternary solution of VC, PA and CA at bare GC electrode in PBS (pH 7) is shown in Fig. 4.4. It shows two peaks at 0.50 V and 1.44 V where three electroactive compounds present in the solution. It also indicates that the bare GC electrode is unable to separate the individual oxidation peaks of VC, PA and CA by using differential pulse voltammetry technique.

4.1.3 Electrochemical behavior of VC, PA and CA at bare Au electrode

Cyclic voltammogram (CV) of the ternary solution of VC, PA and CA at bare Au electrode in Phosphate buffer solution (PBS) (pH 7) is shown in Fig. 4.5. It shows two anodic peaks at 0.63 V and 1.47 V at 0.1 V/s. It also indicates that the bare Au electrode is unable to separate the individual oxidation peaks of VC, PA and CA by using cyclic voltammetry technique.

Differential pulse voltammogram (DPV) of the ternary solution of VC, PA and CA at bare Au electrode in PBS (pH 7) is shown in Fig. 4.6. It shows two peaks at 0.51 V and 1.44 V where three electroactive compounds present in the solution. It also indicates that the bare Au electrode is unable to separate the individual oxidation peaks of VC, PA and CA by using differential pulse voltammetry technique.

4.1.4 Electrochemical behavior of VC, PA and CA at bare Pt electrode

Cyclic voltammogram (CV) of the ternary solution of VC, PA and CA at bare Pt electrode in Phosphate buffer solution (PBS) (pH 7) is shown in Fig. 4.7. It shows two anodic peaks at 0.54 V and 1.44 V at 0.1V/s. It indicates that the bare Pt electrode is unable to separate the individual oxidation peaks of VC, PA and CA by using cyclic voltammetry technique.

Differential pulse voltammogram (DPV) of the ternary solution of VC, PA and CA at bare Pt electrode in PBS (pH 7) is shown in Fig. 4.8. It shows two peaks at 0.50 V and 1.44 V where three electroactive compounds present in the solution. It also indicates that the bare Pt electrode is unable to separate the individual oxidation peaks of VC, PA and CA by using differential pulse voltammetry technique.

4.1.5 Electrochemical behavior of VC, PA and CA at bare PG electrode

Cyclic voltammogram (CV) of the ternary solution of VC, PA and CA at bare PG electrode in Phosphate buffer solution (PBS) (pH 7) is shown in Fig. 4.9. It shows two anodic peaks at 0.54 V and 1.46 V at 0.1V/s. It indicates that the bare PG electrode is unable to separate the individual oxidation peaks of VC, PA and CA by using cyclic voltammetry technique.

Differential pulse voltammogram (DPV) of the ternary solution of VC, PA and CA at bare PG electrode in PBS (pH 7) is shown in Fig. 4.10. It shows two peaks at 0.51 V and 1.45 V where three electroactive compounds present in the solution. It also indicates that the bare PG electrode is unable to separate the individual oxidation peaks of VC, PA and CA by using differential pulse voltammetry technique.

From the observations of the electrochemical behavior of VC, PA and CA ternary solution it is clear that the bare electrodes (WB, GC, Au, Pt and PG) are unable to separate the individual oxidation peaks of VC, PA and CA. Simultaneous determination of these three compounds is not possible at bare electrodes by using any of the CV or DPV techniques.

4.2 Modification of WB electrode with Aspartic acid (APA)

In order to get response from VC, PA and CA in a mixture and to improve the selectivity and sensitivity of WB electrode, it was modified with APA solution prepared in PBS of pH 7.0.

Fig. 4.11 displays the continuous CVs of APA thin film formation onto a bare WB in APA solution over the potential range of – 0.3 V to + 1.8 V for 15 cycles at a scan rate of 0.2 V/s. Aspartic acid contains an amino group and one-electron oxidation of the amino group turns

into its corresponding cation radical, and these cation radicals can form carbon–nitrogen links at the carbon electrode surface. The oxidation peak currents decrease quickly with successive scanning until the fifteen cycles. This is attributed to passivation of the WBE, which is related to grafting of the aspartic acid on the surface of WBE. The modification process was almost complete after fifteen cycles. As a primary amine, the electrochemical behavior of aspartic acid is in agreement with the literature [130]. Accordingly, we have proposed the EC-modification process illustrated in Scheme 1.

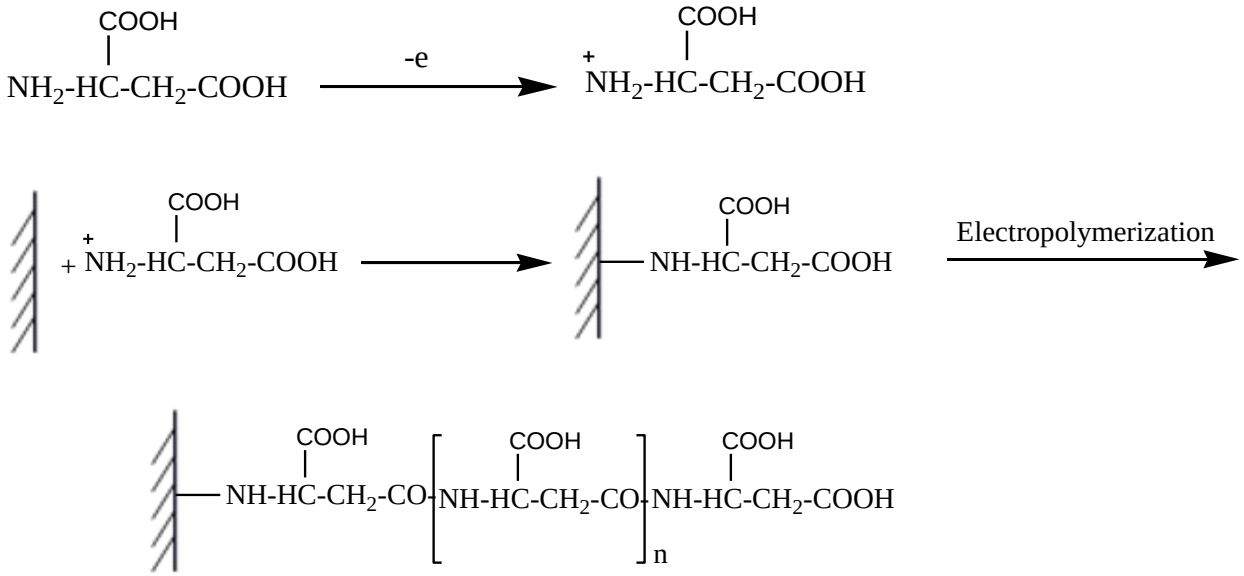

Scheme 1: The modification process of aspartic acid on WBE

4.3 Electrochemical behavior of VC, PA and CA at Aspartic acid (APA) modified different electrodes

4.3.1 Electrochemical behavior of VC, PA and CA at Aspartic acid (APA) modified WB electrode

Cyclic voltammogram (CV) of the ternary solution of VC, PA and CA at APA modified WB electrode in phosphate buffer solution (PBS) (pH 7) is shown in Fig. 4.12. From this voltammogram, it can be seen that three different anodic peaks at 0.24 V for VC, 0.44 V for PA and 1.4 V for CA at 0.1V/s. It indicates that the APA modified WB electrode is enable to separate the individual oxidation peaks of VC, PA and CA by using cyclic voltammetry technique. An electrochemically modified electrode is less prone to surface fouling compared to a bare electrode. It also reduces the overvoltage and overcomes the slow

kinetics of many electrode processes, thus facilitating the redox process of the compounds, which generally results in increased selectivity and sensitivity of determinations [128]. In this point of view, APA enhance the selectivity of WB electrode and gives three separated peaks of VC, PA and CA with good sensitivity compared to the bare electrode.

DPV of the ternary solution of VC, PA and CA at APA modified WB electrode in phosphate buffer solution (PBS) (pH 7) is shown in Fig. 4.13. From this voltammogram, it can be seen that three different anodic peaks at 0.2 V for VC, 0.42 V for PA and 1.4 V for CA at 0.1V/s. It also indicates that the APA modified WB electrode is enable to separate the individual oxidation peaks of VC, PA and CA by using DPV technique.

4.3.2 Electrochemical behavior of VC, PA and CA at Aspartic acid (APA) modified GC electrode

Cyclic voltammogram (CV) of the ternary solution of VC, PA and CA at APA modified GC electrode in Phosphate buffer solution (PBS) (pH 7) is shown in Fig. 4.14. From this CV, it can be seen that there are three different anodic peaks at 0.22 V for VC, 0.42 V for PA and 1.42 V for CA at 0.1V/s. It indicates that the APA modified GC electrode is enable to separate the individual oxidation peaks of VC, PA and CA by using cyclic voltammetry technique. An electrochemically modified electrode is less prone to surface fouling compared to a bare electrode. It also reduces the overvoltage and overcomes the slow kinetics of many electrode processes, thus facilitating the redox process of the compounds, which generally results in increased selectivity and sensitivity of determinations. In this point of view, APA enhance the selectivity of GC electrode and gives three separated peaks of VC, PA and CA with good sensitivity compared to the bare electrode.

DPV of the ternary solution of VC, PA and CA at APA modified GC electrode in Phosphate buffer solution (PBS) (pH 7) is shown in Fig. 4.15. From this DPV, it can be seen that there are three different anodic peaks at 0.22 V for VC, 0.42 V for PA and 1.42 V for CA at 0.1V/s. It also indicates that the APA modified GC electrode is enable to separate the individual oxidation peaks of VC, PA and CA by using DPV technique.

4.3.3 Electrochemical behavior of VC, PA and CA at Aspartic acid (APA) modified Au electrode

Cyclic voltammogram (CV) of the ternary solution of VC, PA and CA at APA modified Au electrode in phosphate buffer solution (PBS) (pH 7) is shown in Fig. 4.16. From this CV, it can be seen that there are three different anodic peaks at 0.28 V for VC, 0.56 V for PA and 1.46 V for CA at 0.1V/s. It indicates that the APA modified Au electrode is enable to separate the individual oxidation peaks of VC, PA and CA by using Cyclic voltammetry technique.

DPV of the ternary solution of VC, PA and CA at APA modified Au electrode in Phosphate buffer solution (PBS) (pH 7) is shown in Fig. 4.17. From this CV, it can be seen that there are three different anodic peaks at 0.26 V for VC, 0.5 V for PA and 1.46 V for CA at 0.1V/s. It also indicates that the APA modified Au electrode is enable to separate the individual oxidation peaks of VC, PA and CA by using DPV technique.

4.3.4 Electrochemical behavior of VC, PA and CA at Aspartic acid (APA) modified Pt electrode

Cyclic voltammogram (CV) of the ternary solution of VC, PA and CA at APA modified Pt electrode in phosphate buffer solution (PBS) (pH 7) is shown in Fig. 4.18. It shows three different anodic peaks at 0.20 V for VC, 0.56 V for PA and 1.44 V for CA at 0.1V/s. It indicates that the APA modified Pt electrode is enable to separate the individual oxidation peaks of VC, PA and CA by using Cyclic voltammetry technique.

DPV of the ternary solution of VC, PA and CA at APA modified Pt electrode in phosphate buffer solution (PBS) (pH 7) is shown in Fig. 4.19. It shows three different anodic peaks at 0.2 V for VC, 0.5 V for PA and 1.44 V for CA at 0.1V/s. It also indicates that the APA modified Pt electrode is enable to separate the individual oxidation peaks of VC, PA and CA by using DPV technique.

4.3.5 Electrochemical behavior of VC, PA and CA at Aspartic acid (APA) modified PG electrode

Cyclic voltammogram (CV) of the ternary solution of VC, PA and CA at APA modified PG electrode in phosphate buffer solution (PBS) (pH 7) is shown in Fig. 4.20. It shows two anodic peaks at 0.22 V and 0.50 V at 0.1V/s. It indicates that the APA modified PG electrode is unable to separate the individual oxidation peaks of VC, PA and CA by using cyclic voltammetry technique. This indicates that APA may not deposit on the surface of PG electrode. The oxidation peak of VC is very small and is much closed and for CA the peak is not well defined.

DPV of the ternary solution of VC, PA and CA at APA modified PG electrode in phosphate buffer solution (PBS) (pH 7) is shown in Fig. 4.21. It shows three different anodic peaks at 0.20 V for VC, 0.42 V for PA and 1.4 V for CA at 0.1V/s. It indicates that the APA modified PG electrode is enable to separate the individual oxidation peaks of VC, PA and CA by using DPV technique. But, the sensitivity is very low for the oxidation peaks of VC, PA and CA. This means that the APA was not deposited at the surface of PG electrode or the oxidation of VC, PA and CA at the surface of PG electrode is not so good.

4.4 Electrode selection

After analyzing CVs and DPVs for the electrochemical behavior of VC+PA+CA at APA modified WB, GC, Au, Pt and PG electrodes (Fig. 4.22 and Fig. 4.23) it is clear that the separation of the oxidation peaks as well as peak current of VC, PA and CA at APA modified WB and GC electrode are prominent than that of Au, Pt and PG electrodes. GC is a commercial electrode and is very expensive whereas WB electrode is very cheap. For this concern, APA modified WB electrode was selected to analysis the electrochemical behavior and quantitative determination of VC, PA and CA.

4.5 pH study

Fig. 4.24 shows the cyclic voltammograms of the ternary mixture of VC, PA and CA in different buffer solutions (pH 3, 5, 7 and 9). Fig. 4.25 shows the plots of peak currents vs pH. Table 4.1 shows that VC, PA and CA have the maximum peak current at pH 7. For this pH 7 was selected for the detection of VC, PA and CA in a ternary mixture.

4.6 Electrochemical Study of VC, PA and CA at bare WB electrode

4.6.1 Cyclic voltammetric behavior of Vitamin-C (VC) at bare WB electrode

Cyclic voltammogram of 5 mM VC in 0.5 M PBS (pH 7) and only 0.5 M PBS (pH 7) is shown in Fig. 4.26. The voltammogram of only 0.5 M PBS (black line) shows no oxidation peak at bare WB electrode. 5 mM VC in 0.5 M PBS (pH 7) (green line) shows one oxidation peak at 0.27 V and peak current is 83 µA. CV of VC in PBS does not show any cathodic peak at bare WB electrode.

4.6.2 Cyclic voltammetric behavior of PA at bare WB electrode

Cyclic voltammogram of 5 mM PA in 0.5 M PBS (pH 7) and only 0.5 M PBS (pH 7) is shown in Fig. 4.27. The voltammogram of only PBS (black line) shows no oxidation peak at bare WB electrode. PA of 5 mM in 0.5 M PBS (pH 7) (red line) shows one oxidation peak at 0.51 V and peak current is 155 µA. CV of 5 mM PA in PBS shows one small cathodic peak at -0.05 V (compared to the anodic peak) at bare WB electrode. This indicates that the redox process of PA at bare WB electrode is a quasi-reversible redox process.

4.6.3 Cyclic voltammetric behavior of Caffeine (CA) at bare WB electrode

Cyclic voltammogram of 5 mM CA in 0.5 M PBS (pH 7) and only PBS (pH 7) is shown in Fig. 4.28. The voltammogram of only PBS (black line) shows no oxidation peak at bare WB electrode. 5 mM CA in 0.5 M PBS (pH 7) (blue line) shows one oxidation peak at 1.44 V and peak current is 296 µA. CV of CA in PBS does not show any cathodic peak at bare WB electrode.

4.6.4 Simultaneous detection of VC and PA at bare WB electrode using cyclic voltammetric technique

CV of 5 mM VC and 5 mM PA was taken for the simultaneous detection at bare WB electrode. The peaks of 5 mM VC and 5 mM PA was overlapped in the simultaneous voltammogram (Fig. 4.29).

VC in PBS gives one anodic peak at + 0.27 V. On the other hand PA in PBS gives anodic and cathodic peaks at + 0.51 V and - 0.05 V respectively. The binary mixture of VC and PA shows a single anodic peak at + 0.50 V which is at high potential than the peaks for individual VC and PA. No cathodic peak observed for the binary mixture of VC and PA at bare WB electrode. The anodic peaks in the binary mixture are the combined peak of both of the species which is due to the fouling effect. As both compounds are oxidized at a close potential their combined solution gives response as if a solution of double concentration. Bare WB electrode does not give separate peaks for simultaneous detection of VC and PA in their binary solution.

4.6.5 Simultaneous detection of PA and CA at bare WB electrode using cyclic voltammetric technique

CV of 5 mM PA and 5 mM CA was taken for the simultaneous detection at bare WB electrode. CV shows two anodic peaks at 0.51 V and 1.44 V. This indicates that the oxidation of PA and CA have a significant potential difference (Fig.4.30). From the individual CVs we can see that the oxidation peak at 0.51 V appeared for PA and 1.44 V is for CA. Simultaneous determination of PA and CA at bare WB electrode is possible but at APA modified WB electrode, they show a significant increase of current that is very important to determine the amount of PA and CA in a low concentration sample.

4.6.6 Simultaneous detection of VC and CA at bare WB electrode using cyclic voltammetric technique

CV of 5 mM PA and 5 mM CA was taken for the simultaneous detection at bare WB electrode. CV shows two anodic peaks at 0.26 V and 1.44 V. This indicates that the oxidation of VC and CA have a significant potential difference (Fig. 4.31). From the individual CVs we can see that the peak at 0.26 V is for VC and at 1.44 V is for CA. Simultaneous determination of VC and CA at bare WB electrode is possible but at APA modified WB electrode they show a significant increase of current that is very important to determine the amount of VC and CA in a low concentration sample.

4.6.7 Simultaneous determination of VC, PA and CA at bare WB electrode using cyclic voltammetric technique

VC in PBS gives one anodic peak at + 0.27 V, PA in PBS gives one anodic and one cathodic peaks at + 0.51 V and - 0.05 V respectively and CA in PBS gives one anodic peak at 1.44 V. Ternary mixture of VC, PA and CA in PBS, two anodic peak was found at + 0.52 V and 1.46 V which is at high potential than the oxidation potential of VC, PA and CA. No cathodic peak observed for the ternary mixture of VC, PA and CA at bare WB electrode (Fig. 4.32). The anodic peaks of VC and PA in the ternary mixture are the combined peak of both of the species which is due to the fouling effect where CA gives an individual peak for the difference of oxidation potential compared to VC and PA. VC and PA are oxidized at a close potential, their combined solution gives response as if a solution of double concentration. Bare WB electrode does not give separate peaks for simultaneous detection of VC, PA and CA in their ternary solution.

4.7 Cyclic voltammetric behavior of APA solution at modified WB electrode

Cyclic voltammogram of APA solution at modified WB electrode is shown in Fig. 4.33. APA in PBS solution shows no anodic or cathodic peak in the measurement potential of VC, PA and CA within - 0.3 V to + 1.8 V. It indicates that the deposited APA film on WB electrode surface just enhance the signals of analytes without interfering with their oxidation potential and sensitivity.

4.8 Cyclic voltammetric behavior of VC at APA modified WB electrode

Cyclic voltammogram of 5 mM VC in PBS (pH 7) solution and only PBS at APA modified WB electrode is shown in Fig. 4.34. There is no peak for only PBS but a sharp and well defined peak is observed for VC in PBS solution at 0.18 V.

The oxidation peak of VC is shifted to less positive potential (E_{pa} = 0.18 V) at the APA modified WBE, because of a kinetic effect, and thus a substantial increase in the rate of electron transfer from VC is observed [130]. The electrochemical oxidation reaction of VC at APA modified WBE is shown in scheme 2.

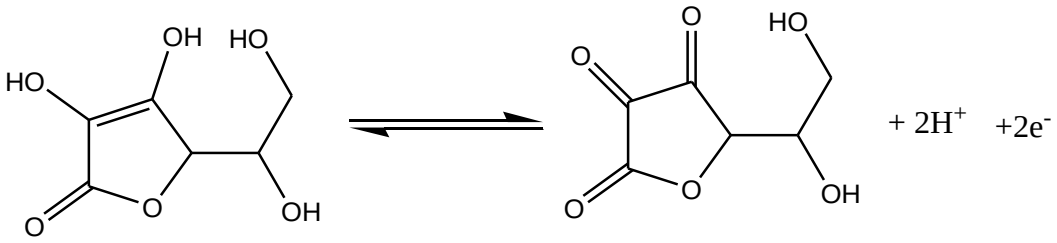

Vitamin C

Scheme 2: Electrochemical oxidation reaction of VC at APA modified WBE

4.8.1 Comparison of the CV of VC in PBS at bare and APA modified WB electrode

Fig. 4.35 shows the comparison between the behaviors of VC at bare and APA modified WB electrode. At bare WB electrode VC gives an anodic peak at 0.27 V having peak current 83 µA. But, at APA modified WB electrode VC gives an anodic peak at 0.18 V having peak current 117 µA. It is clear that the anodic peak of VC at APA modified WB electrode is sharper and well defined than that of bare WB electrode. The position of the anodic peak of VC at APA modified WB electrode is shifted significantly and the currents are prominent than that of bare WB electrode.

4.8.2 Scan rate effect of VC in PBS at APA modified WB electrode

The CVs of 5 mM VC in PBS (pH 7) at APA modified WB electrode at different scan rates is shown in Fig. 4.36. The current potential data, peak potential separation, peak currents are represented in table 4.2.

From table 4.2 it is clear that the peak current of VC is gradually increased with the increased of scan rate. The peak current of VC increased with the increased of square root of scan rate ($v^{1/2}s^{-1/2}$) (Fig. 4.37), the corresponding trend line is a straight line which passes through the origin indicates that the oxidation process of VC is a diffusion controlled process [129].

4.8.3 Cyclic voltammetric behavior of PA in PBS at APA modified WB electrode

Cyclic voltammogram of 5 mM PA in PBS (pH 7) solution and only PBS at APA modified WB electrode is shown in Fig. 4.38. There is no peak for PBS but a sharp and well defined anodic and cathodic peak is observed for PA at 0.42 V and 0.24 V.

The oxidation peak of PA is shifted at slightly higher positive potential (E_{pa} = 0.42 V) at the APA modified WBE, and thus a substantial increase in the rate of electron transfer from PA is observed. This is attributed to the improved reversibility of the electron-transfer processes [131]. The electrochemical oxidation reaction of PA at APA modified WBE is shown in scheme 3.

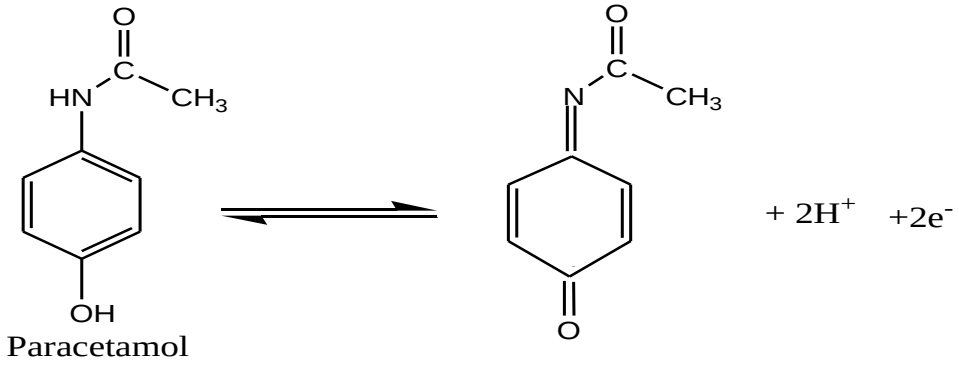

Scheme 3: Electrochemical oxidation reaction of PA at APA modified WBE

4.8.4 Comparison of the CV of PA in PBS at bare and APA modified WB electrode

Fig. 4.39 shows the comparison between the behaviors of PA at bare and APA modified WB electrode. At bare WB electrode PA gives an anodic and a cathodic peak at 0.51 V and -0.05 V having peak current 155 µA and 46 µA. But, at APA modified WB electrode, PA gives an anodic peak at 0.42 V having peak current 222 µA and a cathodic peak at 0.24 V having peak current 110 µA. It is clear that the anodic and cathodic peak of PA at APA modified WB electrode is sharper and well defined than that of bare WB electrode. The position of the anodic peak of PA at APA modified WB electrode is shifted significantly and the currents are prominent than that of bare WB electrode.

4.8.5 Scan rate effect of PA in PBS at APA modified WB electrode

The CVs of 5 mM PA in PBS (pH 7) at APA modified WB electrode at different scan rates is shown in Fig. 4.40. The current potential data, peak potential separation, peak currents are represented in Table 4.3.

From table 4.3 it is clear that the anodic and cathodic peak currents of PA is gradually increased with the increased of scan rate. The peak current of PA increased with the

increased of square root of scan rate ($v^{1/2}s^{-1/2}$) (Fig. 4.41), the corresponding trend lines are straight lines and they are not pass through the origin indicates that the redox process of PA is an impurely diffusion controlled process [129].

4.8.6 Cyclic voltammetric behavior of CA in PBS at APA modified WB electrode

Cyclic voltammogram of 5 mM CA in PBS (pH 7) solution and only PBS at APA modified WB electrode is shown in Fig. 4.42. There is no peak for PBS but a sharp and well defined peak is observed for CA at 1.42 V.

The oxidation peak of CA is shifted at higher positive potential (E_{pa} = 1.42 V) at the APA modified WBE. The oxidation reaction of CA is the two electron transfer process which matches the cyclic voltammetric behavior of CA [132]. The electrochemical oxidation reaction of CA at APA modified WBE is shown in scheme 4.

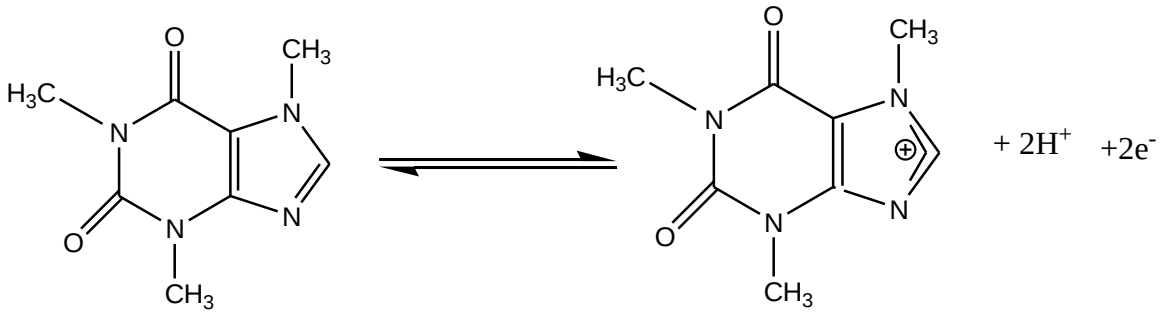

Caffeine

Scheme 4: Electrochemical oxidation reaction of CA at APA modified WBE

4.8.7 Comparison of the CV of CA in PBS at bare and APA modified WB electrode

Fig. 4.43 shows the comparison between the behaviors of CA at bare and APA modified WB electrode. At bare WB electrode CA gives an anodic peak at 1.44 V having peak current 296 µA. But, at APA modified WB electrode CA gives an anodic peak at 1.41 V having peak current 369 µA. It is clear that the anodic peak of CA at APA modified WB electrode is sharper and well defined than that of bare WB electrode. The position of the anodic peak of CA at APA modified WB electrode is shifted slightly but the currents are prominent than that of bare WB electrode.

4.8.8 Scan rate effect of CA in PBS at APA modified WB electrode

The CVs of 5 mM VC in PBS (pH 7) at APA modified WB electrode at different scan rates is shown in Fig. 4.44. The current potential data, peak potential separation, peak currents are represented in Table 4.4.

From table 4.4 it is clear that the peak current of CA is gradually increased with the increased of scan rate. The peak current of CA increased with the increased of square root of scan rate ($v^{1/2}s^{-1/2}$) (Fig. 4.45), the corresponding trend line is a straight line which is not passed through the origin indicates that the oxidation process of CA is an impurely diffusion controlled process [129].

4.9 Simultaneous detection of VC, PA and CA at APA modified WB electrode using CV

4.9.1 Simultaneous detection of VC and PA at APA modified WB electrode using CV

CV of a binary mixture (5 mM) of VC and PA in PBS at bare WB and APA modified WB electrode is shown in Fig.4.46. The CVs of VC, PA and the binary mixture (5 mM) of VC and PA in PBS at APA modified WB electrode is shown in Fig.4.47. For the mixture of VC and PA, there only one peak was observed at + 0.51 V at bare WB electrode. At APA modified WB electrode, VC and PA gives two anodic peaks + 0.18 V and + 0.42 V respectively, and one cathodic peak at + 0.24 V. From the positions of the anodic and cathodic peaks it can be explained that the peaks of both VC and PA are separated at APA modified WB electrode. The APA modified WB electrode can separate the peaks of VC and PA when they are present in a mixture.

4.9.2 Simultaneous detection of PA and CA at APA modified WB electrode using CV

CV of a binary mixture (5 mM) of PA and CA in PBS both at bare WB and APA modified WB electrode is shown in Fig. 4.48. The CVs of PA, CA and their binary mixture (5 mM) in PBS at APA modified WB electrode is shown in Fig. 4.49. At APA modified WB electrode PA and CA shows two anodic peaks at + 0.42 V and + 1.41 V respectively. The peak currents of PA and CA are 207 µA and 365 µA. Binary mixture of PA and CA shows two peaks at + 0.51 V and + 1.45 V at bare WB electrode for their difference of oxidation

potential. The peak currents of PA and CA were 155 µA and 296 µA at bare WB electrode. From the positions and currents of the peaks it can be explained that the peaks of both PA and CA are sharp and well defined at APA modified WB electrode having peak current prominent than that of bare WB electrode. So APA modified WB electrode can determine the amount of PA and CA accurately compared to bare WB electrode.

4.9.3 Simultaneous detection of VC and CA at APA modified WB electrode using CV

CV of a binary mixture (5 mM) of VC and CA in PBS at bare WB and APA modified WB electrode is shown in Fig. 4.50. The CVs of VC, CA and their binary mixture (5 mM) in PBS at APA modified WB electrode is shown in Fig. 4.51. At APA modified WB electrode the binary mixture of VC and CA shows two anodic peaks + 0.18 V and + 1.42 V respectively. The peak currents of VC and CA are 117 µA and 369 µA. Binary of VC and CA shows two oxidation peaks at + 0.27 V and + 1.44 V at bare WB electrode for their difference of oxidation potential. The peak currents of VC and CA were 83 µA and 296 µA respectively at bare WB electrode. From the positions and currents of the peaks it can be explained that the peaks of both VC and CA are sharp and well defined at APA modified WB electrode having peak current prominent than that of bare WB electrode. So APA modified WB electrode can determine the amount of VC and CA accurately compared to bare WB electrode.

4.9.4 Simultaneous detection VC, PA and CA ternary solution in PBS at APA modified WB electrode using CV

CV of a ternary mixture (5 mM) of VC, PA and CA in PBS both at bare WB and APA modified WB electrode is shown in Fig. 4.52. The CVs of VC, PA and CA and their ternary mixture (5mM) at APA modified WB electrode is shown in Fig. 4.53. At APA modified WB electrode ternary mixture of VC, PA and CA shows three anodic peaks + 0.18 V, + 0.42 and + 1.42V respectively. The peak current of VC, PA and CA are 117 µA, 222 µA and 369 µA. For the mixture of VC, PA and CA, two peaks were observed at + 0.51 V and + 1.44 V respectively at bare WB electrode. In fig. 4.53, the positions and currents of the peaks indicates that the APA modified WB electrode can separate the peaks with good sensitivity

compared to the bare WB electrode. So, APA modified WB electrode can be used to simultaneous detection of VC, PA and CA in a ternary mixture.

4.10 Simultaneous detection of VC, PA and CA at APA modified WB electrode using differential pulse voltammetric (DPV) technique

4.10.1 Simultaneous detection of VC and PA in PBS at APA modified WB electrode using DPV

DPVs of a binary mixture (5 mM) of VC and PA in PBS at bare WB and APA modified WB electrode is shown in Fig. 4.54. The DPVs of VC, PA and their binary mixture (5 mM) in PBS at APA modified WB electrode is shown in Fig. 4.55. Binary mixture of VC and PA in PBS shows two anodic peaks at + 0.18 V and + 0.42 V respectively. For the mixture of VC and PA, there only one peak was observed at + 0.50 V that was the overlapped peak of both VC and PA at bare WB electrode. In fig. 4.55, the positions of the anodic peaks indicates that the peaks of both VC and PA are separated at APA modified WB electrode. The APA modified WB electrode can separate the peaks of VC and PA when they are present in a mixture using DPV technique.

4.10.2 Simultaneous detection of PA and CA in PBS at APA modified WB electrode using DPV

DPVs of a binary mixture (5 mM) of PA and CA in PBS at bare WB and APA modified WB electrode in shown in Fig. 4.56. The DPVs of PA, CA and their binary mixture (5 mM) in PBS at APA modified WB electrode is shown in Fig. 4.57. At APA modified WB electrode, binary mixture of PA and CA in PBS shows two anodic peaks + 0.42 V and + 1.41 V respectively. The peak currents of PA and CA are 130 µA and 127 µA at APA modified WB electrode. From the positions and currents of the peaks (Fig. 4.57) it can be explained that the peaks of both PA and CA are sharp and well defined at APA modified WB electrode having peak current prominent than that of bare WB electrode. So APA modified WB electrode can determine the amount of PA and CA accurately compared to bare WB electrode using DPV technique.

4.10.3 Simultaneous detection of VC and CA in PBS at APA modified WB electrode using DPV

DPV of a binary mixture (5 mM) of VC and CA in PBS at bare WB and APA modified WB electrode is shown in Fig.4.58. The DPVs of VC, CA and their binary mixture (5 mM) in PBS at APA modified WB electrode is shown in Fig.4.59. At APA modified WB electrode binary mixture of VC and CA in PBS shows two anodic peaks + 0.18 V and + 1.41 V respectively. The peak currents of VC and CA are 48 µA and 152 µA. From the positions and currents of the peaks (fig. 4.59) it can be explained that the peaks of both VC and CA are sharp and well defined at APA modified WB electrode having peak current prominent than that of bare WB electrode. So APA modified WB electrode can determine the amount of VC and CA accurately compared to bare WB electrode using DPV technique.

4.10.4 Simultaneous detection VC, PA and CA in PBS at APA modified WB electrode using DPV

DPV of a ternary mixture (5 mM) of VC, PA and CA in PBS both at bare WB and APA modified WB electrode is shown in Fig. 4.60. The DPVs of VC, PA and CA and their ternary mixture (5 mM) in PBS at APA modified WB electrode are shown in Fig. 4.61. At APA modified WB electrode ternary mixture of VC, PA and CA in PBS shows three anodic peaks + 0.18 V, + 0.40 and + 1.42V respectively. The peak currents of VC, PA and CA are 31 µA, 124 µA and 127 µA. For the mixture of VC, PA and CA in PBS, two peaks were observed at + 0.48 V and + 1.44 V respectively at bare WB electrode. In fig. 4.61, the positions and currents of the peaks indicates that the APA modified WB electrode can separate the peaks with high sensitivity compared to the bare WB electrode. So, APA modified WB electrode can be used to simultaneous detection (qualitative & quantitative) of VC, PA and CA in a ternary mixture using DPV technique.

4.11 Quantitative estimation of VC, PA and CA in PBS at APA modified WB electrode in binary and ternary mixture

For the calculation of sensitivity and detection limits of the analytes we need the surface area of APA modified WB electrode. The surface area experiments are given below:

4.11.1 Electrode surface area calculation

Fig. 4.62 and 4.64 shows the CVs of ferrocyanide in KCl solution at bare WB electrode and at APA modified WB electrode respectively. Table 4.5 and table 4.6 shows the peak current of ferrocyanide in KCl solution at different scan rate using bare WB electrode and at APA modified WB electrode respectively.

Electrode surface area was calculated Randles–Sevcik equation using 2 mM ferrocyanide at different scan rate in 1M KCl solution.

In general, the peak current of diffusion controlled reversible or quasi-reversible electro - chemical reaction follows Randles–Sevcik equation

$$Ip = 0.4463nF\sqrt{\frac{nFD}{RT}}AC\sqrt{v} \quad \text{(1)}$$

Where Ip = the peak current, n = the number of electrons, F = Faraday constant, T = the temperature in Kelvin, R = the gas constant, A = the surface area of the working electrode, D = the diffusion coefficient of the electroactive species, C = the bulk concentration of the electroactive species and *v* = the scan rate of voltammograms.

From Equation (1) we get,

$$Slope = 0.4463nF\sqrt{\frac{nFD}{RT}}AC$$

$$A = \frac{Slope}{0.4463nF\sqrt{\frac{nFD}{RT}}C}$$

For the surface area of bare WB electrode,

Fig. 4.63 shows the corresponding straight line and from the straight line, the value of slope is ~7.5×10^{-5} and the standard value of diffusion coefficient for ferrocyanide in WBE is 1.52×10^{-6} cm^2/s. where concentration C = 2×10^{-6} mol/cm^3 so we get,

$$A = \frac{7.5\times10^{-5}}{0.4463\times1\times96500\sqrt{\frac{1\times96500\times 1.52\times10^{-6}}{8.314\times 298}}\times2\times10^{-6}}$$

$A = 0.11\ cm^2$

Again, for the surface area of APA modified WB electrode,

Fig. 4.65 shows the corresponding straight line and from the straight line, the value of slope is ~10.4×10^{-5} and the standard value of diffusion coefficient for ferrocyanide in WBE is 1.52×10^{-6} cm^2/s. where concentration C = 2×10^{-6} mol/cm^3 so we get,

$$A = \frac{10.4\times10^{-5}}{0.4463\times1\times96500\sqrt{\frac{1\times96500\times 1.52\times10^{-6}}{8.314\times 298}}\times2\times10^{-6}}$$

$A = 0.15\ cm^2$

Bare WB electrode has the surface area 0.11 cm^2. Surface area of APA modified WB electrode is 0.15 cm^2 indicates that the surface area of WB electrode increased after modify.

4.11.2 Simultaneous quantitative estimation of VC and PA in PBS at APA modified WB electrode

DPVs of simultaneous change of VC and PA (1-5 mM) in PBS are shown in fig. 4.66. Peak currents of VC and PA in PBS were increased linearly with the increase of their concentrations. The linear regression equations for VC and PA are, Ip (VC) = 7.807vc + 6.0748 (R^2 = 0.9946) and Ip (PA) = 12.715_{PA} + 23.063 (R^2 = 0.9848) respectively (Fig. 4.67). The average current increase for VC and PA is 7.8 µA and 12.96 µA. The sensitivity was calculated for the binary mixture of VC and PA. The sensitivity of VC and PA are 52.0 µA/mM/cm^2 and 93.1 µA/mM/cm^2. Limit of detection (LoD) was calculated by signal to noise ratio (S/N = 3). The LoD of VC and PA are 0.565 µmol L^{-1} and 0.411 µmol L^{-1}.

4.11.3 Simultaneous quantitative estimation of PA and CA in PBS at APA modified WB electrode

DPVs of simultaneous change of PA and CA (1-5 mM) in PBS are shown in fig. 4.68. Peak currents of PA and CA in PBS were increased linearly with the increase of their concentrations. The linear regression equations for PA and CA are Ip (PA) = 15.991_{PA} + 36.175 (R^2 = 0.9985) and Ip (CA) = 13.208_{CA} + 52.654 (R^2 = 0.9977) (Fig. 4.69)

respectively. The average current increase for PA and CA is 16.05 µA and 13.08 µA. The sensitivity was calculated for the binary mixture of PA and CA. The sensitivity of PA and CA are 106.9 µA/mM/cm^2 and 128.1 µA/mM/cm^2. Limit of detection (LoD) was calculated by signal to noise ratio (S/N = 3). The LoD of PA and CA are 0.370 µmol L^{-1} and 0.673 µmol L^{-1}.

4.11.4 Simultaneous quantitative estimation of VC and CA in PBS at APA modified WB electrode

DPVs of simultaneous change of VC and CA (1-5 mM) are shown in fig. 4.70. Peak currents of VC and CA were increased linearly with the increase of their concentrations. The linear regression equation for VC and CA is Ip (VC) = 9.0902_{VC} + 1.5193 (R^2 = 0.9996) and Ip (CA) = 25.308_{CA} + 40.719 (R^2 = 0.9981) (Fig. 4.71). The average current increases for VC and CA is 9.04 µA and 25.83 µA. The sensitivity was calculated for the binary mixture of VC and CA. The sensitivity of VC and CA are 60.2 µA/mM/cm^2 and 158.6 µA/mM/cm^2. Limit of detection (LoD) was calculated by signal to noise ratio (S/N = 3). The LoD of VC and CA are 0.394 µmolL^{-1} and 0.750 µmolL^{-1} respectively.

4.12 Quantitative estimation of VC, PA and CA in ternary mixture at APA modified WB electrode

4.12.1 Quantitative estimation of VC at constant PA + CA concentration in PBS at APA modified WB electrode

DPV of the ternary mixture of VC, PA and CA in PBS at APA modified WB electrode is shown in fig. 4.72 where concentration of PA and CA in PBS were kept constant and the concentration of VC in PBS was varied successively. Fig. 4.73 shows the calibration curve for different concentrations of VC. This calibration curve can be used to determine VC in presence of PA and CA quantitatively in a ternary mixture. In case of VC the peak current increases with increasing their concentrations over the range of 1-5mM. The linear regression equation of VC is, Ip (VC) = 9.8344_{VC} + 4.5448 (R^2 = 0.9979).

4.12.2 Quantitative estimation of PA at constant VC + CA concentration in PBS at APA modified WB electrode

DPV of the ternary mixture of VC, PA and CA in PBS at APA modified WB electrode is shown in fig. 4.74 where concentration of VC and CA in PBS were kept constant and the concentration of PA in PBS was varied successively. Fig. 4.75 shows the calibration curve for different concentrations of PA. This calibration curve can be used to determine PA in presence of VC and CA quantitatively in a ternary mixture. In case of PA the peak current increases with increasing their concentrations over the range of 1-5mM. The linear regression equation of PA is, Ip (PA) = 16.298_{PA} + 8.2454 (R^2 = 0.9982).

4.12.3 Quantitative estimation of CA at constant VC + PA concentration in PBS at APA modified WB electrode

DPV of the ternary mixture of VC, PA and CA in PBS at APA modified WB electrode is shown in fig. 4.76 where concentration of VC and PA in PBS were kept constant and the concentration of CA in PBS was varied successively. Fig. 4.77 shows the calibration curve for different concentrations of CA. This calibration curve can be used to determine CA in presence of VC and PA quantitatively in a ternary mixture. In case of CA the peak current increases with increasing their concentrations over the range of 1-5mM. The linear regression equation of CA is, Ip (CA) = 14.87_{CA} + 59.894 (R^2 = 0.9967).

4.12.4 Quantitative estimation of VC + PA at constant CA concentration in PBS at APA modified WB electrode

DPV of the ternary mixture of VC, PA and CA in PBS at APA modified WB electrode is shown in fig. 4.78 where concentration of CA was kept constant and the concentration of VC and PA was varied successively. Fig. 4.79 shows the calibration curve for different concentrations of VC and PA in PBS. This calibration curve can be used to determine VC and PA in presence of CA quantitatively in a ternary mixture. In case of VC and PA the peak current increases with increasing their concentrations over the range of 1-5mM. The linear regression equations of VC and PA are, Ip (VC) = 8.9262_{VC} + 2.8865 (R^2 = 0.9974) and Ip (PA) = 15.582_{PA} + 11.807 (R^2 = 0.995) respectively.

4.12.5 Quantitative estimation of PA + CA at constant VC concentration in PBS at APA modified WB electrode

DPV of the ternary mixture of PA, CA and VC in PBS at APA modified WB electrode is shown in fig. 4.80 where concentration of VC was kept constant and the concentration of PA and CA were varied successively. Fig. 4.81 shows the calibration curve for different concentrations of PA and CA. This calibration curve can be used to determine PA and CA in presence of VC quantitatively in a ternary mixture. In case of PA and CA the peak current increases with increasing their concentrations over the range of 1-5mM. The linear regression equations of PA and CA are Ip (PA) = 17.656_{PA} + 1.1519 (R^2 = 0.9981) and Ip (CA) = 14.883_{CA} + 70.561 (R^2 = 0.9918) respectively.

4.12.6 Quantitative estimation of VC + CA at constant PA concentration in PBS at APA modified WB electrode

DPV of the ternary mixture of PA, CA and VC in PBS at APA modified WB electrode is shown in fig. 4.82 where concentration of PA was kept constant and the concentration of VC and CA were varied successively. Fig. 4.83 shows the calibration curve for different concentrations of VC and CA. This calibration curve can be used to determine VC and CA in presence of PA quantitatively in a ternary mixture. In case of VC and CA the peak current increases with increasing their concentrations over the range of 1-5mM. The linear regression equation of VC and CA are Ip (VC) = 10.961_{VC} + 1.6947 (R^2 = 0.9991) and Ip (CA) = 22.86_{CA} + 35.044 (R^2 = 0.9961) respectively.

4.12.7 Simultaneous quantitative estimation of VC, PA and CA in PBS at APA modified WB electrode in a ternary mixture

DPVs of the ternary mixture of the different concentrations of PA, CA and VC in PBS at APA modified WB electrode are shown in fig. 4.84. The calibration curve for different concentrations of VC, PA and CA are shown in Fig 4.85. These calibration curve can be used to determine VC, PA and CA quantitatively in a ternary mixture. The anodic currents of VC, PA and CA increased linearly with increasing their concentrations over the range of 1-5mM. The linear regression equation of VC, PA and CA are Ipa (VC) = 8.0478_{VC} + 14.87

(R^2 = 0.9975), Ipa (PA) = 14.813_{PA} + 36.666 (R^2=0.9972) and Ipa (CA) = 22.269_{CA} + 41.147 (R^2 = 0.9922), respectively. The sensitivity of VC, PA and CA are 54.4 µA/mM/cm^2, 99.9 µA/mM/cm^2 and 151.7 µA/mM/cm^2 and detection limits are 0.20 µmol L^{-1}, 0.16 µmol L^{-1} and 0.33 µmol L^{-1} respectively.

The linear regression equations of the calibration curves for single concentration change, binary concentration change and ternary concentration changes are nearly equal, indicating that they do not interfere in the determination of each other. So, this sensor can be used to determine the target analytes (VC, PA and CA) individually, in a binary mixture and simultaneously in a ternary mixture.

4.13 Interference study

Figure 4.86 shows the DPV of the ternary solution of VC, PA and CA in the presence of lysine, arginine, glycine, thiamine (vitamin B1), nicotinamide (vitamion B3), pyridoxine (PD) (vitamin B6) and glucose as interfering agents. From the voltammogram it is clear that the peak positions of VC (0.20 V), PA (0.48 V) and CA (1.42 V) are not influenced by the interfering substances. The peak positions are remaining unchanged like they appeared when no interfering substances present (Fig. 4.8). An oxidation peak appeared for pyridoxine at 0.74 V without interfering the peaks positions of VC, PA and CA. So, APA modified WB electrode does not show any interference in the peak potential range of VC, PA and CA by the mentioned interfering substances.

Simultaneous determination of VC, PA and CA using diethylamine modified Glassy carbon (GC) electrode has been reported in this laboratory as an unpublished work. The limit of detection (LoD) of VC, PA and CA were 0.4 µmol L^{-1}, 0.2 µmol L^{-1} and 0.3 µmol L^{-1} respectively at diethylamine modified GC electrode. In this work, the aspartic acid modified WB electrode gives the limit of detection (LoD) of VC, PA and CA are 0.20 µmol L^{-1}, 0.16 µmol L^{-1} and 0.33 µmol L^{-1} respecttively. The sensitivity for VC, PA and CA were 40.7 µA/mM/cm^2, 95.5 µA/mM/cm^2 and 76.2 µA/mM/cm^2 respectively at diethylamine modified GC electrode. On the other hand, the sensitivity for VC, PA and CA are 54.4 µA/mM/cm^2, 99.9 µA/mM/cm^2 and 151.7 µA/mM/cm^2 respectively at the aspartic acid modified WB electrode. From this comparison, it can be seen that the limit of detection at APA modified WB electrode for VC, PA and CA are lower than that of diethylamine modified GC electrode

and the sensitivity of APA modified WB electrode is higher than that of diethylamine modified GC electrode.

4.14 Quantitative Analysis of standard and tablet samples of VC, PA and CA by APA modified WB electrode

Quantitative analysis in real and tablet samples was done by this method. For each analyte recovery percentage (R %) and standard deviation (SD) were calculated to evaluate the consistency of the sensor. The quantitative determination of each tablet samples was valided by UV-Vis method.

4.14.1 Quantitative analysis of vitamin C in standard and tablet samples

4.14.1.1 Quantitative analysis of standard VC

DPVs of different amount of standard VC in 30 mL PBS (pH 7) under optimum condition are shown in fig. 4.87. Table 4.7 shows the current for different amount of VC. Fig.4.88 shows the calibration curve of VC with response to different amount. The regression equation for the calibration curve of VC is Ip = 1.1349x + 1.3915 (R^2 = 0.9974). This equation was used to determine the unknown amount in the real and tablet samples where, "Ip" is the current of the sample and "x" is the amount.

Table 4.8 shows the recovery percentage data of standard VC calculated from the regression equation of the calibration curve. The recovery percentage is found 99-104% indicates that the sensor has the ability to determine the amount of VC with high accuracy.

Table 4.9 shows the data of the determination of known 35mg standard VC sample (5 times) for standard deviation calculation. The standard deviation was found ± 0.4mg. It indicates that the sensor can determine the amount with high consistency.

4.14.1.2 Determination of VC in tablet samples using APA modified WB electrode sensor

For each determination 1/20 parts of the tablet was dissolved in 30 mL of PBS (pH 7).

Calculation of the amount

Fig. 4.89 shows the DPVs of the tablet samples in 30 mL PBS (pH 7) and table 4.10 shows the current of tablet samples.

VC in Cevit tablet

The linear regression equation of VC (Fig. 4.88) is Ip = 1.1349x + 1.3915 where, "Ip" is the current of the VC in cevit and "x" is the amount.

For Cevit the current found 15.53μA.

So, x = (15.53-1.3915)/1.1349

X = 12.46 mg in 1/20 parts of the tablet. [For each determination 1/20 parts of the tablet was dissolved in 30 mL of PBS (pH 7).

So, total amount of VC in Cevit tablet is 20 × 12.46 = 249.2 mg.

Same calculation for every tablet samples. Table 4.11 shows amount of VC in different tablet samples.

4.14.1.3 Determination of VC in tablet samples using UV-Vis method

For each determination 1/6 parts of the tablet was dissolved in 100 mL of water.

Fig. 4.90 shows the UV-Vis spectra of different concentrations of VC using water as solvent. Table 4.12 shows the absorbance for different concentrations of VC. Fig. 4.91 shows the calibration curve of VC with response to different concentration. The regression equation for the calibration curve of VC is A = 0.0403x + 0.3129 (R^2 = 0.9928). This equation was used to determine the unknown amount in the real and tablet samples where, "A" is the absorbance of the sample and "x" is the amount.

Table 4.13 shows the quantitative determination of VC in different commercial tablets of different pharmaceuticals using UV-Visible technique with standard deviations. Each replicates were repeated by 4 times. Table 4.14 shows the comparison of the determination of VC using UV-Visible technique with the determination of VC using APA modified WB electrode.

The table 4.14 shows the amount of VC determined using APA modified WB electrode in commercial samples are very close or nearly equal to the determination of VC using UV-

Visible method. So, APA modified WB electrode sensor can be used in pharmaceuticals to determine the actual quantity of VC in relevant tablets.

4.14.2 Quantitative analysis of Paracetamol in standard and tablet samples

4.14.2.1 Quantitative analysis of standard PA

DPVs of different amount of standard PA in 50 mL PBS (pH 7) under optimum condition are shown in fig. 4.92. Table 4.15 shows the current for different amount of PA. Fig. 4.93 shows the calibration curve of PA with response to different amount. The regression equation for the calibration curve of PA is Ip = 2.4768x + 133.81 (R^2 = 0.9927). This equation was used to determine the unknown amount in the real and tablet samples where, "Ip" is the current of the sample and "x" is the amount.

Table 16 shows the recovery percentage data of standard PA using the regression equation of the calibration curve. The recovery percentage is found 98-102% indicates that the sensor has the ability to determine the amount of PA with high consistency.

Table 17 shows the data of the determination of known 30 mg standard PA samples (5 times) for standard deviation calculation. The standard deviation was found ± 0.3 mg. It indicates that the sensor can determine the amount with high consistency.

4.14.2.2 Determination of PA in tablet samples using APA modified WB electrode sensor

For each determination 1/20 parts of the tablet was dissolved in 50 mL of PBS (pH 7).

Calculation of the amount

Fig. 4.94 shows the DPVs of the tablet samples in 50 mL PBS (pH 7) and table 4.18 shows the current of tablet samples.

PA in Napa tablet:

The linear regression equation of PA (Fig. 4.93) is Ip = 2.4768x + 121.43 where, "Ip" is the current of the PA in napa and "x" is the amount.

For napa the current found 183.2262 μA.

So, x = (183.2262-121.43) / 2.4768

X = 24.95 mg in 1/20 parts of the tablet. [For each determination 1/20 parts of the tablet was dissolved in 50 mL of PBS (pH 7)].
So, total amount of PA in Napa tablet is 20 × 24.95 = 499.1 mg.

Same calculation for every tablet sample. Table 4.19 shows the amount of PA in different commercial tablets of different pharmaceuticals.

4.14.2.3 Determination of PA in tablet samples using UV-Vis method

For each determination 1/5 parts of the tablet was dissolved in 100 mL of water.

Fig. 4.95 shows the UV-Visible spectra of different concentrations of PA using water as solvent. Table 4.20 shows the absorbance for different concentrations of PA. Fig. 4.96 shows the calibration curve of PA. The regression equation for the calibration curve of PA is A = 0.0265x + 0.0308 (R^2 = 0.9934). This equation was used to determine the unknown amount in the real and tablet samples where, "A" is the absorbance of the sample and "x" is the amount.

Table 4.21 shows the quantitative determination of PA in different commercial tablets of different pharmaceuticals using UV-Visible technique with standard deviations. Each replicates were repeated by 4 times. Table 4.22 shows the comparison of the determination of PA using UV-Visible technique with the determination of PA using APA modified WB electrode.

The table 4.22 shows the amount of PA determined using APA modified WB electrode in commercial samples are very close or nearly equal to the determination of PA using UV-Visible method. So, APA modified WB electrode sensor can be used in pharmaceuticals to determine the actual quantity of PA in relevant tablets.

4.14.3 Simultaneous quantitative determination of Paracetamol and Caffeine in standard and combined tablet samples

4.14.3.1 Quantitative analysis of standard PA + CA at APA modified WB electrode

DPVs of different amount of standard PA + CA in 50 mL PBS (pH 7) under optimum condition are shown in fig. 4.97. Table 4.23 shows the peak current for different amount of

PA and CA. Fig. 4.98 shows the calibration curve of PA with response to different amount. The regression equation for the calibration curve of PA is Ipa = 1.902pa + 84.993 (R^2 = 0.9899). This equation was used to determine the unknown amount in the real and tablet samples where, "Ipa" is the current of the sample and "pa" is the amount of PA in unknown PA+CA samples. Fig. 4.99 shows the calibration curve of CA with response to different amount. The regression equation for the calibration curve of CA is Ica = 2.0615ca + 18.377 (R^2 = 0.9929). This equation was used to determine the unknown amount in the real and tablet samples where, "Ica" is the current of the sample and "ca" is the amount of CA in unknown PA + CA samples.

Table 4.24 shows the recovery percentage data of standard CA using the regression equation of the calibration curve (fig. 4.89). The recovery percentage is found 98-102% indicates that the sensor can determine the amount of CA in PA + CA solution with high accuracy.

Table 4.25 shows the data of the determination of known 10 mg standard CA samples (5 times) for standard deviation calculation. The standard deviation was found ± 0.2 mg. It indicates that the sensor can determine the amount with high consistency.

4.14.3.2 Simultaneous determination of PA + CA in tablet samples using APA modified WB electrode sensor

For each determination 1/15 parts of the tablet was dissolved in 50 mL of PBS (pH 7).

Fig. 4.100 shows the DPVs of the tablet samples in 50 mL PBS (pH 7) and table 4.26 shows the current of tablet samples. Table 4.26 shows the amount of PA and CA in different commercial PA + CA containing tablets of different pharmaceuticals.

The table 4.26 shows the amount of PA and CA determined using APA modified WB electrode in commercial samples are close to the actual quantity of PA and CA in relevant tablets. So, APA modified WB electrode sensor can be used in pharmaceuticals for simultaneously determine the actual quantity of PA and CA in relevant tablets.

Table 4.1: Peak currents (Ip) of VC, PA and CA in different pH solutions at Aspartic acid (APA) modified WB electrode

Buffer solution (pH)	Peak current of VC (Ip/µA)	Peak current of PA (Ip/µA)	Peak current of CA (Ip/µA)
3	114.26	148.85	204.57
5	158.27	198.23	326.41
7	178.46	212.78	370.27
9	102.31	77.52	270.36

Table 4.2: Peak current (Ip) of 5 mM VC in PBS (pH 7) at APA modified WB electrode at different scan rates

Scan rate (v/Vs^{-1})	Sq. root of scan rate ($v^{1/2}$/$V^{1/2}s^{-1/2}$)	Peak current (Ip/µA)
0.05	0.22	83.72
0.10	0.32	113.29
0.20	0.45	142.36
0.30	0.55	161.58
0.40	0.63	192.38

Table 4.3: Peak current (Ipa and Ipc) of 5 mM PA in PBS (pH 7) at APA modified WB electrode at different scan rates

Scan rate (v/Vs^{-1})	Sq. root of scan rate ($v^{1/2}$/$V^{1/2}s^{-1/2}$)	Peak current (Ipa/µA)	Peak current (Ipc/µA)
0.05	0.22	133.18	57.21
0.10	0.32	190.53	102.57
0.20	0.45	270.99	157.29
0.30	0.55	319.55	195.49
0.40	0.63	375.45	234.68

Table 4.4: Peak current (Ip) of 5 mM CA in PBS (pH 7) at APA modified WB electrode at different scan rates

Scan rate (v/Vs^{-1})	Sq. root of scan rate ($v^{1/2}/V^{1/2}s^{-1/2}$)	Peak current (Ip/µA)
0.05	0.22	228.05
0.10	0.32	368.16
0.20	0.45	478.14
0.30	0.55	594.79
0.40	0.63	728.58

Table 4.5: Peak current (Ipa and Ipc) of 2 mM potassium ferrocyanide in KCl at bare WB electrode at different scan rates

Scan rate (v/Vs^{-1})	Sq. root of scan rate ($v^{1/2}/V^{1/2}s^{-1/2}$)	Anodic peak current (Ipa/µA)	Cathodic peak current (Ipc/µA)
0.05	0.22	22.16	-23.26
0.10	0.32	30.80	-32.11
0.15	0.39	34.04	-35.51
0.20	0.45	39.08	-40.74
0.25	0.50	44.03	-43.50

Table 4.6: Peak current (Ipa and Ipc) of 2 mM potassium ferrocyanide in KCl at APA modified WB electrode at different scan rates

Scan rate (v/Vs^{-1})	Sq. root of scan rate ($v^{1/2}/V^{1/2}s^{-1/2}$)	Anodic peak current (Ipa/µA)	Cathodic peak current (Ipc/µA)
0.05	0.22	23.34	-23.47
0.10	0.32	32.25	-33.41
0.15	0.39	40.11	-41.47
0.20	0.45	47.09	-48.71
0.25	0.50	52.21	-53.49

Table 4.7: Peak current of different amount (mg) of VC in PBS at APA modified WB electrode

Amount (mg)	Peak current (Ip/µA)
10.0	12.98
15.0	18.69
20.0	23.02
25.0	30.05
30.0	35.79
35.0	41.03

Table 4.8: Recovery percentage of the determination of standard VC using APA modified WB electrode

Amount (mg)	Added (mg)	Total (mg)	Found (mg)	Recovery (%)
15.0	0.0	15.0	15.6	104.0
15.0	5.0	20.0	20.3	101.5
15.0	10.0	25.0	25.2	100.7
15.0	15.0	30.0	30.6	102.0
15.0	20.0	35.0	34.8	99.4

Table 4.9: Determination of the standard deviation of standard VC using APA modified WB electrode

Standard VC (mg)	Peak current (Ip/µA)	Found (mg)	Average (mg)	Standard deviation (± mg)
35.0	41.31	35.17	35.27	0.4
35.0	42.27	36.02		
35.0	41.29	35.16		
35.0	41.48	35.33		
35.0	40.73	34.67		

Table 4.10: Peak Current (Ip) of VC in different tablet samples

Tablet sample	Peak current (Ip/μA)
Cevit	15.53
Nutrivit C	15.33
Ascobex	15.63
Cecon	14.52
Vasco	15.29

Table 4.11: Amount found (mg) of VC in tablet samples of different pharmaceutical company using APA modified WB electrode sensor

Tablets	Pharmaceutical name	Amount found (mg)	Amount labeled (mg)
Cevit	Square	249.4	250.0
Nutrivit C	ACI	245.6	250.0
Ascobex	Beximco	253.8	250.0
Cecon	ACME	237.4	250.0
Vasco	Opsonin	245.0	250.0

Table 4.12: Concentration (ppm) and absorbance (A) of standard VC using UV-Vis method

Concentration (ppm)	Absorbance (A)
10.0	0.657
20.0	1.147
30.0	1.596
40.0	1.918
50.0	2.284

Table 4.13: Determination of VC in different tablet samples using UV-Visible technique

Tablets	Pharmaceutical name	Observations No.	Absorbance (A)	Quantity (mg)	Average value ± SD (mg)	Amount labeled (mg)
Cevit	Square	1	1.989	249.5	249.5 ± 0.3	250.0
		2	1.990	249.7		
		2	1.988	249.4		
		4	1.992	250.1		
Nutrivit C	ACI	1	1.972	247.0	246.7 ± 0.6	250.0
		2	1.97	246.7		
		3	1.967	246.2		
		4	1.977	247.8		
Ascobex	Beximco	1	2.005	250.9	250.8 ± 0.4	250.0
		2	2.008	250.4		
		3	2.01	250.7		
		4	2.005	250.9		
Cecon	ACME	1	1.918	238.9	238.9 ± 0.3	250.0
		2	1.915	238.5		
		3	1.917	238.8		
		4	1.92	239.3		
Vasco	Opsonin	1	1.952	245.5	245.9 ± 0.2	250.0
		2	1.952	246.0		
		3	1.95	245.7		
		4	1.953	245.2		

Table 4.14: Comparison of the amount of VC determined by APA modified WB electrode sensor with UV-visible method

Tablets	Pharmaceutical name	Amount found by APA modified WB electrode sensor (mg)	Amount found by UV-Visible method (mg)	Amount labeled (mg)
Cevit	Square	249.4	249.5 ± 0.3	250.0
Nutrivit C	ACI	245.6	246.7 ± 0.6	250.0
Ascobex	Beximco	251.1	250.8 ± 0.4	250.0
Cecon	ACME	237.4	238.9 ± 0.3	250.0
Vasco	Opsonin	245.0	245.9 ± 0.2	250.0

Table 4.15: Amount (mg) and peak current (Ip) of PA in PBS at APA modified WB electrode

Amount (mg)	Peak current (Ip/μA)
10.0	146.61
15.0	154.95
20.0	172.10
25.0	186.06
30.0	198.07
35.0	206.51
40.0	219.16

Table 4.16: Recovery percentage of the determination of standard PA using APA modified WB electrode

Amount (mg)	Added (mg)	Total Amount (mg)	Amount Found (mg)	Recovery (%)
15.0	0.0	15.0	14.74	98.3
15.0	5.0	20.0	20.40	102.0
15.0	10.0	25.0	25.20	100.8
15.0	15.0	30.0	30.13	100.4
15.0	20.0	35.0	34.67	99.1

Table 4.17: Standard deviation of the determination of standard PA using APA modified WB electrode

Known amount of PA (mg)	Current (µA)	Amount found (mg)	Average (mg)	Standard deviation (± mg)
15.0	159.73	15.3	15.72	0.3
15.0	161.31	16.1		
15.0	160.36	15.7		
15.0	160.14	15.5		
15.0	160.94	16.0		

Table 4.18: Peak current (Ip) of PA in different tablet samples

Tablet	Current(Ip/μA)
Xpa XR	203.38
Ace	183.05
Napa	183.23
Renova	182.51
Parapyrol	182.11
Longpara	201.62

Table 4.19: Amount found (mg) of PA in tablet samples of different pharmaceutical company using APA modified WB electrode

Tablets	Pharmaceutical name	Amount found (mg)	Amount labeled (mg)
Xpa XR	Aristopharma	661.8	665.0
Ace	Square	497.6	500.0
Napa	Beximco	499.0	500.0
Renova	Opsonin	493.2	500.0
Parapyrol	GlaxoPharma	490.0	500.0
Longpara	IBN Sina	657.8	665.0

Table 4.20: Concentration (ppm) and absorbance (A) of standard PA using UV-Vis method

Concentration (ppm)	Absorbance (A)
10.0	0.247
20.0	0.484
30.0	0.736
40.0	1.084
50.0	1.273

Table 4.21: Determination of PA in different tablet samples using UV-Visible technique

Tablets	Pharmaceutical name	Observations No.	Absorbance (A)	Quantity (mg)	Average value ± SD (mg)	Amount labeled (mg)
Xpa XR	Aristopharma	1	1.137	661.1	661.8 ± 0.3	665.0
		2	1.138	661.6		
		2	1.139	662.2		
		4	1.139	662.2		
Ace	Square	1	0.848	497.4	497.4 ± 0.5	500.0
		2	0.849	498.0		
		3	0.848	497.4		
		4	0.847	496.9		
Napa	Beximco	1	0.850	498.6	499.1 ± 0.4	500.0
		2	0.851	499.1		
		3	0.851	499.1		
		4	0.852	499.7		
Renova	Opsonin	1	0.821	493.2	493.1 ± 0.3	500.0
		2	0.820	493.6		
		3	0.822	492.9		
		4	0.821	492.7		
Parapyrol	GlaxoPharma	1	0.836	490.6	490.6 ± 0.2	500.0
		2	0.836	490.6		
		3	0.835	490.1		
		4	0.837	491.2		
Longpara	IBN Sina	1	1.112	657.0	657.6 ± 0.3	665.0
		2	1.113	657.4		
		2	1.113	657.4		
		4	1.114	658.1		

Table 4.22: Comparison of the amount of PA determined by APA modified WB electrode sensor with UV-visible method

Tablets	Pharmaceutical name	Amount found by APA modified WB electrode sensor (mg)	Amount found by UV-Visible method (mg)	Amount labeled (mg)
Xpa XR	Aristopharma	661.8	661.8 ± 0.3	665.0
Longpara	IBN Sina	657.8	657.6 ± 0.3	665.0
Ace	Square	497.6	497.4 ± 0.5	500.0
Napa	Beximco	499.0	499.1 ± 0.4	500.0
Parapyrol	GlaxoPharma	490.0	490.6 ± 0.2	500.0
Renova	Opsonin	493.2	493.1 ± 0.3	500.0

Table 4.23: Amount (mg) and peak current (Ip) of the binary solution of PA and CA in PBS at APA modified WB electrode

Amount of PA + CA (mg)	Peak Current (Ip/μA)	
	Paracetamol	Caffeine
10 + 2	99.96	21.35
15 + 4	113.68	27.85
20 + 6	125.44	31.78
25 + 8	135.10	34.37
30 + 10	144.19	38.67
35 + 12	151.64	42.39
40 + 14	159.74	47.08
45 + 16	168.64	51.94

Table 4.24: Recovery percentage of the determination of standard CA in PA + CA binary solution using APA modified WB electrode

Amount (mg)	Added (mg)	Total (mg)	Found (mg)	Recovery (%)
4.0	0.0	4.0	4.1	102.5
4.0	2.0	6.0	6.1	101.7
4.0	4.0	8.0	7.9	98.1
4.0	6.0	10.0	9.2	99.2
4.0	8.0	12.0	11.8	98.3

Table 4.25: Standard deviation of the determination of standard CA in PA + CA binary solution using APA modified WB electrode

Known amount of CA (mg)	Current (µA)	Amount found (mg)	Average (mg)	Standard deviation (± mg)
10.0	39.27	10.14	10.02	0.2
10.0	38.76	9.89		
10.0	38.90	9.96		
10.0	38.68	9.85		
10.0	39.48	10.23		

Table 4.26: Amount found (mg) of PA and CA in PA + CA tablet samples of different pharmaceutical company using APA modified WB electrode

Tablet	Pharmaceutical name	Current (Ip/µA)		Amount of PA + CA found (mg)	PA + CA labeled value (mg)
		Paracetamol	Caffeine		
Ace Plus	Square	148.05	26.36	497.3 + 59.9	500 + 65
Feva Plus	Ad-din	149.45	26.00	508.3 + 55.5	500 + 65
Fast Plus	Acme	150.26	25.03	514.7 + 48.4	500 + 65
Napa Extra	Beximco	148.78	27.09	503.1 + 63.4	500 + 65
Reset Plus	Incepta	147.47	27.34	492.7 + 65.2	500 + 65
Nor Plus	Novelta	146.68	26.11	486.5 + 56.3	500 + 65
Tamen X	Eskayef	144.83	24.98	471.9 + 47.6	500 + 65

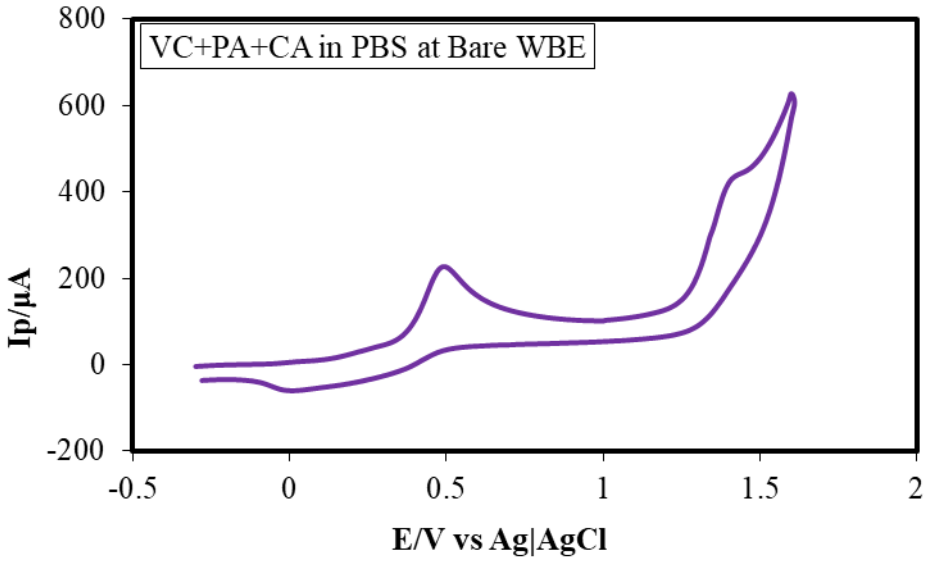

Fig. 4.1: Cyclic voltammogram (CV) of the ternary solution of VC, PA and CA in phosphate buffer solution (PBS) (pH 7) at bare WB electrode at scan rate 0.1 V/s.

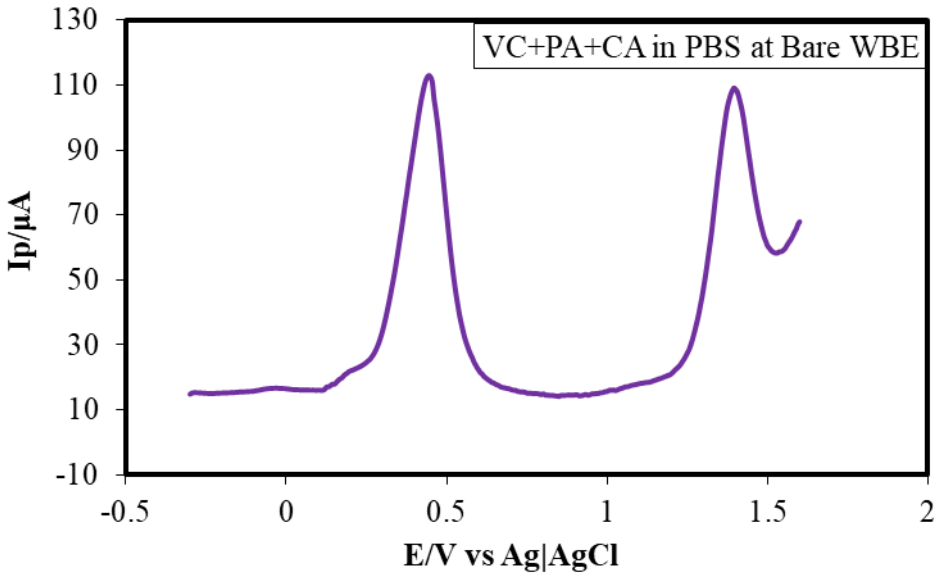

Fig. 4.2: Differential pulse voltammogram (DPV) of the ternary solution of VC, PA and CA in phosphate buffer solution (PBS) (pH 7) at bare WB electrode at scan rate 0.1 V/s.

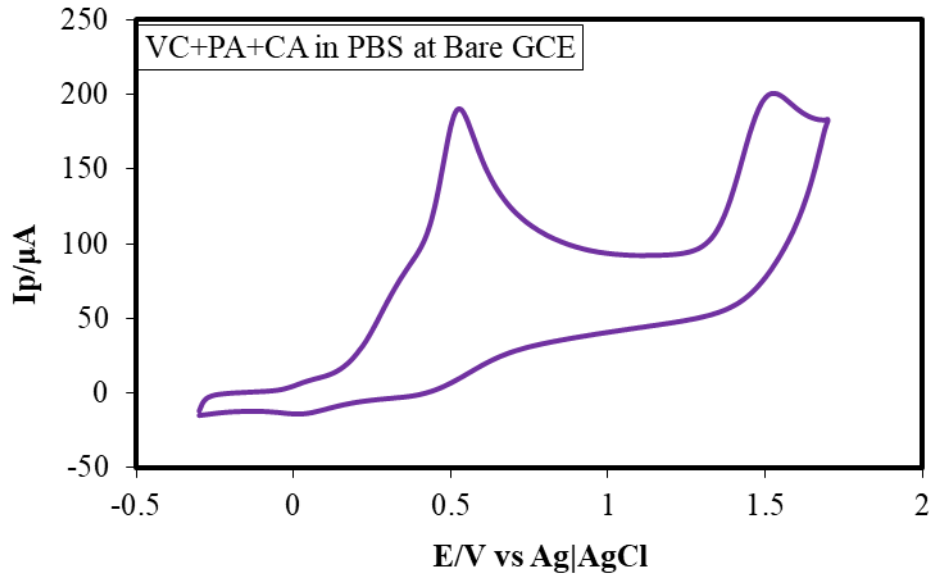

Fig. 4.3: Cyclic voltammogram (CV) of the ternary solution of VC, PA and CA in phosphate buffer solution (PBS) (pH 7) at bare GC electrode at scan rate 0.1 V/s.

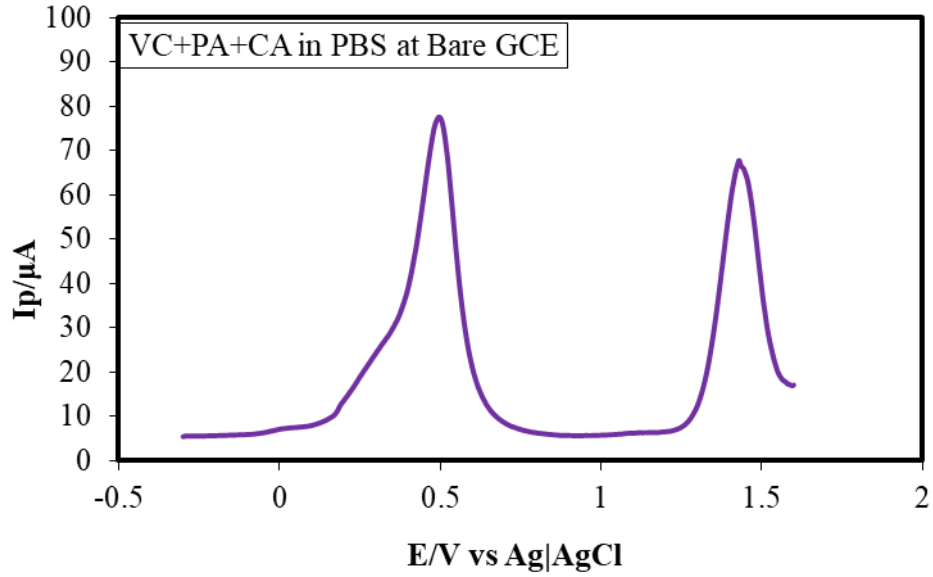

Fig. 4.4: Differential pulse voltammogram (DPV) of the ternary solution of VC, PA and CA in phosphate buffer solution (PBS) (pH 7) at bare GC electrode at scan rate 0.1 V/s.

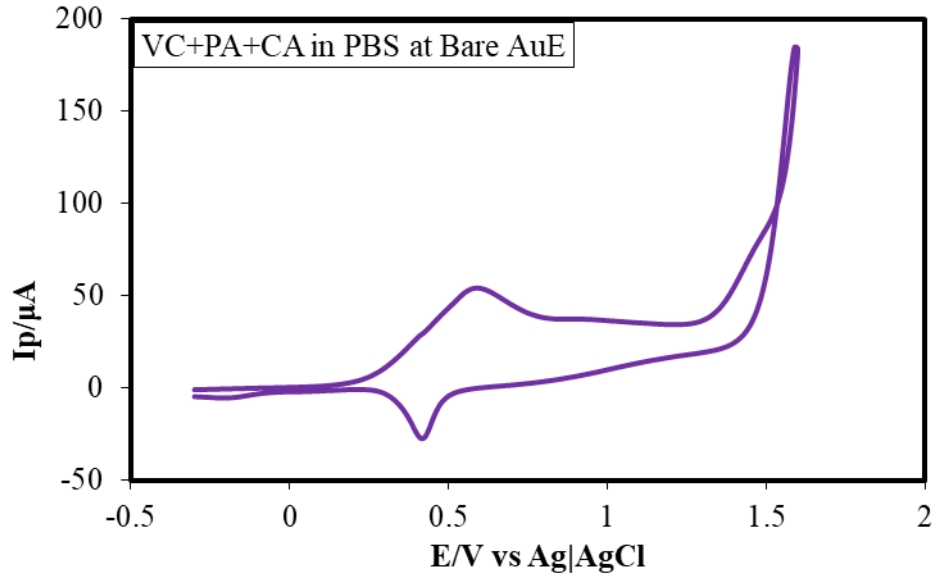

Fig. 4.5: Cyclic voltammogram (CV) of the ternary solution of VC, PA and CA in phosphate buffer solution (PBS) (pH 7) at bare Au electrode at scan rate 0.1 V/s.

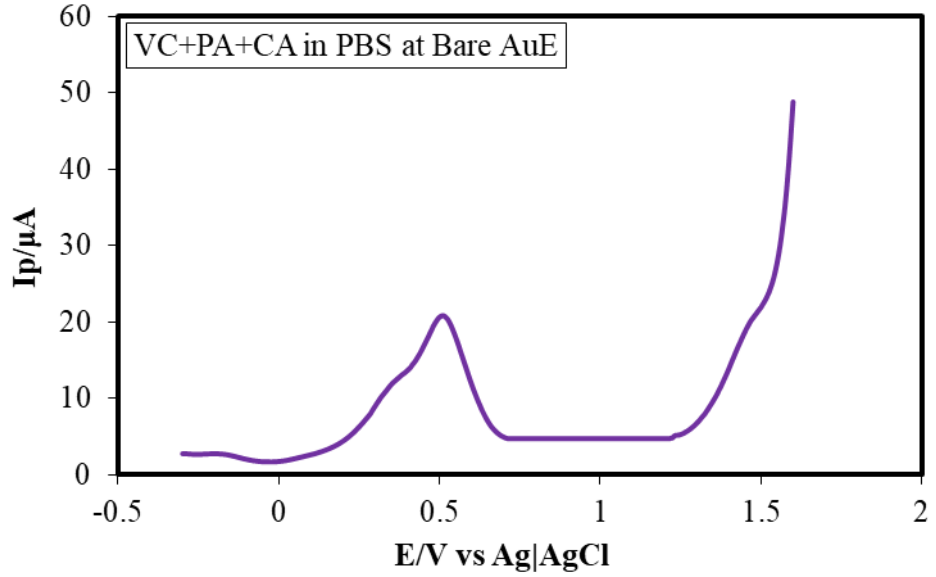

Fig. 4.6: Differential pulse voltammogram (DPV) of the ternary solution of VC, PA and CA in phosphate buffer solution (PBS) (pH 7) at bare Au electrode at scan rate 0.1 V/s.

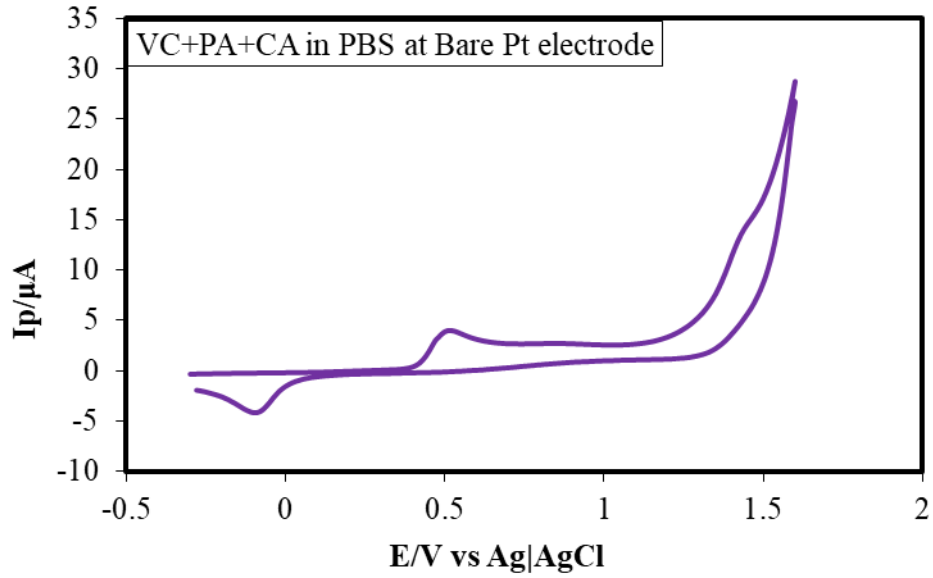

Fig. 4.7: Cyclic voltammogram (CV) of the ternary solution of VC, PA and CA in phosphate buffer solution (PBS) (pH 7) at bare Pt electrode at scan rate 0.1 V/s.

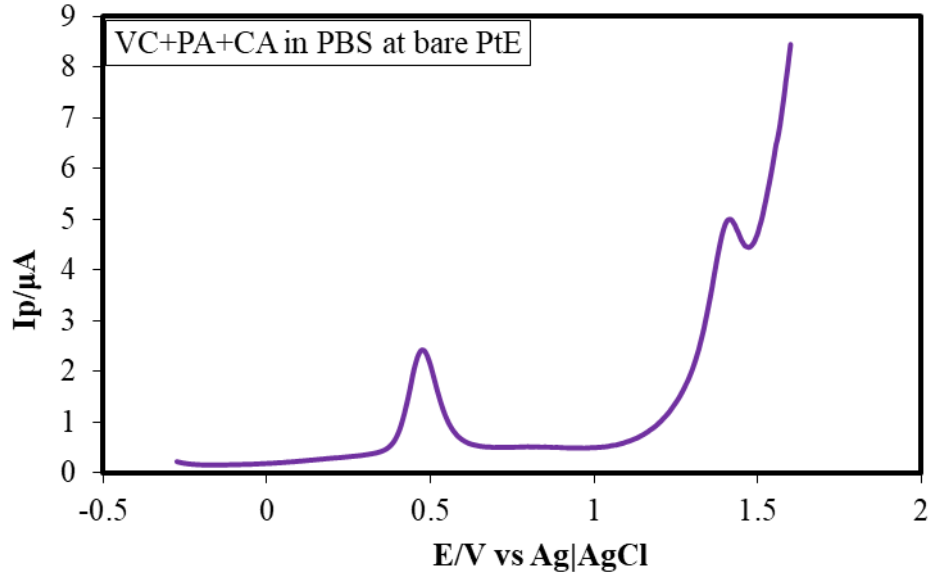

Fig. 4.8: Differential pulse voltammogram (DPV) of the ternary solution of VC, PA and CA in phosphate buffer solution (PBS) (pH 7) at bare Pt electrode at scan rate 0.1 V/s.

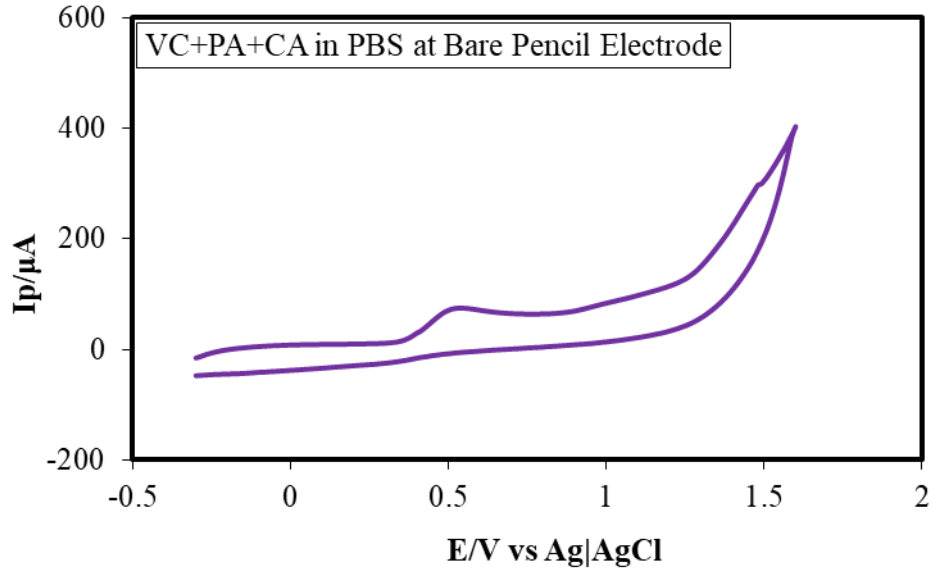

Fig. 4.9: Cyclic voltammogram (CV) of the ternary solution of VC, PA and CA in phosphate buffer solution (PBS) (pH 7) at bare pencil electrode at scan rate 0.1 V/s.

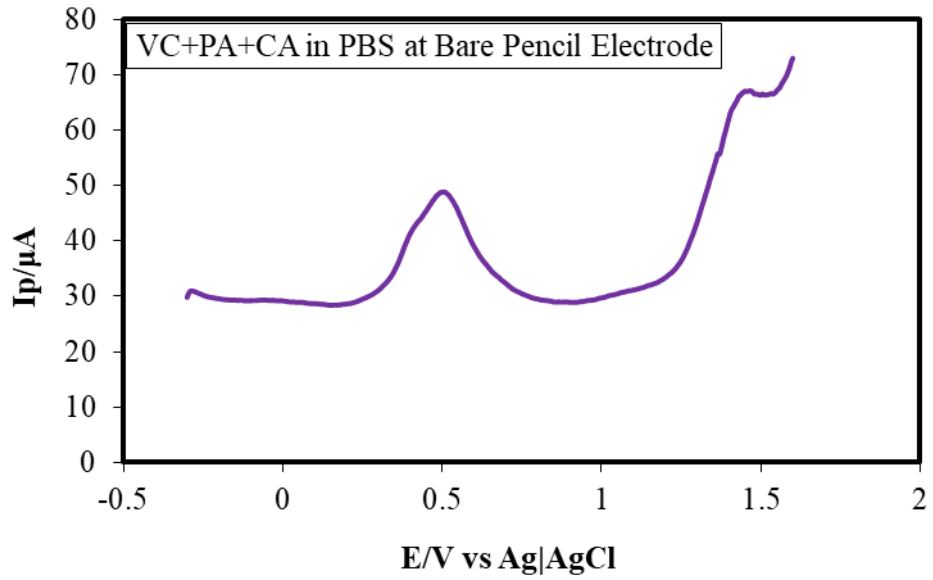

Fig. 4.10: Differential pulse voltammogram (DPV) of the ternary solution of VC, PA and CA in phosphate buffer solution (PBS) (pH 7) at bare pencil electrode at scan rate 0.1 V/s.

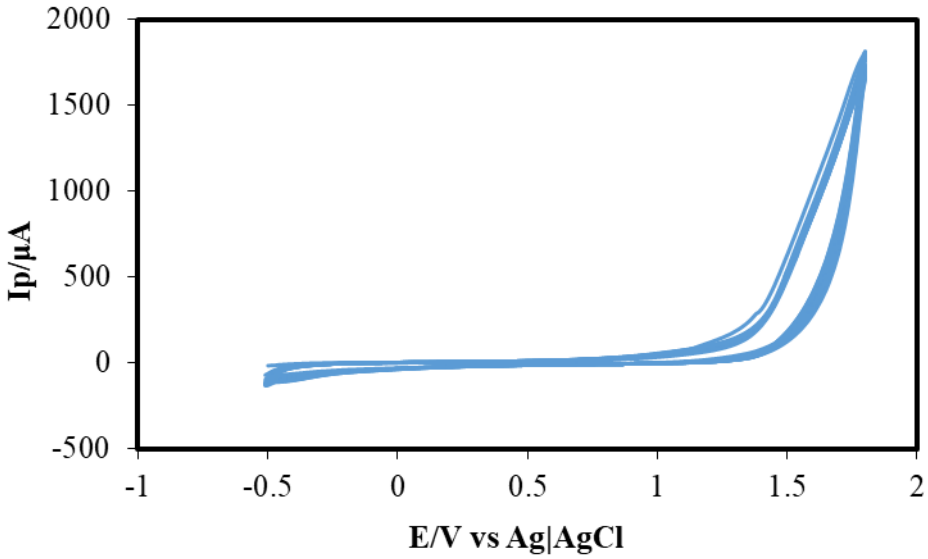

Figure 4.11: Cyclic voltammogram (CV) of Aspartic acid (APA) thin film growth by 15 cycles on the surface of bare WB electrode at scan rate 0.2 V/s.

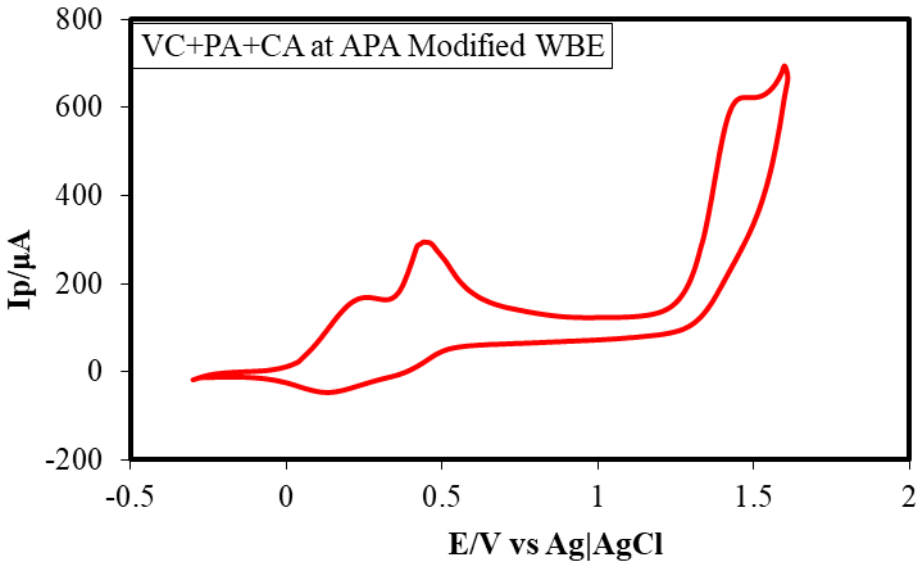

Fig. 4.12: Cyclic voltammogram (CV) of the ternary solution of VC, PA and CA in phosphate buffer solution (PBS) (pH 7) at APA modified WB electrode at scan rate 0.1 V/s.

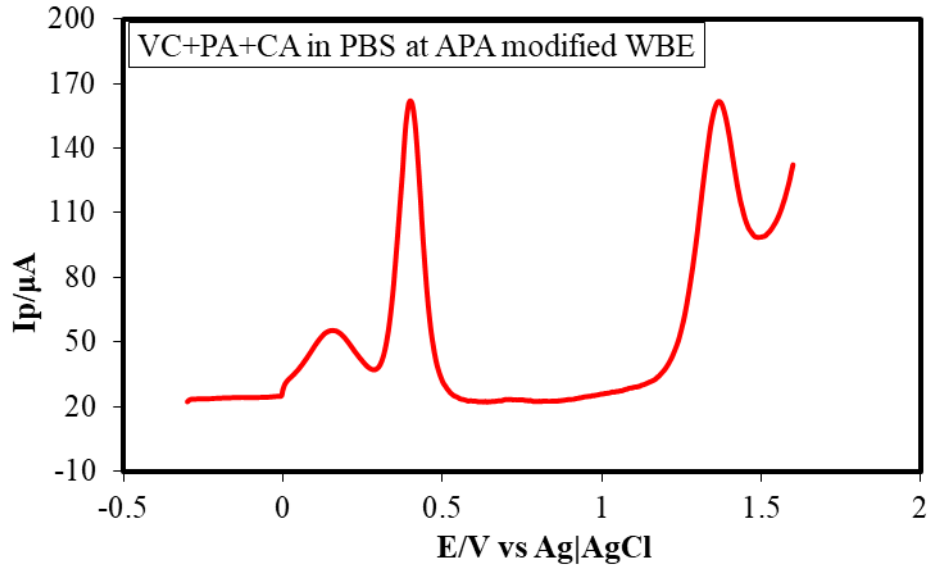

Fig. 4.13: Differential pulse voltammogram (DPV) of the ternary solution of VC, PA and CA in phosphate buffer solution (PBS) (pH 7) at APA modified WB electrode at scan rate 0.1 V/s.

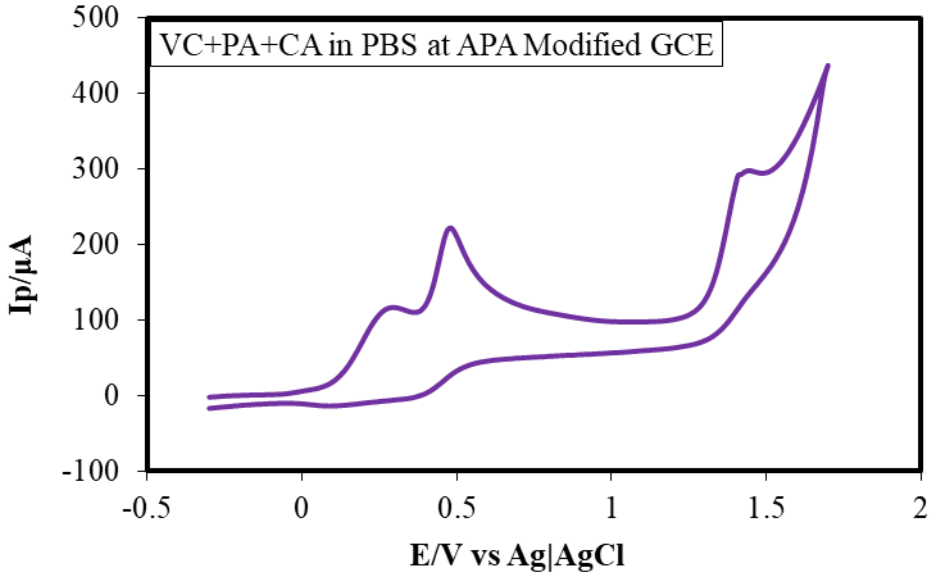

Fig. 4.14: Cyclic voltammogram (CV) of the ternary solution of VC, PA and CA in phosphate buffer solution (PBS) (pH 7) at APA modified GC electrode at scan rate 0.1 V/s.

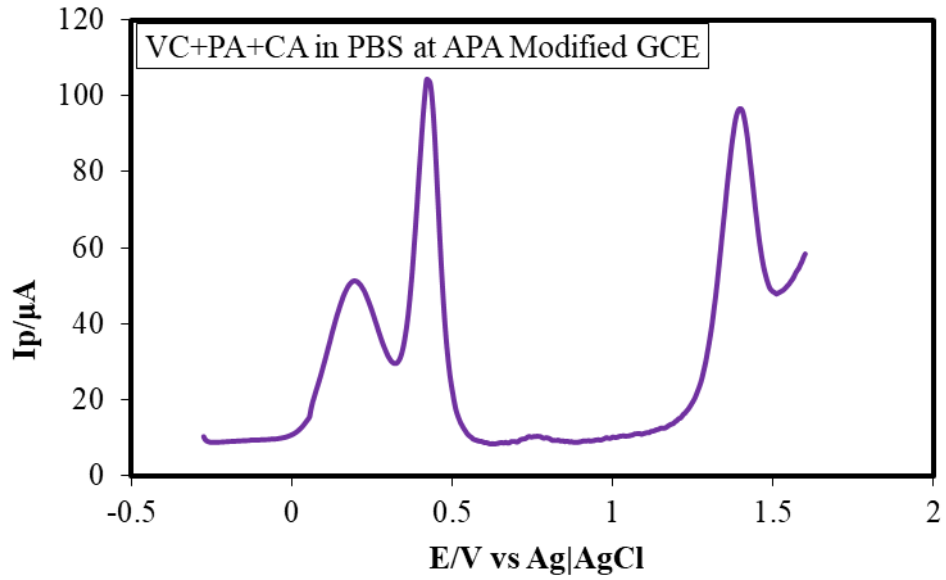

Fig. 4.15: Differential pulse voltammogram (DPV) of the ternary solution of VC, PA and CA in phosphate buffer solution (PBS) (pH 7) at APA modified GC electrode at scan rate 0.1 V/s.

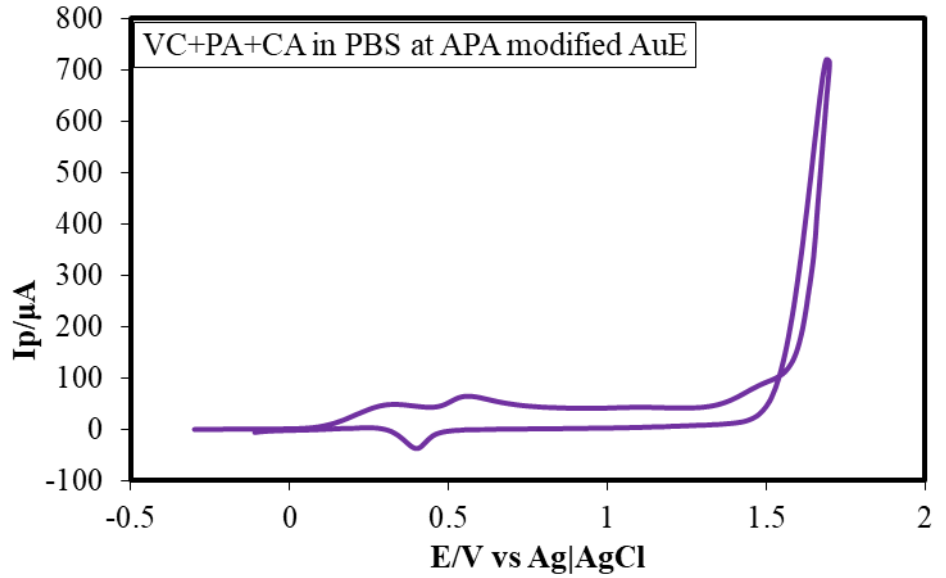

Fig. 4.16: Cyclic voltammogram (CV) of the ternary solution of VC, PA and CA in phosphate buffer solution (PBS) (pH 7) at APA modified Au electrode at scan rate 0.1 V/s.

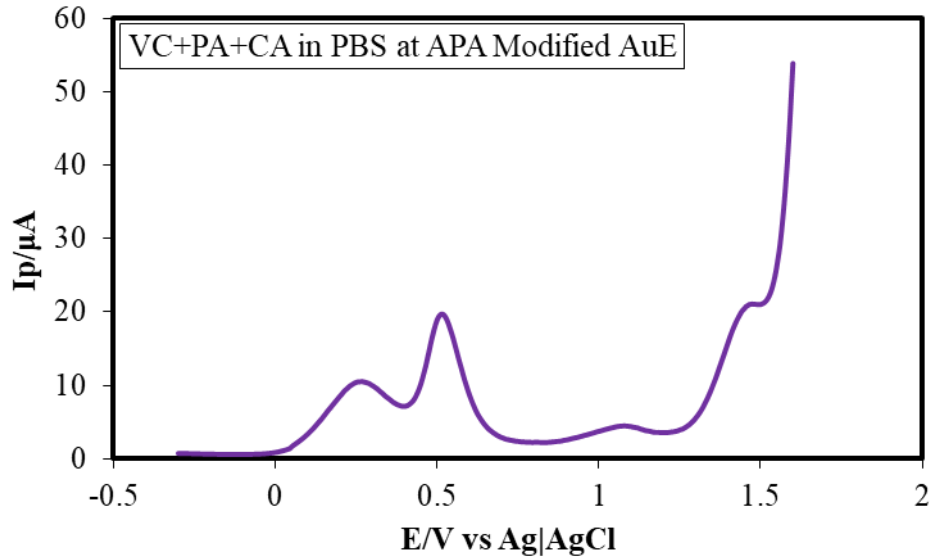

Fig. 4.17: Differential pulse voltammogram (DPV) of the ternary solution of VC, PA and CA in phosphate buffer solution (PBS) (pH 7) at APA modified Au electrode at scan rate 0.1 V/s.

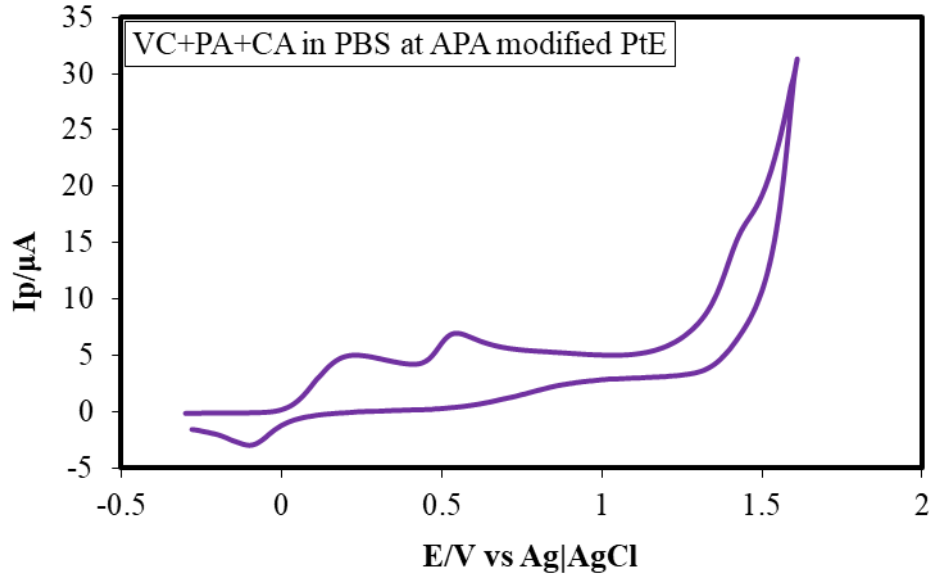

Fig. 4.18: Cyclic voltammogram (CV) of the ternary solution of VC, PA and CA in phosphate buffer solution (PBS) (pH 7) at APA modified Pt electrode at scan rate 0.1 V/s.

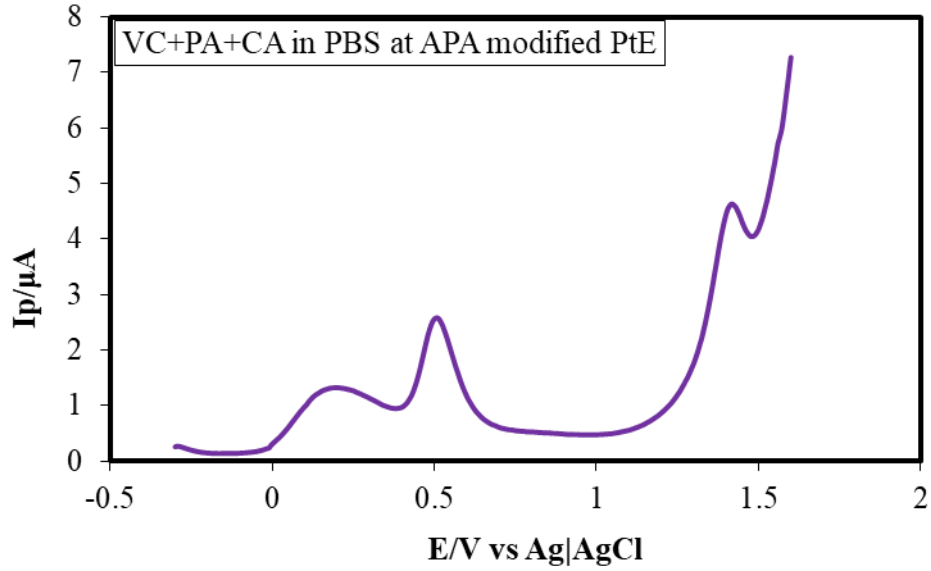

Fig. 4.19: Differential pulse voltammogram (DPV) of the ternary solution of VC, PA and CA in phosphate buffer solution (PBS) (pH 7) at APA modified Pt electrode at scan rate 0.1 V/s.

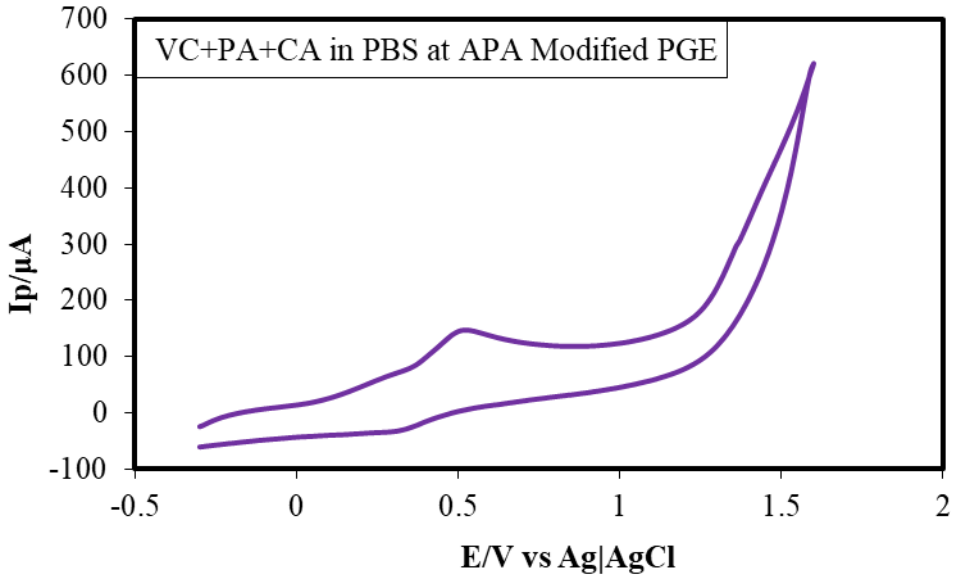

Fig. 4.20: Cyclic voltammogram (CV) of the ternary solution of VC, PA and CA in phosphate buffer solution (PBS) (pH 7) at APA modified pencil graphite electrode electrode at scan rate 0.1 V/s.

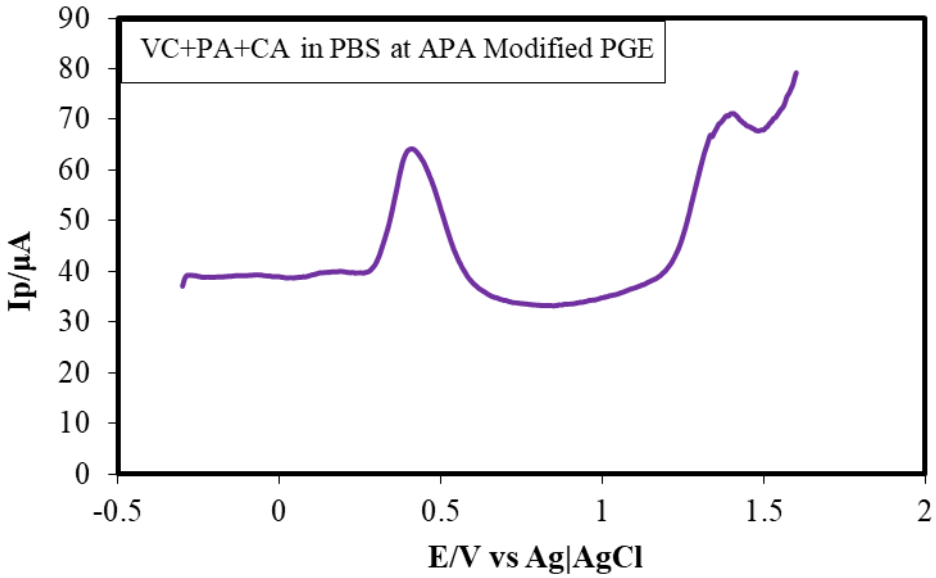

Fig. 4.21: Differential pulse voltammogram (DPV) of the ternary solution of VC, PA and CA in phosphate buffer solution (PBS) (pH 7) at APA modified pencil graphite electrode electrode at scan rate 0.1 V/s.

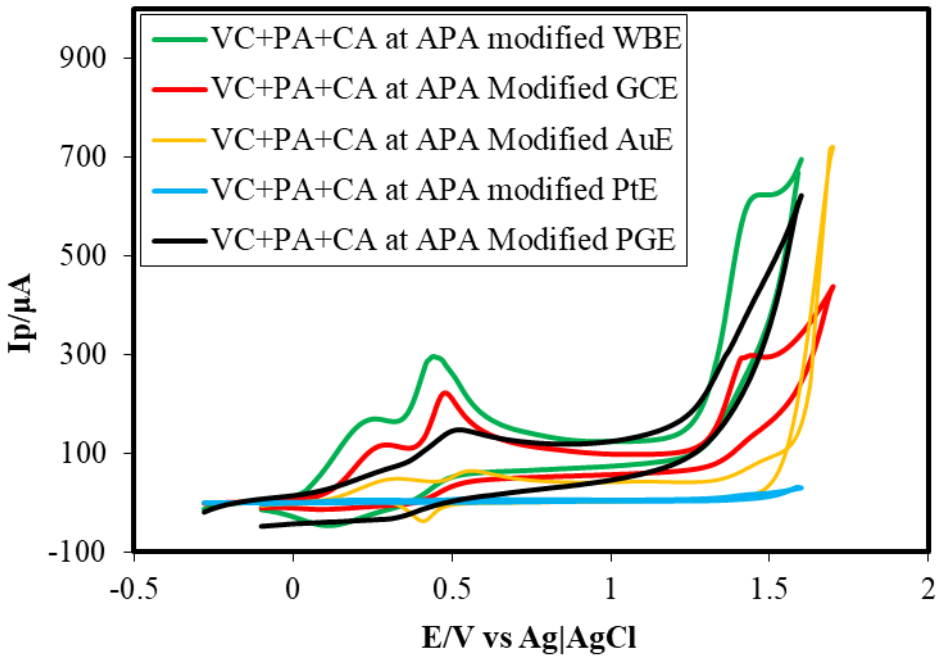

Fig. 4.22: Cyclic voltammograms (CVs) of the ternary solution of VC, PA and CA in phosphate buffer solution (PBS) (pH 7) at APA modified WB (red line), GC (green line), Au (violet line), Pt (light blue line) and PG (black line) electrode at scan rate 0.1 V/s.

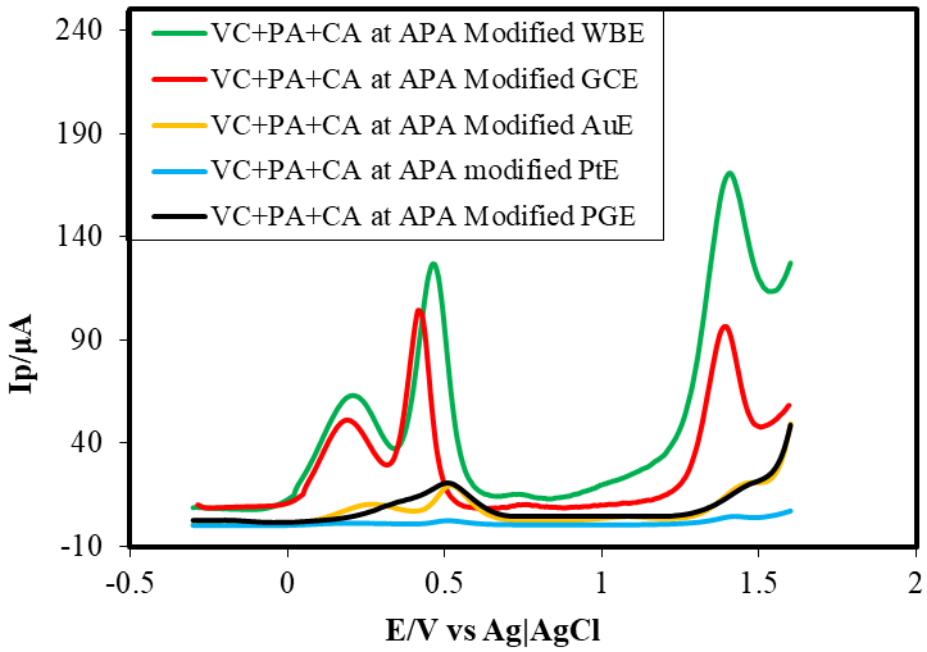

Fig. 4.23: Cyclic voltammograms (CVs) of the ternary solution of VC, PA and CA in phosphate buffer solution (PBS) (pH 7) at APA modified WB (green line), GC (red line), Au (light blue line), Pt (violet line) and PG (black line) electrode at scan rate 0.1 V/s.

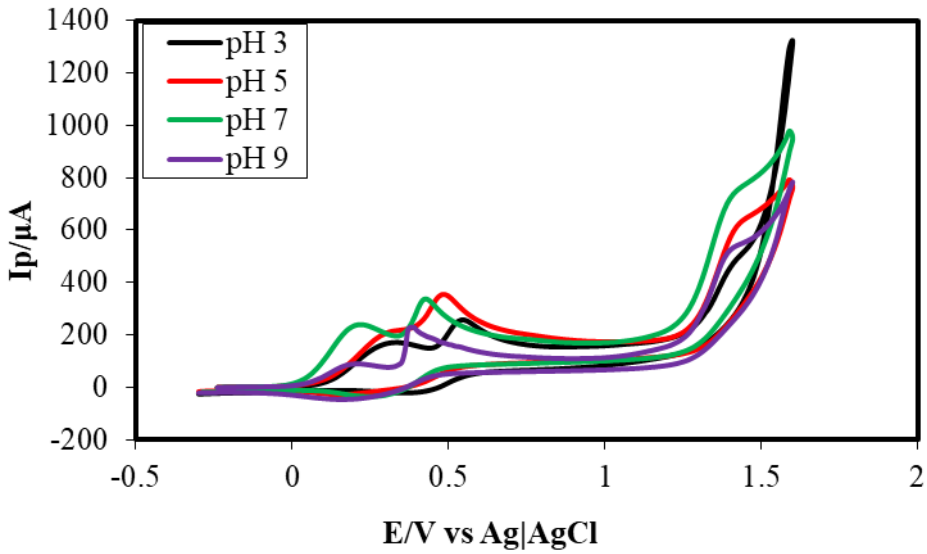

Fig. 4.24: Cyclic voltammograms (CVs) of the ternary solution of VC, PA and CA in different buffer solution (pH 3, 5, 7 and 9) at APA modified WB electrode.

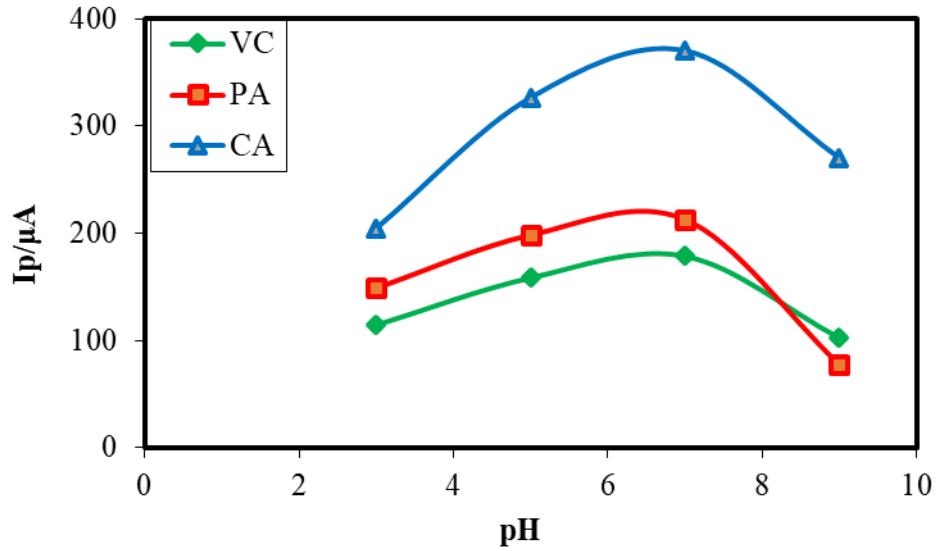

Figure 4.25: Plots of peak current (I_p) vs pH (3, 5, 7 and 9) of VC (green line), PA (red line) and CA (violet line).

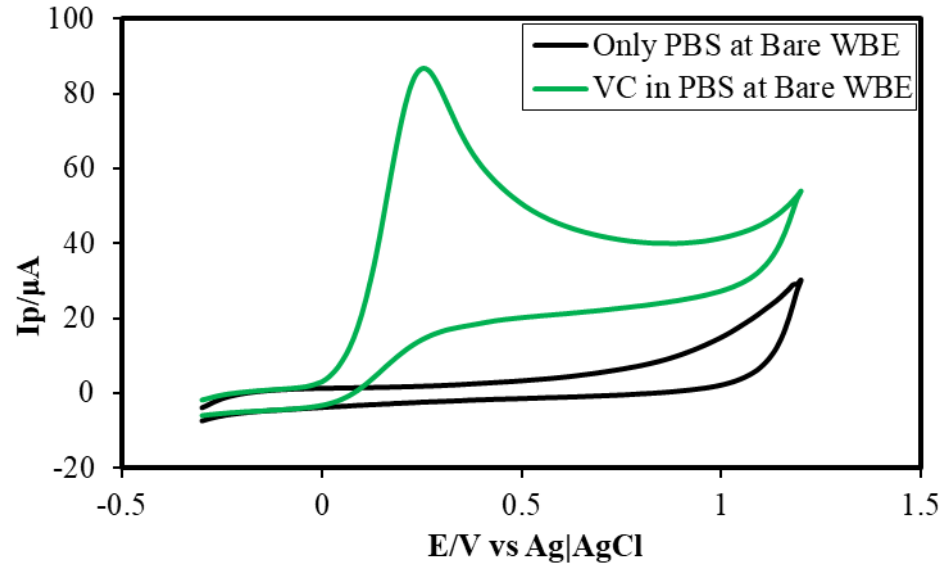

Fig. 4.26: Cyclic voltammogrm (CV) of 5 mM VC in 0.5 M PBS (pH 7) (green line) and only 0.5 M PBS (pH 7) (black line) of Bare WB Electrode at scan rate 0.1 V/s.

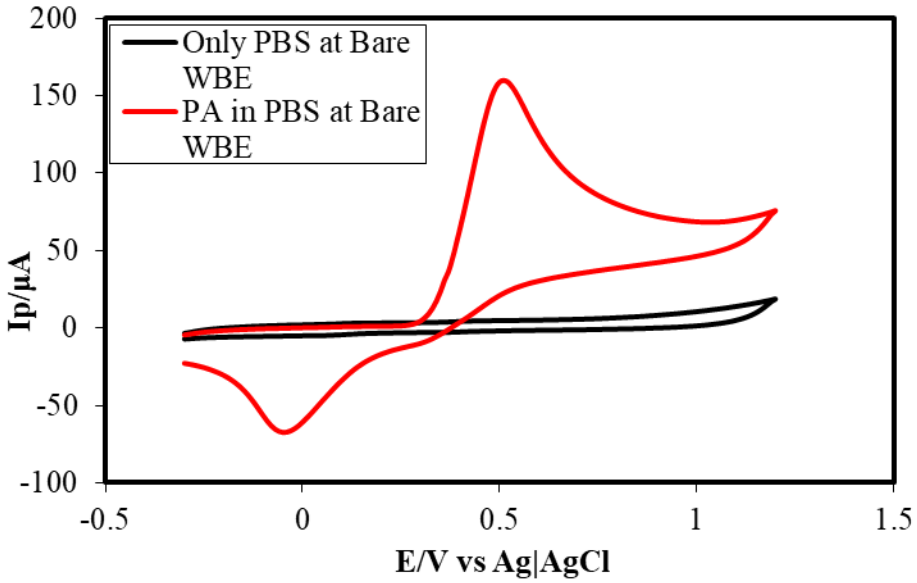

Fig. 4.27: Cyclic voltammogrm (CV) of 5 mM PA in 0.5 M PBS (pH 7) (red line) and only 0.5 M PBS (pH 7) (black line) of Bare WB Electrode at scan rate 0.1 V/s.

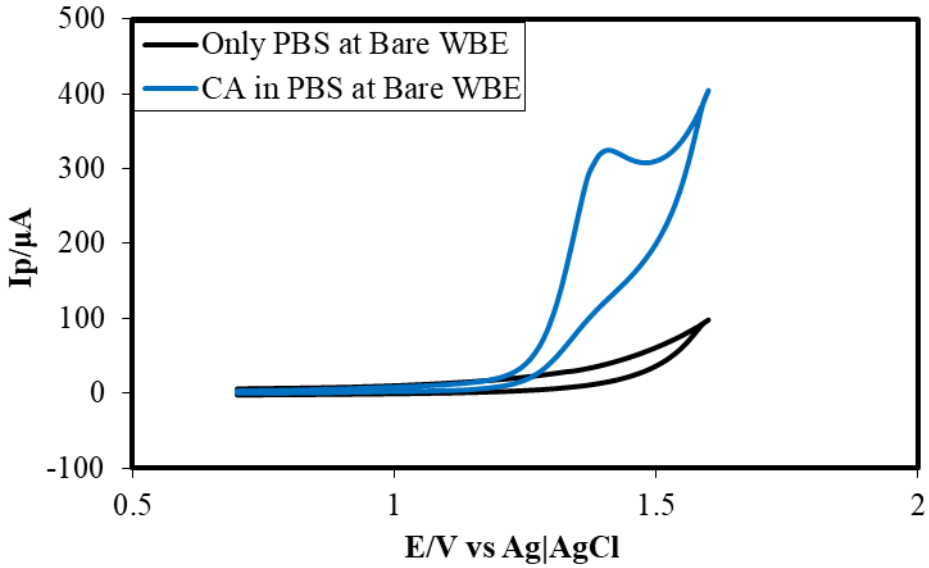

Fig. 4.28: Cyclic voltammogrm (CV) of 5 mM CA in 0.5 M PBS (pH 7) (black line) and only 0.5 M PBS (pH 7) (blue line) of Bare WB Electrode at scan rate 0.1 V/s.

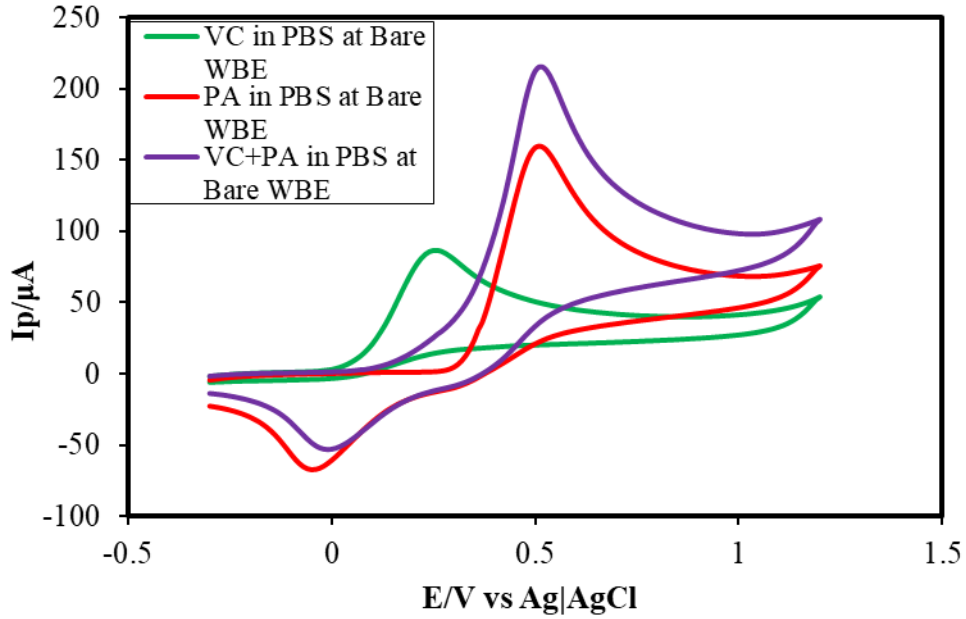

Fig. 4.29: Cyclic voltammogram (CV) of 5 mM VC (red line), 5 mM PA (green line) and 5 mM VC + 5 mM PA (violate line) of Bare WB Electrode in PBS (pH 7) at scan rate 0.1 V/s.

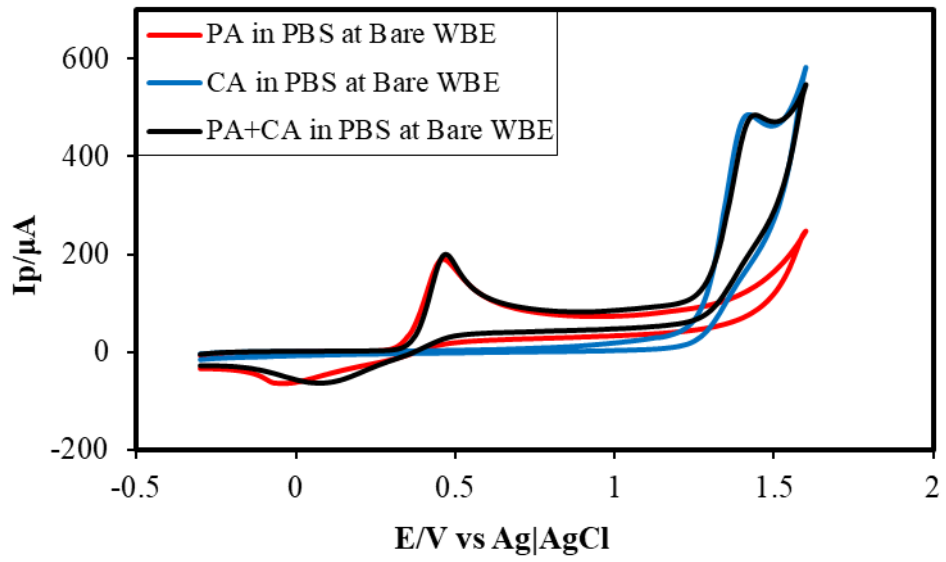

Fig. 4.30: Cyclic voltammogram (CV) of 5 mM PA (red line), 5 mM CA (blue line) and 5 mM PA + 5 mM CA (black line) of Bare WB Electrode in PBS (pH 7) at scan rate 0.1 V/s.

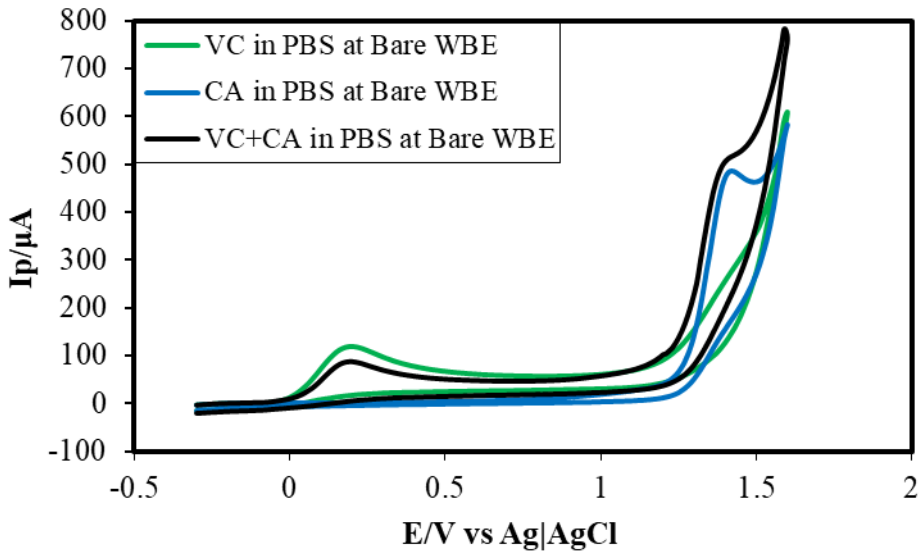

Fig. 4.31: Cyclic voltammogram (CV) of 5 mM VC (green line), 5 mM CA (blue line) and 5 mM VC + 5 mM CA (black line) of Bare WB Electrode in PBS (pH 7) at scan rate 0.1 V/s.

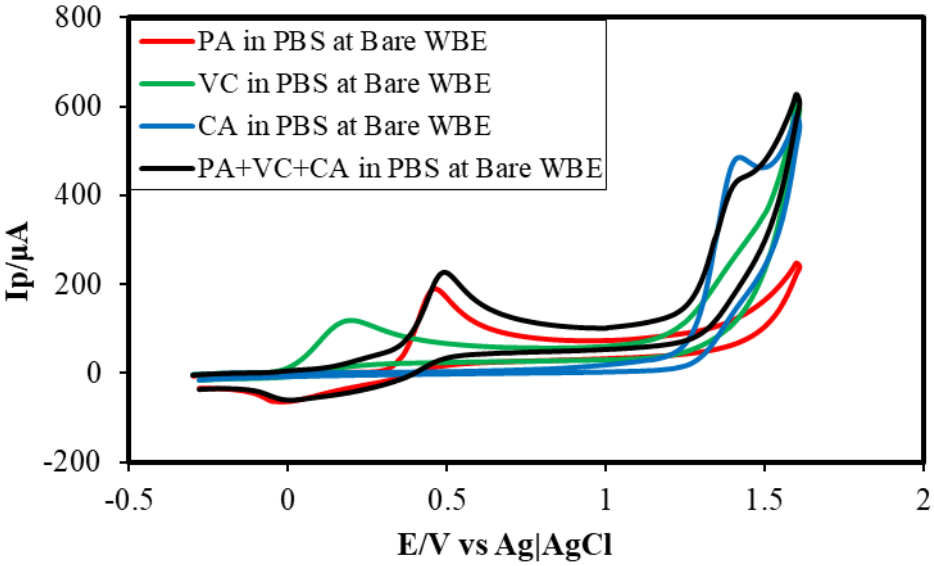

Fig. 4.32: Cyclic voltammogram (CV) of 5 mM VC (green line), 5 mM PA (red line) and 5 mM CA (blue line) and 5 mM VC + 5 mM PA + 5 mM CA (black line) of Bare WB Electrode in PBS (pH 7) at scan rate 0.1 V/s.

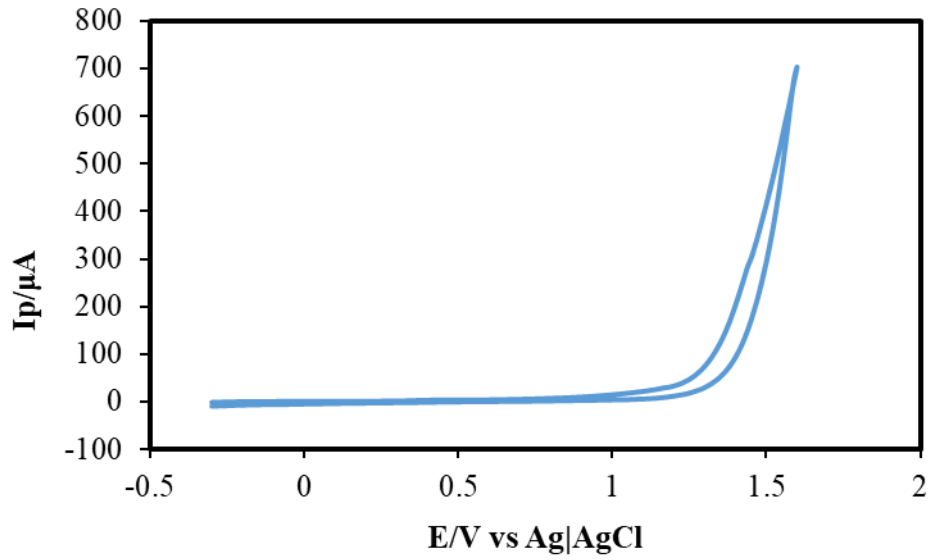

Figure 4.33: Cyclic voltammogram (CV) of APA in PBS (pH 7) at Modified WB electrode at scan rate 0.1 V/s.

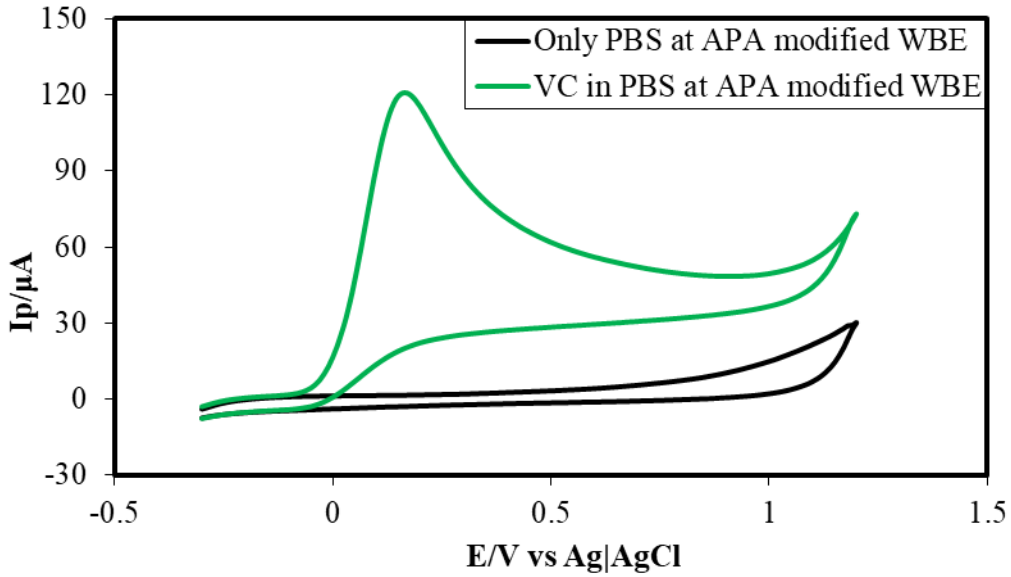

Fig. 4.34: Cyclic voltammogram (CV) of 5 mM VC in 0.5 M PBS (pH 7) (green line) and only 0.5 M PBS (pH 7) (black line) at APA modified WB electrode at scan rate 0.1 V/s.

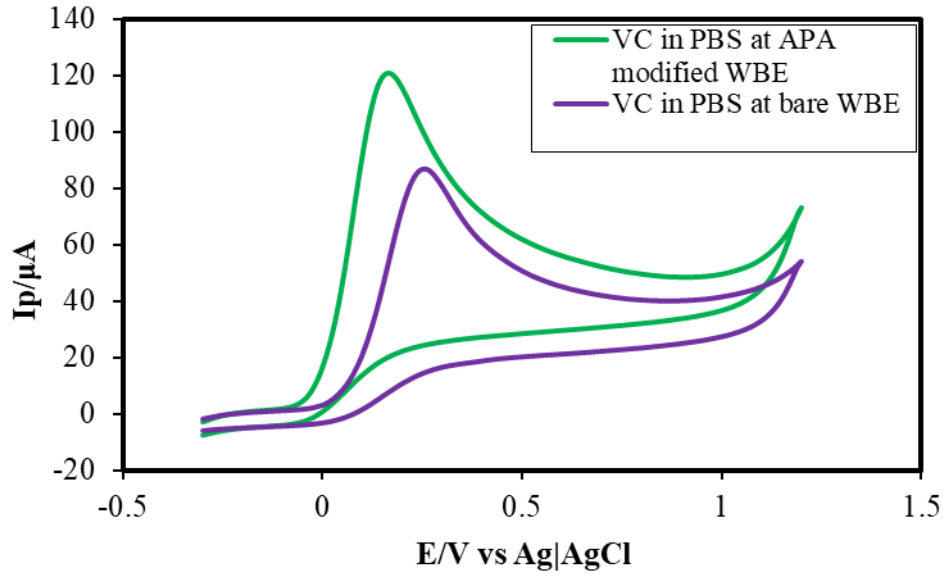

Fig. 4.35: Cyclic voltammogram (CV) of 5 mM VC in 0.5 M PBS (pH 7) at bare (violet line) and APA modified (green line) WB Electrode at scan rate 0.1 V/s.

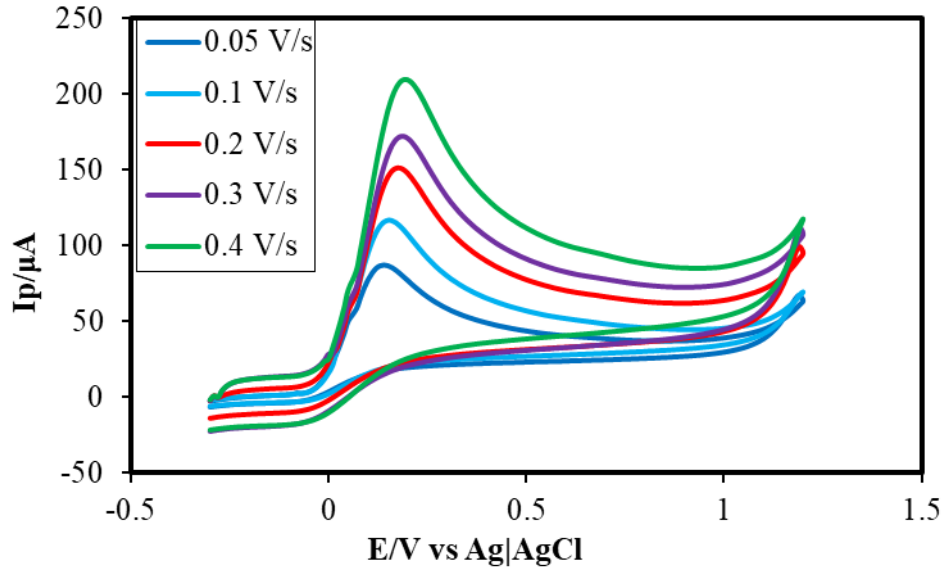

Fig. 4.36: Cyclic Voltammogram (CV) of 5 mM VC at APA Modified WB Electrode in PBS (pH 7) at different scan rate 0.05 V/s, 0.1 V/s, 0.2 V/s, 0.3 V/s and 0.4 V/s.

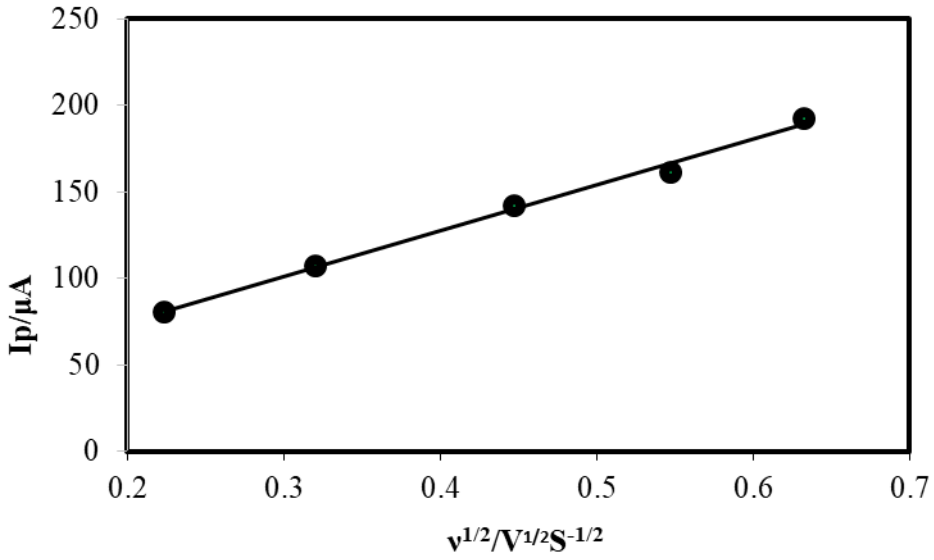

Fig. 4.37: Plots of peak current (Ip) of VC vs square root of scan rate ($v^{1/2}s^{-1/2}$).

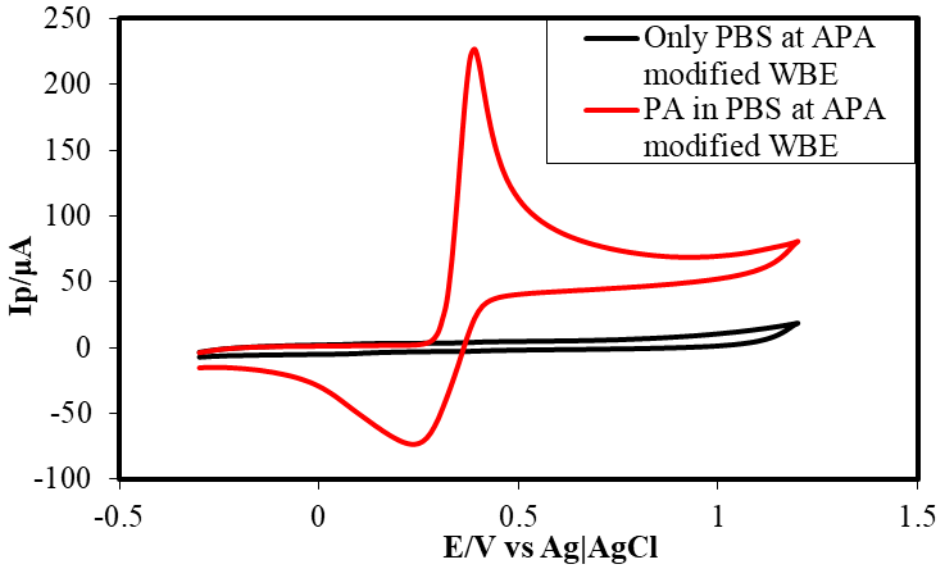

Fig. 4.38: Cyclic Voltammogram (CV) of 5 mM PA in 0.5 M PBS (pH 7) (red line) and only 0.5 M PBS (pH 7) (black line) at APA modified WB Electrode at scan rate 0.1 V/s.

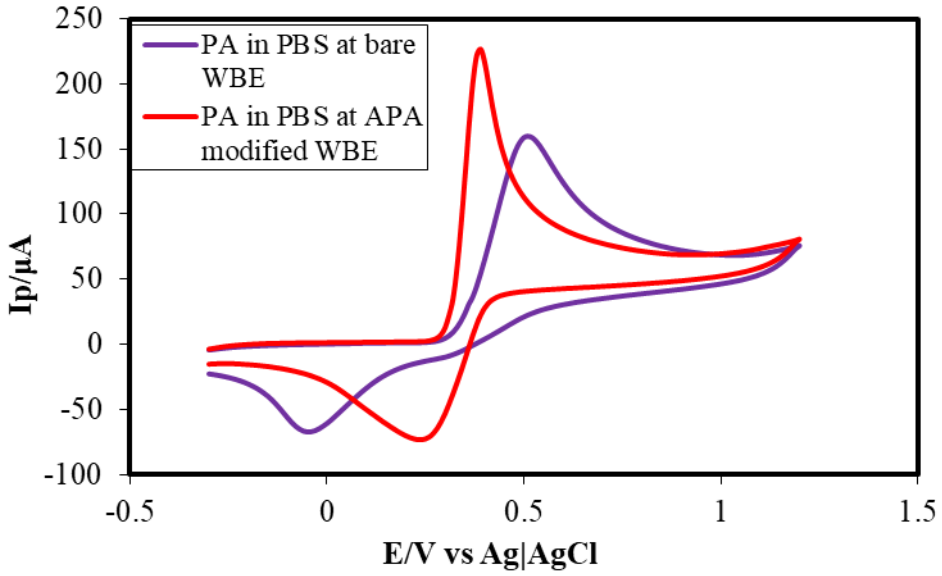

Fig. 4.39: Cyclic Voltammogram (CV) of 5 mM PA in 0.5 M PBS (pH 7) at bare (violet line) and APA modified (red line) WB Electrode at scan rate 0.1 V/s.

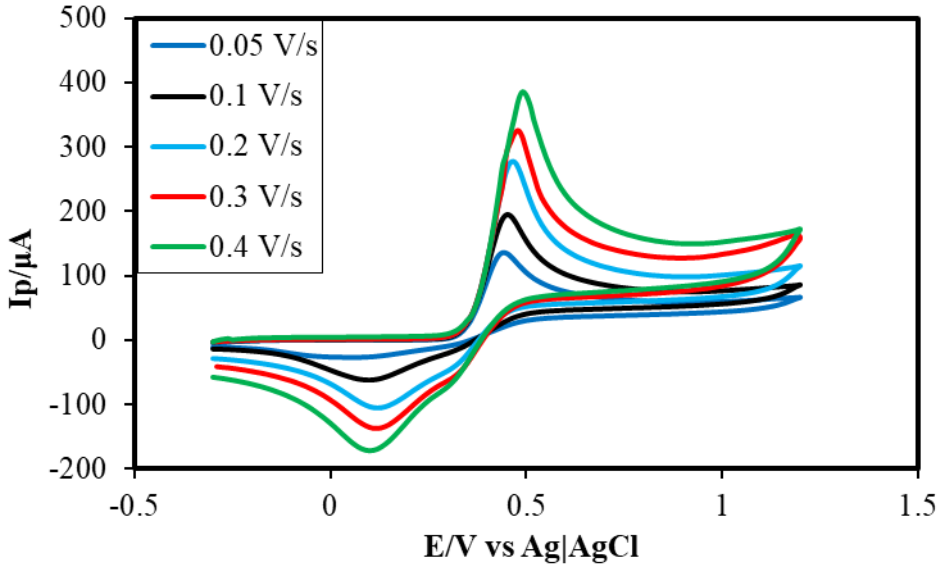

Fig. 4.40: Cyclic Voltammogram (CV) of 5 mM PA at APA Modified WB Electrode in PBS (pH 7) at different scan rate 0.05 V/s, 0.1 V/s, 0.2 V/s, 0.3 V/s and 0.4 V/s.

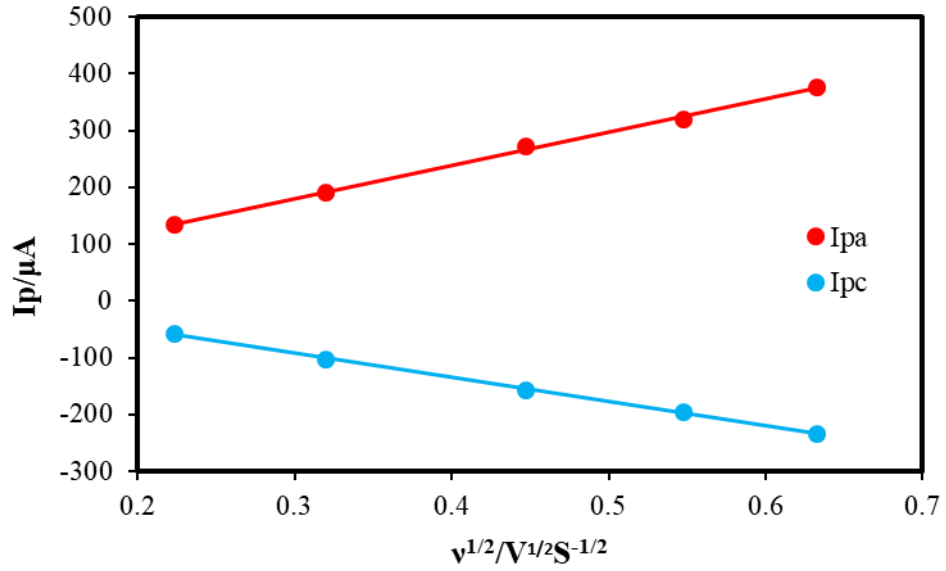

Fig. 4.41: Plots of peak currents (Ipa and Ipc) of PA vs square root of scan rate ($v^{1/2}s^{-1/2}$).

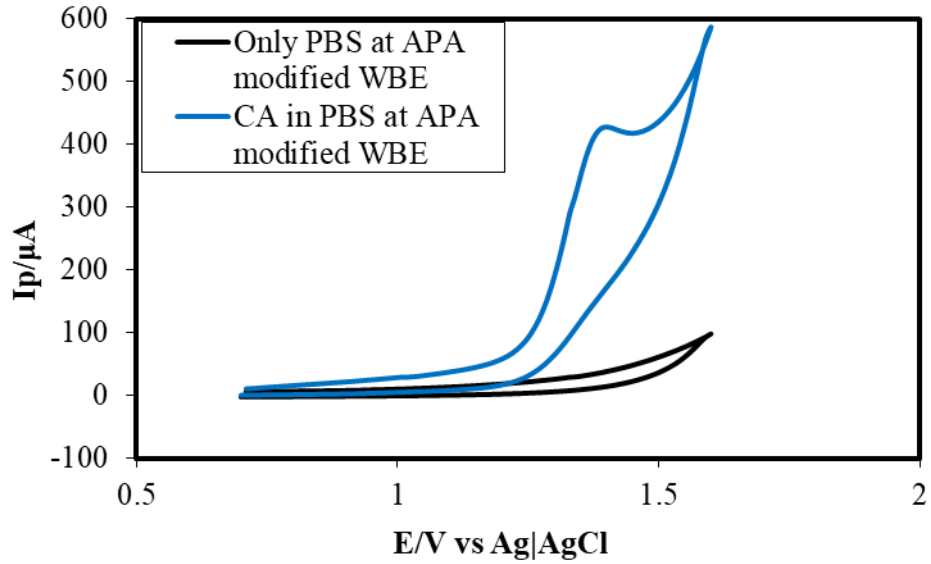

Fig. 4.42: Cyclic voltammogram (CV) of 5 mM CA in 0.5 M PBS (pH 7) (blue line) and only 0.5 M PBS (pH 7) (black line) at APA modified WB Electrode at scan rate 0.1 V/s.

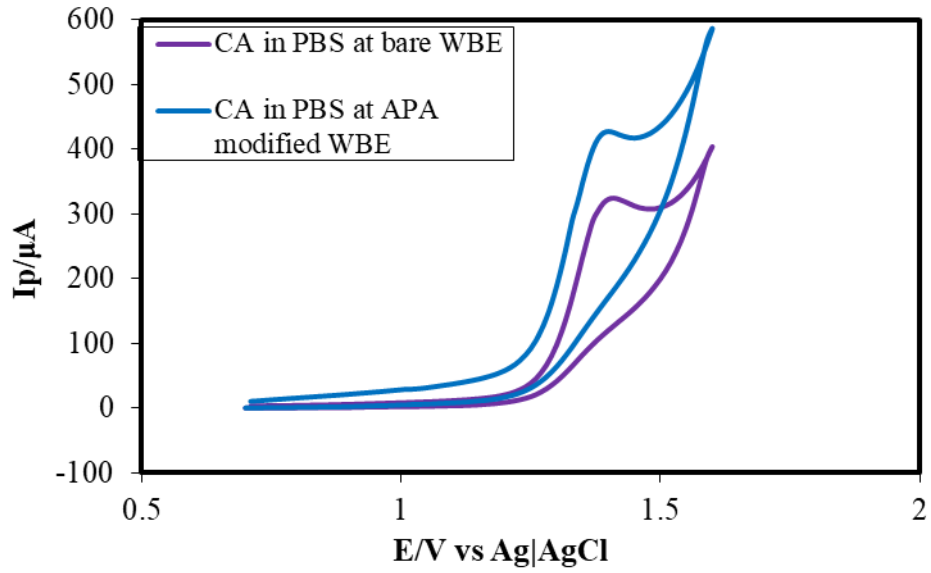

Fig. 4.43: Cyclic voltammogram (CV) of 5 mM CA in 0.5 M PBS (pH 7) at bare (violet line) and APA modified (blue line) WB Electrode at scan rate 0.1 V/s.

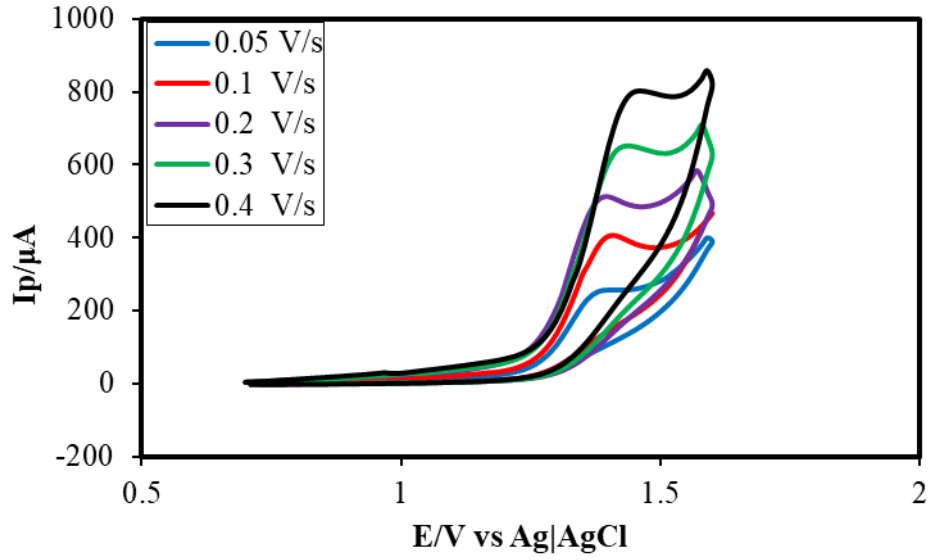

Fig. 4.44: Cyclic Voltammogram (CV) of 5 mM CA at APA Modified WB Electrode in PBS (pH 7) at different scan rate 0.05 V/s, 0.1 V/s, 0.2 V/s, 0.3 V/s and 0.4 V/s.

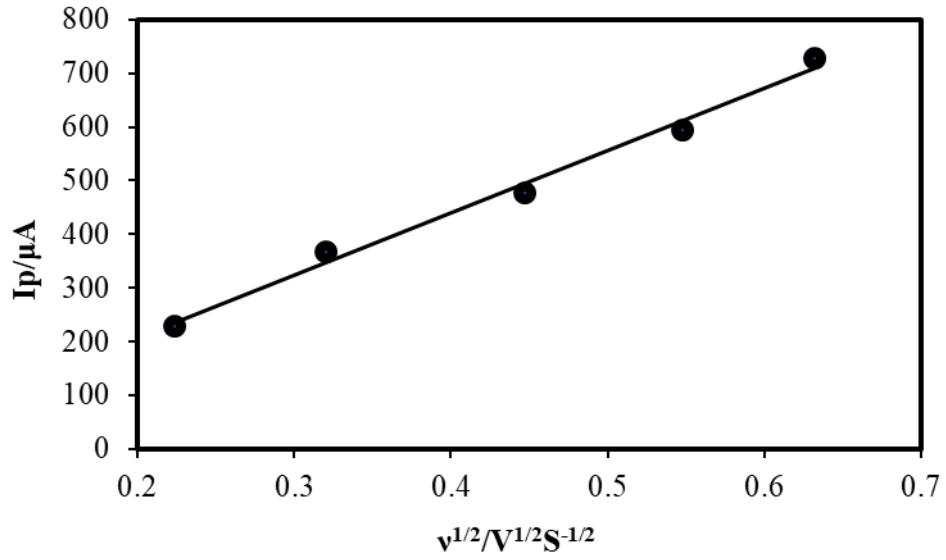

Fig. 4.45: Plots of peak current (Ip) of CA vs square root of scan rate ($v^{1/2}s^{-1/2}$).

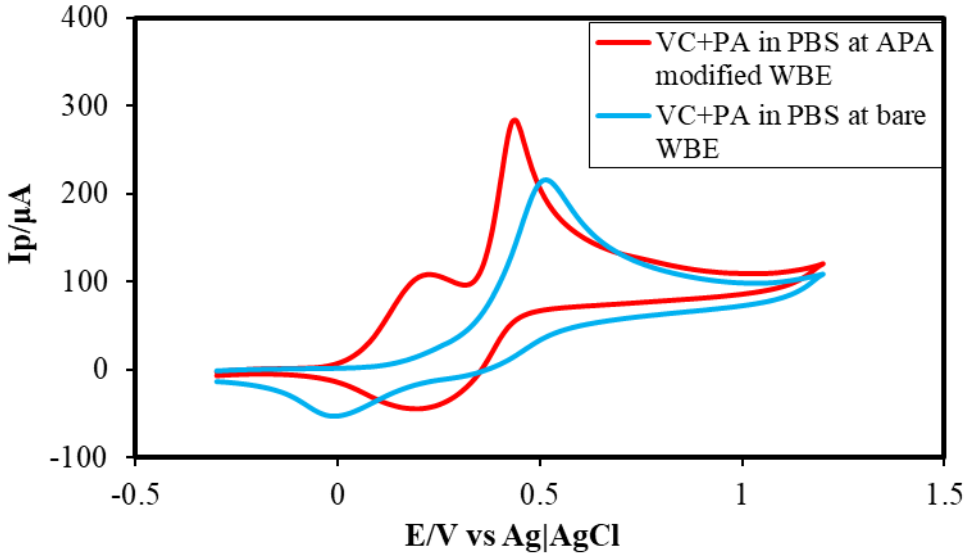

Fig. 4.46: CV comparison of 5 mM VC + 5 mM PA at bare (blue line) and APA modified WB electrode (red line) at scan rate 0.1 V/s.

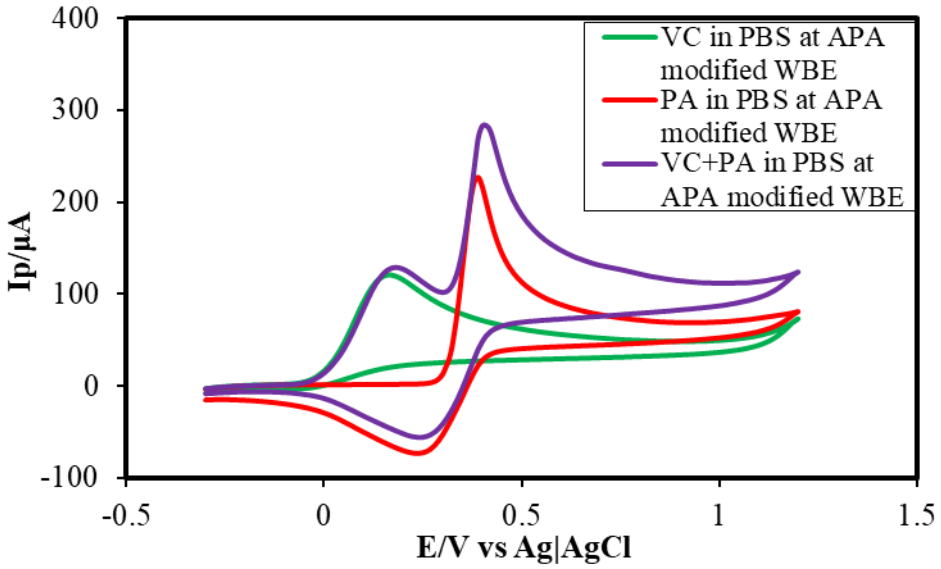

Fig. 4.47: CVs of 5 mM VC (green line), 5 mM PA (red line) and simultaneous 5 mM VC + 5 mM PA (violate line) at APA modified WB electrode at scan rate 0.1 V/s.

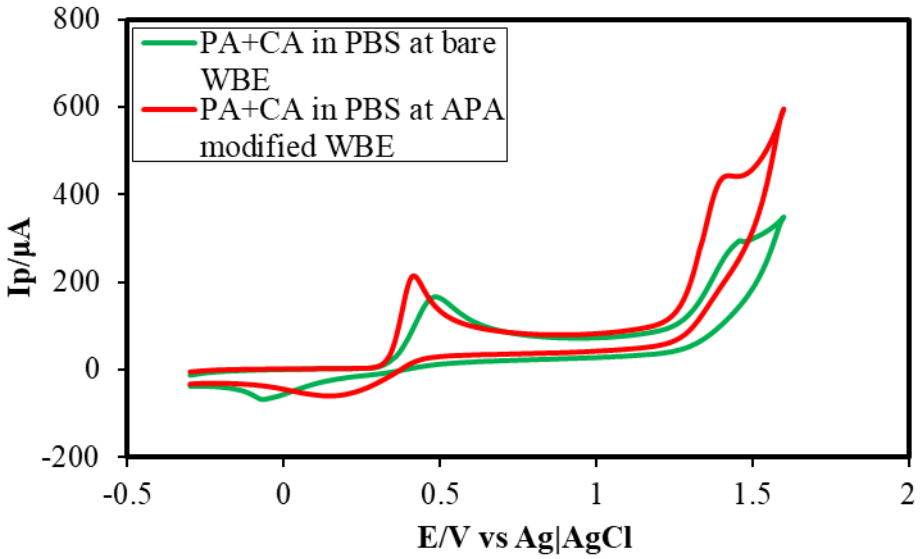

Fig. 4.48: CV comparison of 5 mM PA + 5 mM CA at bare (green line) and APA modified WB electrode (red line) at scan rate 0.1 V/s.

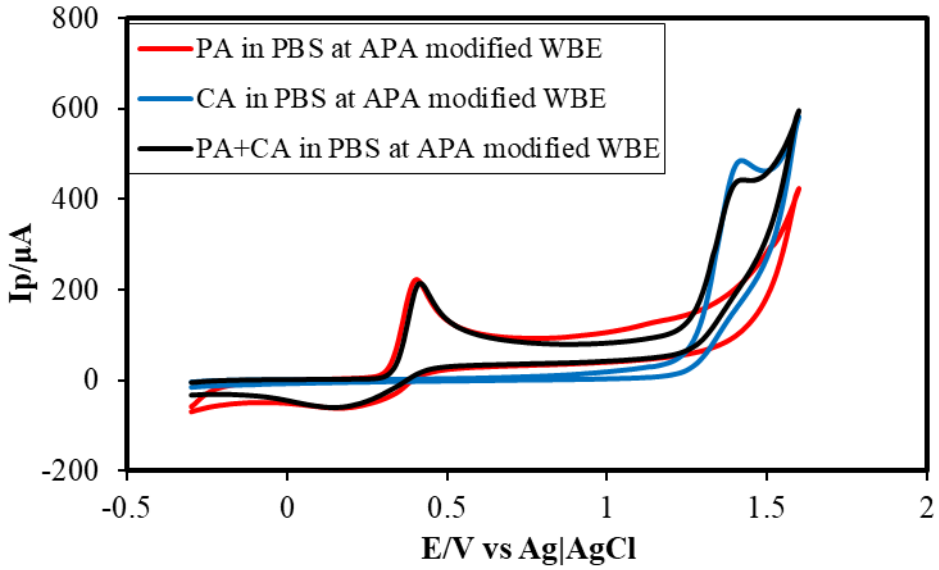

Fig. 4.49: Cyclic voltammograms (CVs) of 5 mM PA (red line), 5 mM CA (blue line) and simultaneous 5 mM PA + 5 mM CA (black line) at APA modified WB electrode at scan rate 0.1 V/s.

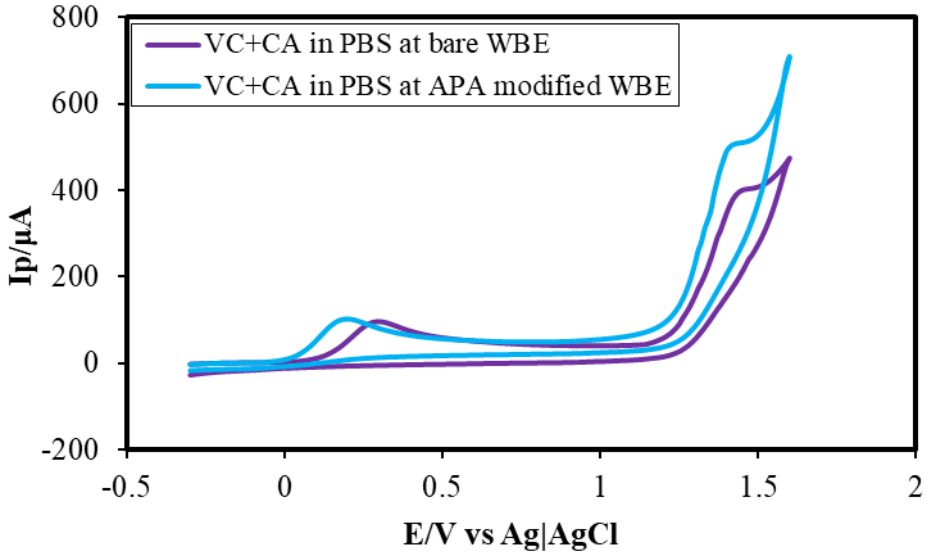

Fig. 4.50: CV comparison of 5 mM VC + 5 mM CA at bare (violet line) and APA modified WB electrode (blue line) at scan rate 0.1 V/s.

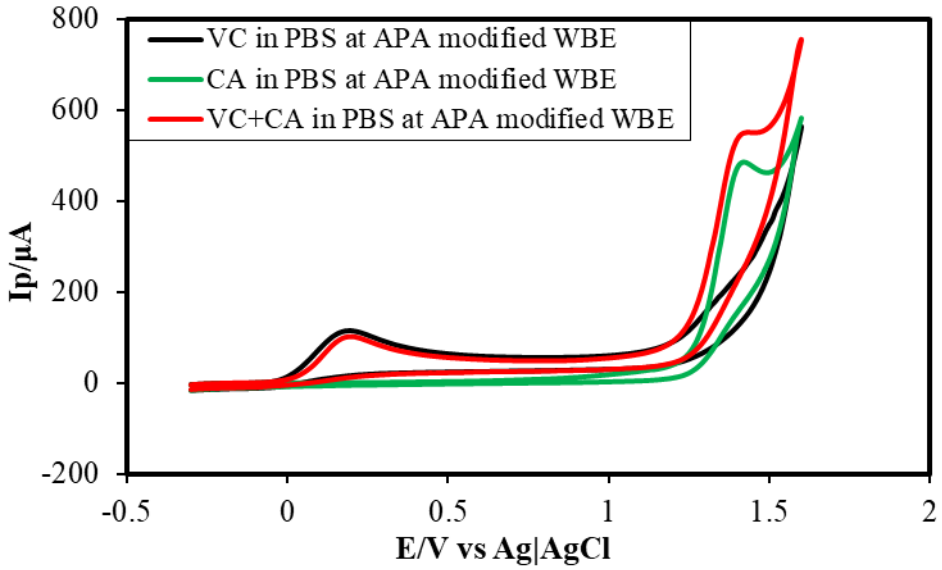

Fig. 4.51: Cyclic voltammograms (CVs) of 5 mM VC (black line), 5 mM CA (green line) and simultaneous 5 mM PA + 5 mM CA (red line) at APA modified WB electrode at scan rate 0.1V/s.

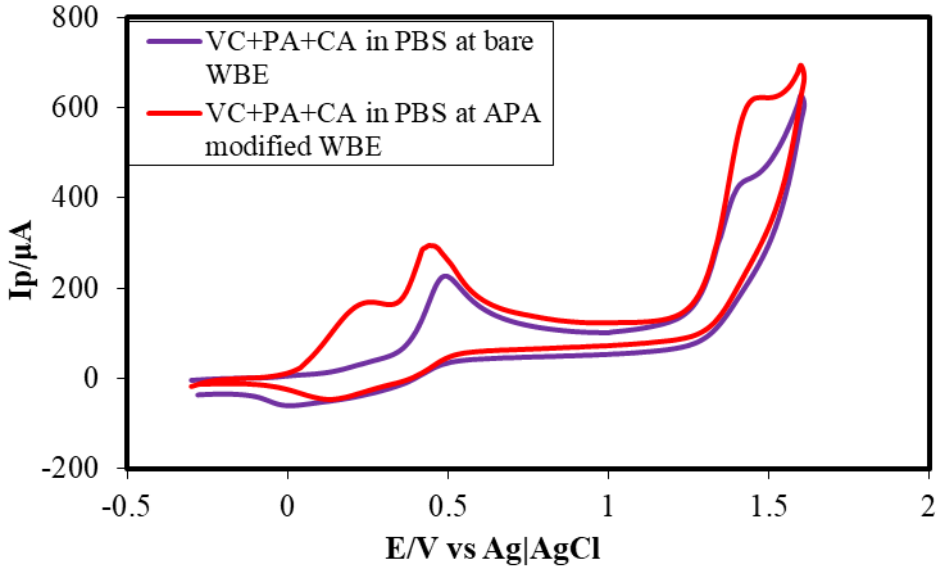

Fig. 4.52: CV comparison of 5 mM VC + 5 mM PA + 5 mM CA at bare (violate line) and APA modified WB electrode (red line) at scan rate 0.1 V/s.

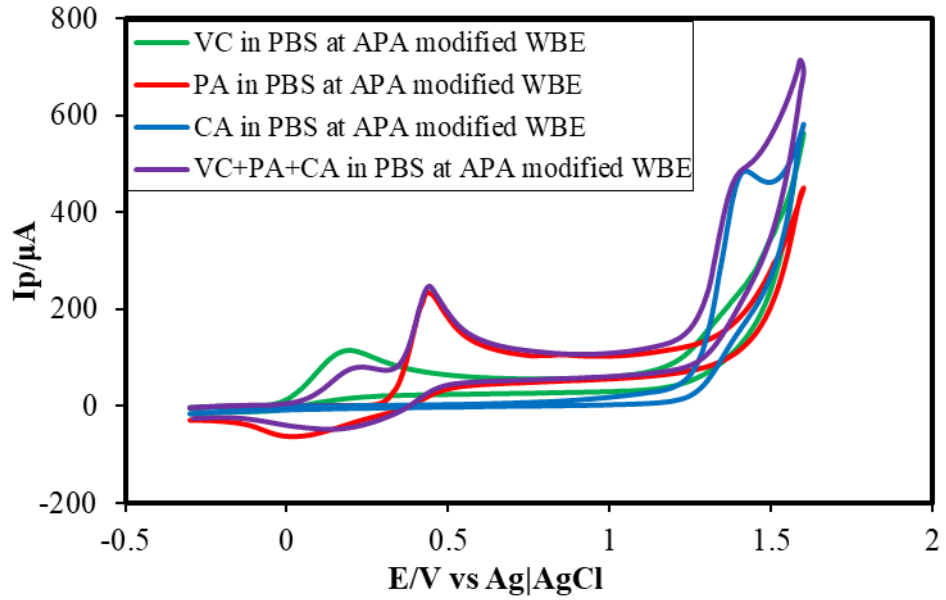

Fig. 4.53: Cyclic voltammograms (CVs) of 5 mM VC (green line), 5 mM PA (red line), 5 mM CA (blue line) and simultaneous 5 mM VC + 5 mM PA + 5 mM CA (violate line) at APA modified WB electrode at scan rate 0.1 V/s.

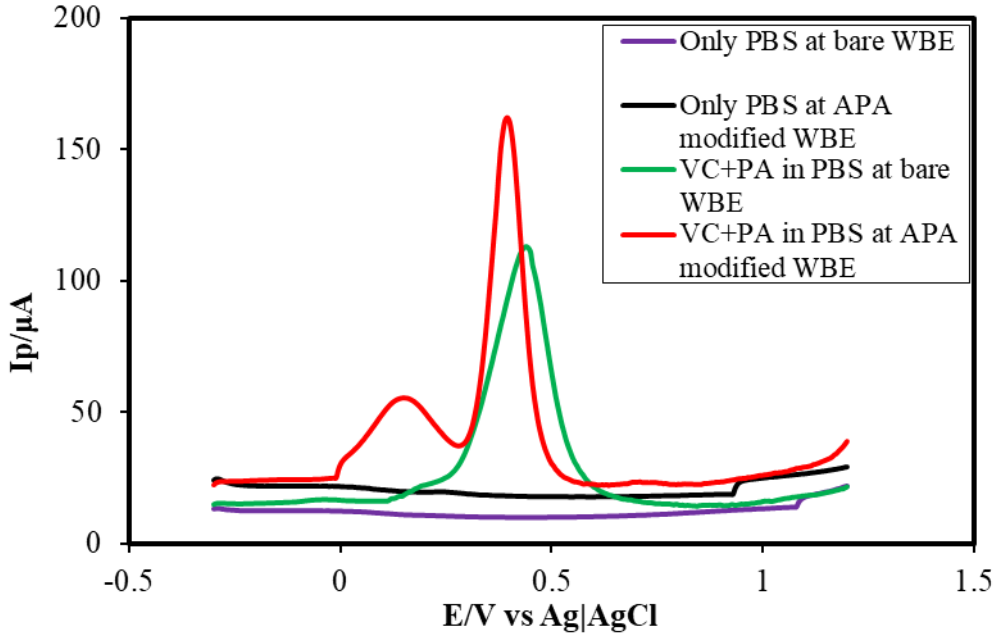

Fig. 4.54: Differential pulse voltammogramms (DPVs) comparison of only PBS (pH 7) at bare (violet line) and APA modified WB electrode (black line) and 5 mM VC + 5 mM PA at bare (green line) and APA modified WB electrode (red line) at scan rate 0.1 V/s.

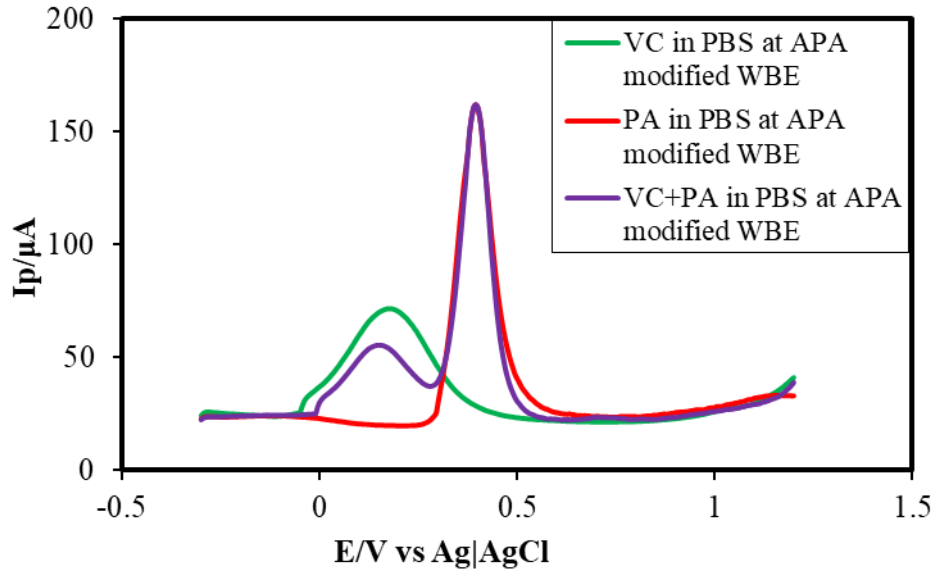

Fig. 4.55: Differential pulse voltammogramms (DPVs) of 5 mM VC (green line), 5 mM PA (red line) and 5 mM VC + 5 mM PA (violate line) in PBS (pH 7) at APA modified WB electrode at scan rate 0.1 V/s.

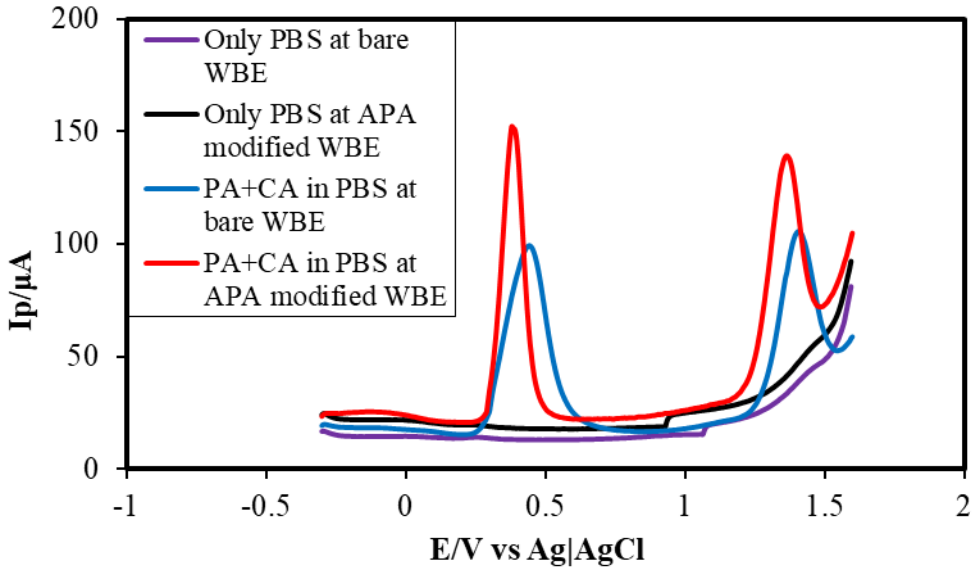

Fig. 4.56: Differential pulse voltammogramms (DPVs) comparison of only PBS (pH 7) at bare (violet line) and APA modified WB electrode (black line) and 5 mM PA + 5 mM CA at bare (blue line) and APA modified WB electrode (red line) at scan rate 0.1 V/s.

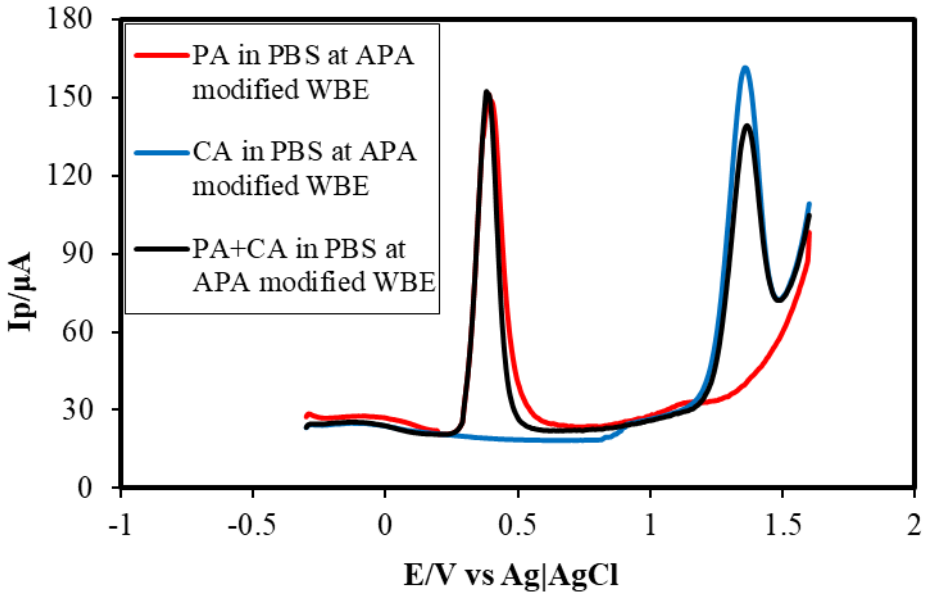

Fig. 4.57: Differential pulse voltammogramms (DPVs) of 5 mM PA (red line), 5 mM CA (blue line) and 5 mM PA + 5 mM CA (black line) in PBS (pH 7) at APA modified WB electrode at scan rate 0.1 V/s.

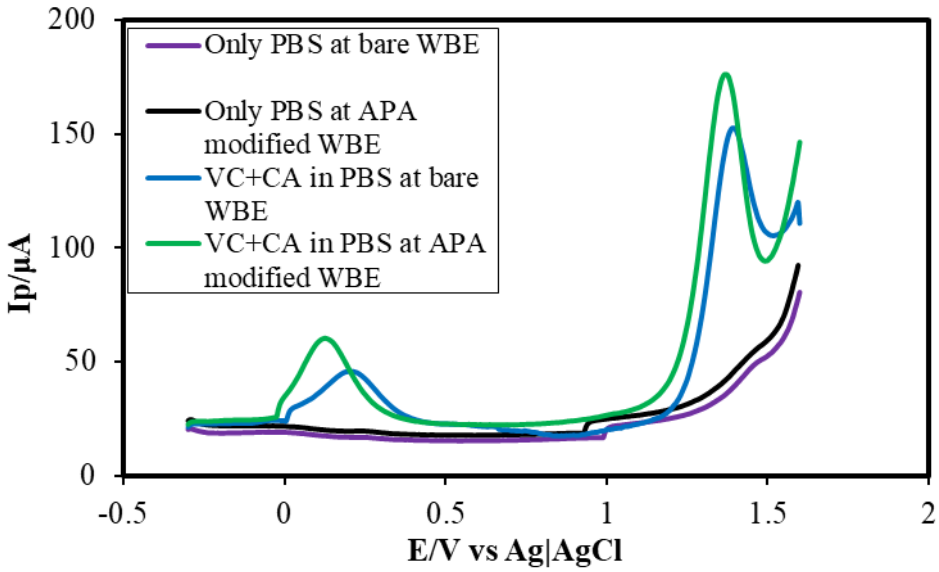

Fig. 4.58: Differential pulse voltammogramms (DPVs) comparison of only PBS (pH 7) at bare (violet line) and APA modified WB electrode (black line) and 5 mM VC + 5mM CA at bare (blue line) and APA modified WB electrode (green line) at scan rate 0.1 V/s.

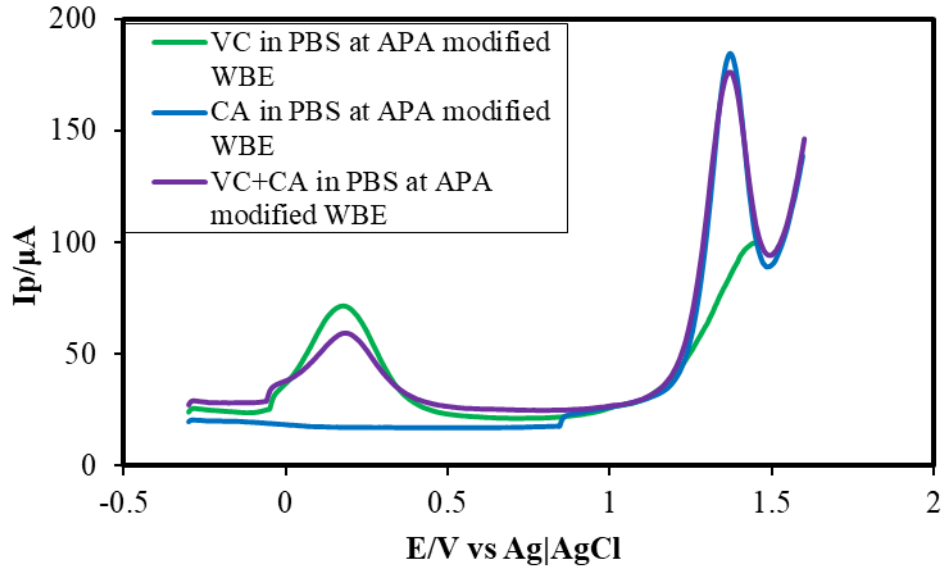

Fig. 4.59: Differential pulse voltammogramms (DPVs) of 5 mM VC (green line), 5 mM CA (blue line) and 5 mM VC + 5 mM CA (violate line) in PBS (pH 7) at APA modified WB electrode at scan rate 0.1 V/s.

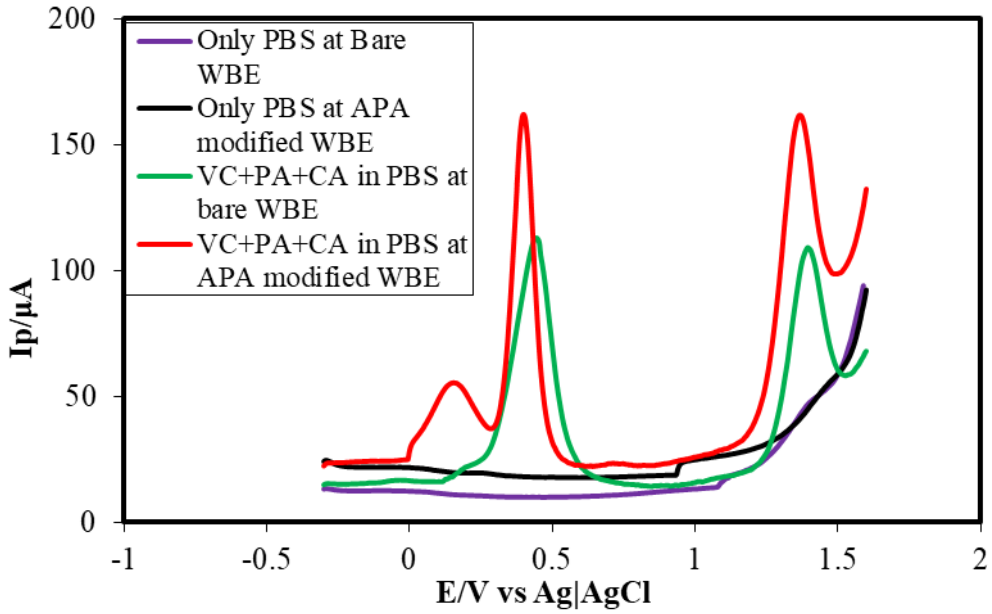

Fig. 4.60: Differential pulse voltammogramms (DPVs) comparison of only PBS (pH 7) at bare (orange line) and APA modified WB electrode (black line) and 5 mM VC + 5 mM PA + 5 mM CA at bare (green line) and APA modified WB electrode (red line) at scan rate 0.1 V/s.

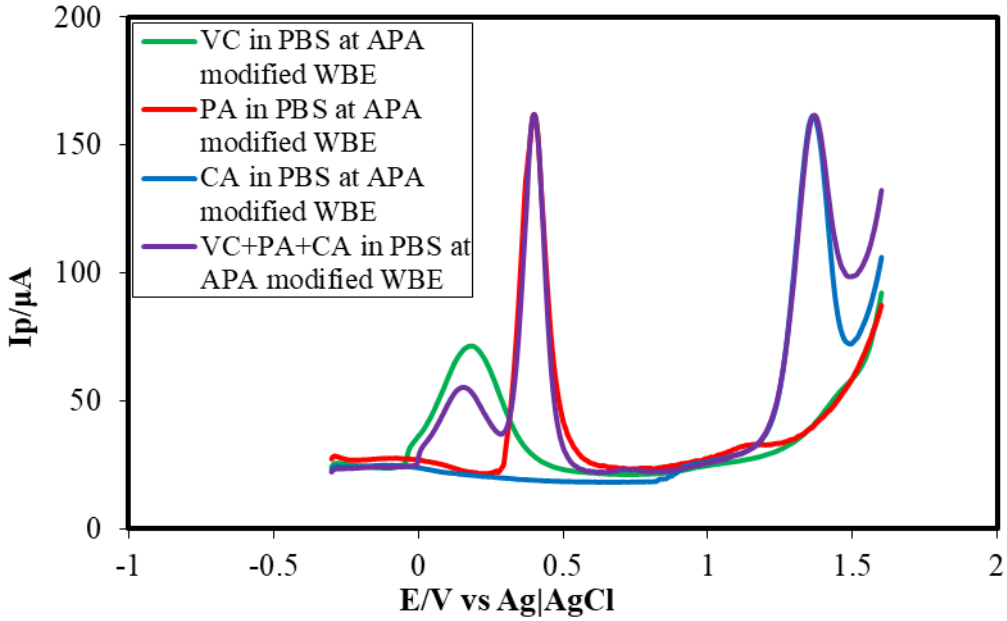

Fig. 4.61: Differential pulse voltammogramms (DPVs) of 5 mM VC (green line), 5 mM PA (red line) and 5 mM CA (blue line) and 5 mM VC + 5 mM PA + 5 mM CA (violate line) in PBS (pH 7) at APA modified WB electrode at scan rate 0.1 V/s.

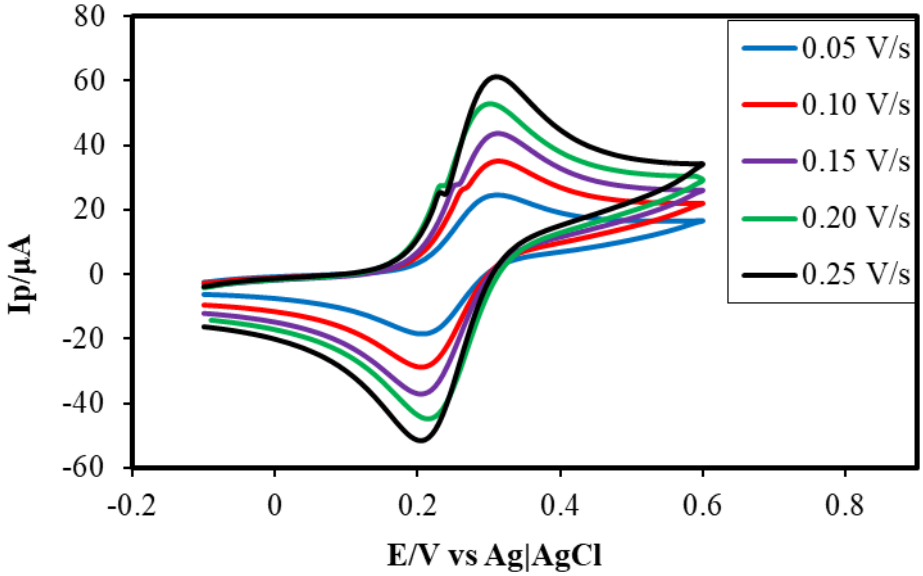

Figure 4.62: Cyclic voltammograms (CVs) of 2 mM potassium ferrocyanide at bare WB electrode at the scan rate of 0.05 V/s, 0.10 V/s, 0.15 V/s, 0.20 V/s and 0.25 V/s in 1 M KCl as supporting electrolyte.

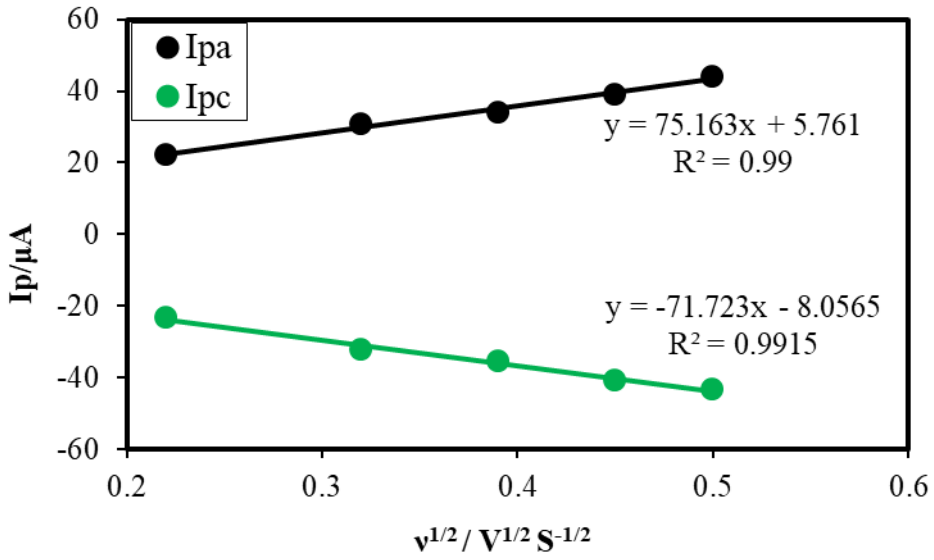

Fig. 4.63: The anodic and the cathodic peak current of ferrocyanide vs square root of the scan rates.

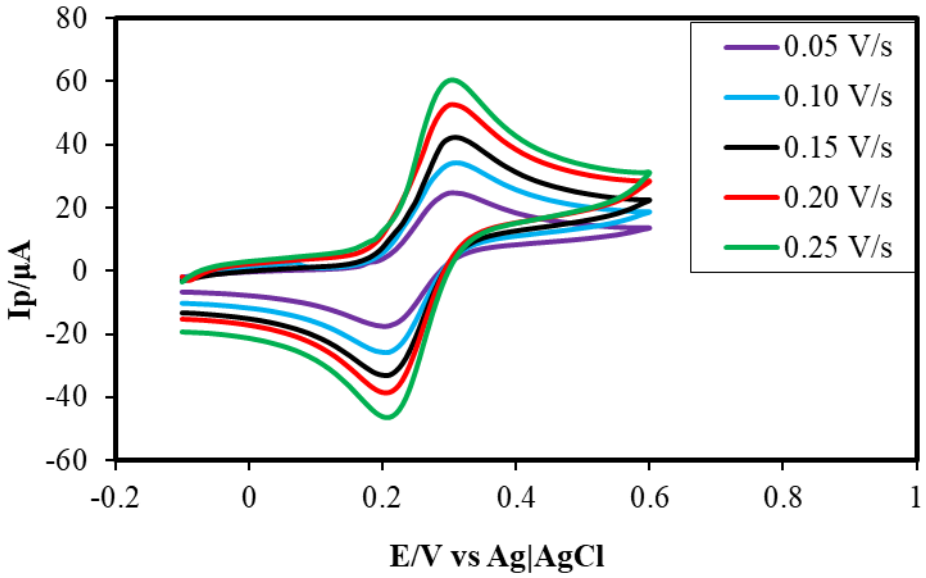

Figure 4.64: Cyclic voltammograms (CVs) of 2 mM potassium ferrocyanide on APA modified WB electrode at different scan rate of 0.05 V/s, 0.10 V/s, 0.15 V/s, 0.20 V/s and 0.25 V/s in 1 M KCl as supporting electrolyte.

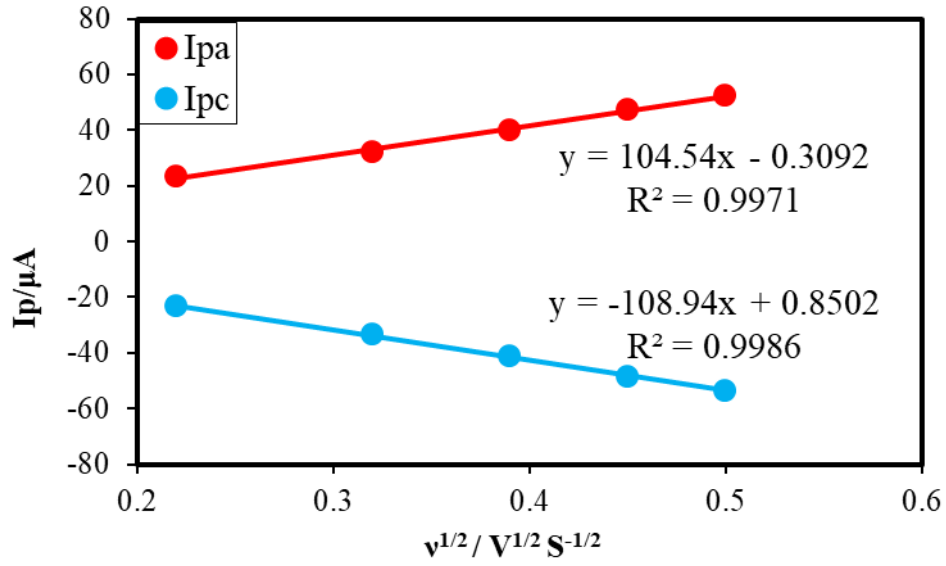

Fig. 4.65: The anodic and the cathodic peak current of ferrocyanide vs square root of the scan rates.

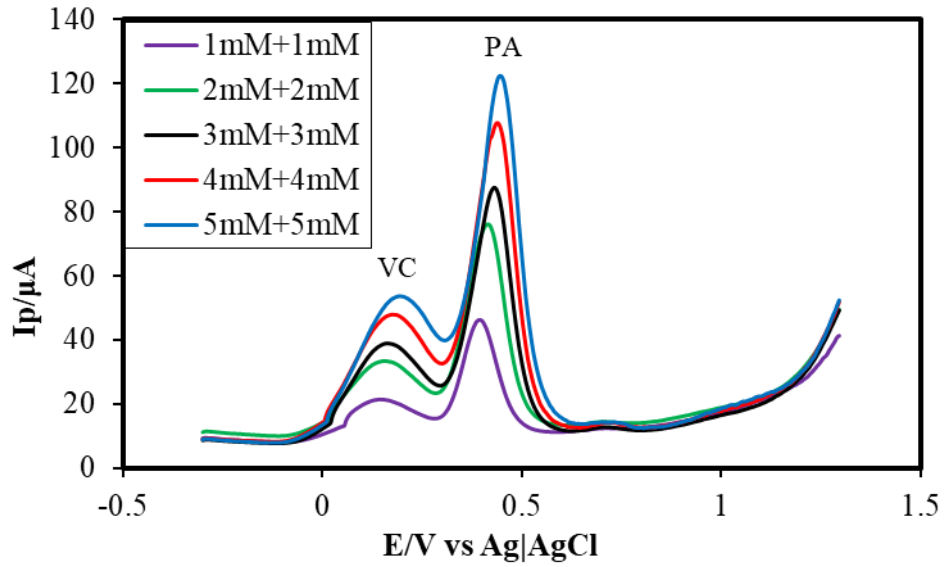

Fig. 4.66: DPVs of simultaneous change of VC + PA (1-5 mM) at APA modified WB electrode in PBS (pH 7) at scan rate 0.1 V/s.

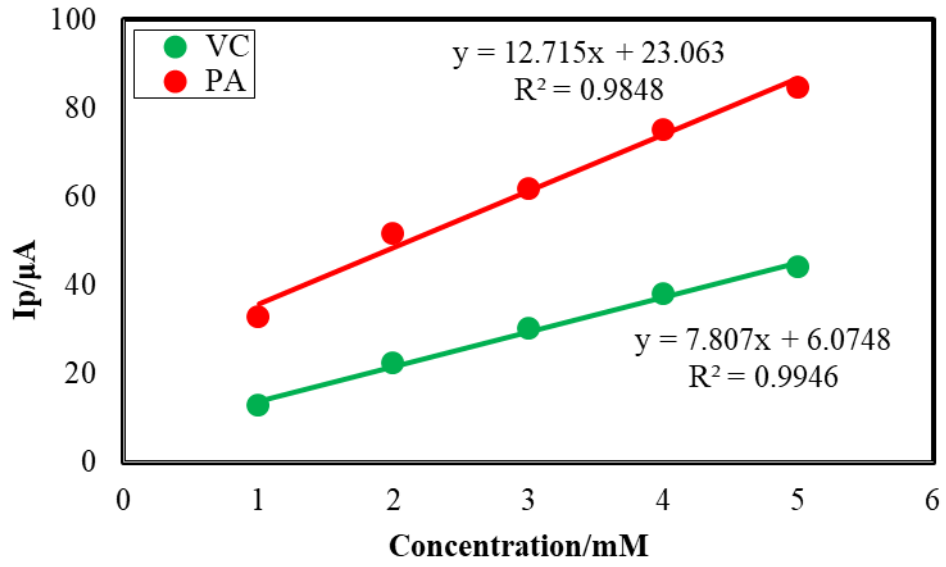

Fig. 4.67: Calibration curve for simultaneous estimation of VC (green markers) and PA (red markers) in a binary mixture at APA modified WB electrode.

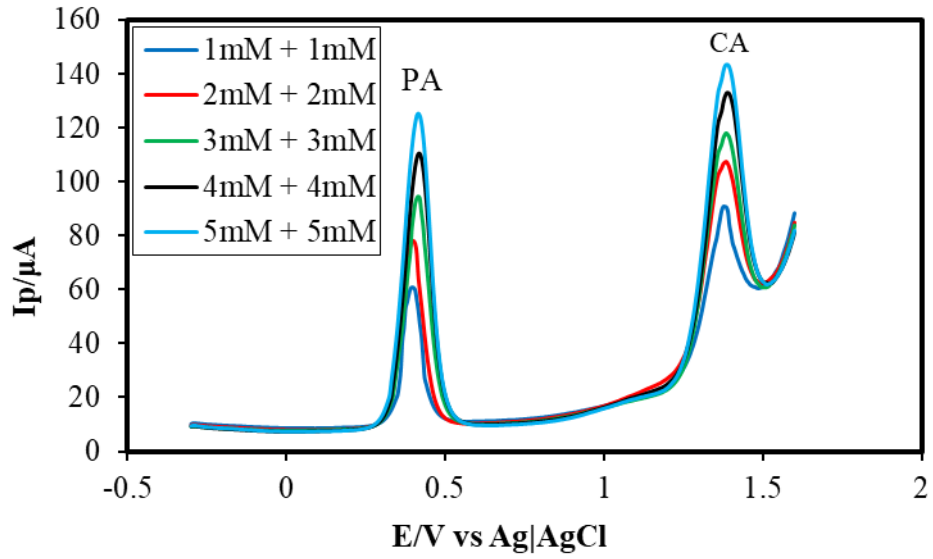

Fig. 4.68: DPVs of simultaneous change of PA + CA (1-5 mM) at APA modified WB electrode in PBS (pH 7) at scan rate 0.1 V/s.

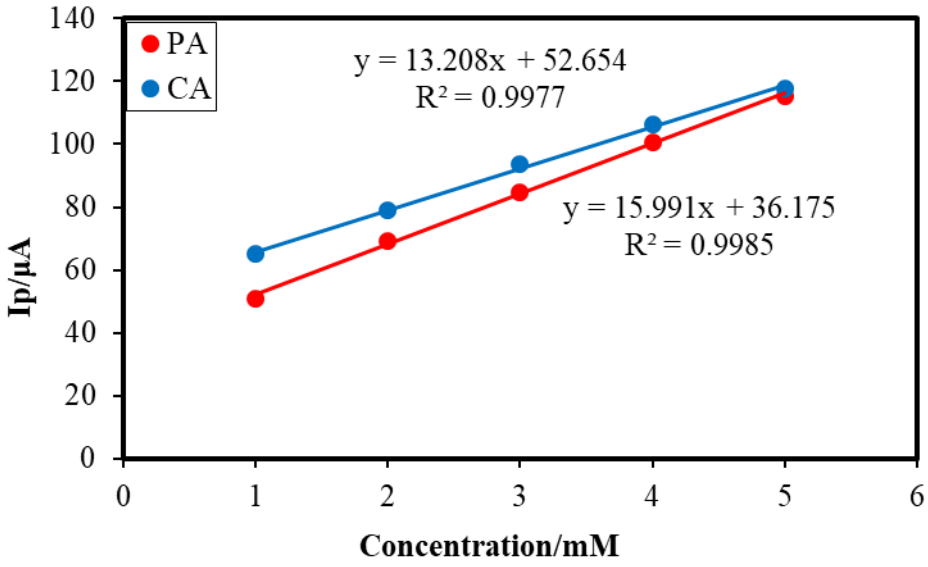

Fig. 4.69: Calibration curve for simultaneous estimation of PA (red markers) and CA (blue markers) in a binary mixture at APA modified WB electrode.

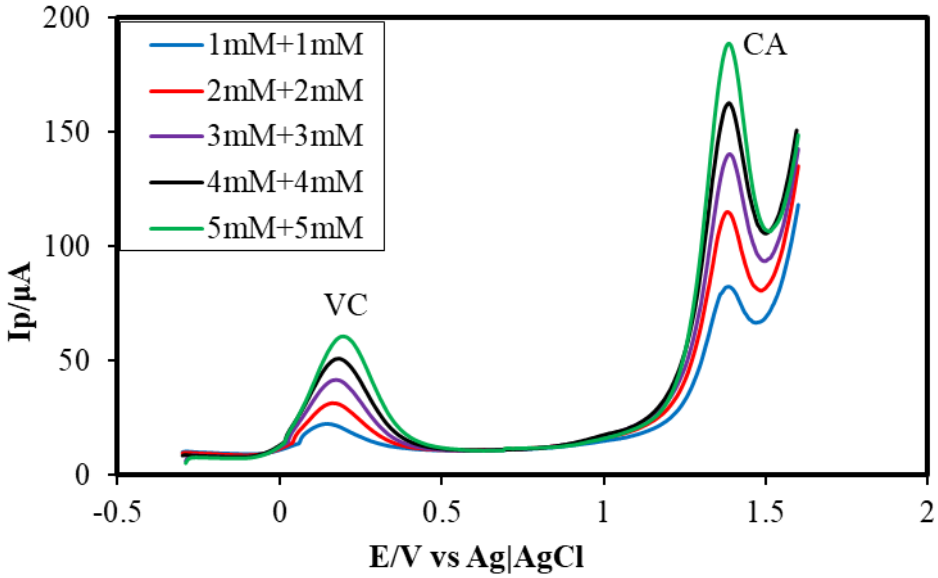

Fig. 4.70: DPVs of simultaneous change of VC + CA (1-5 mM) of APA modified WB electrode in PBS (pH 7) at scan rate 0.1 V/s.

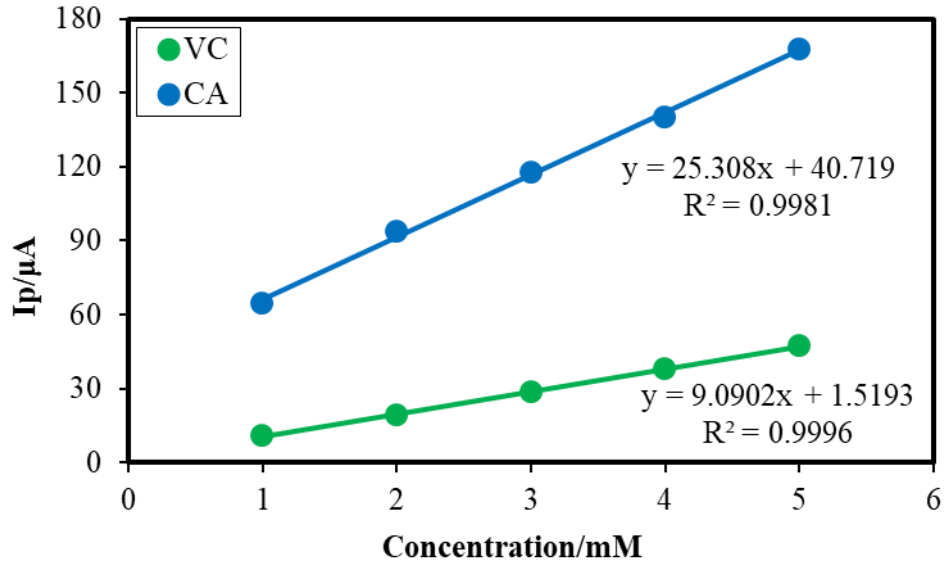

Fig. 4.71: Calibration curve for simultaneous estimation of VC (green markers) and CA (blue markers) in a binary mixture at APA modified WB electrode.

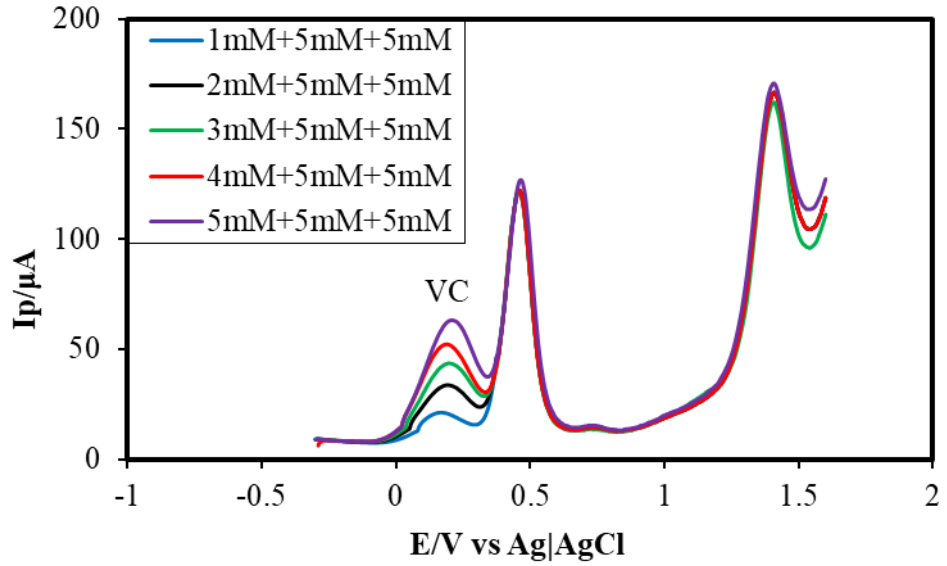

Fig. 4.72: DPV of different concentration of VC (1-5 mM) in constant PA + CA concentration (5 mM) ternary mixture in PBS (pH 7) at APA modified WB electrode at scan rate 0.1 V/s.

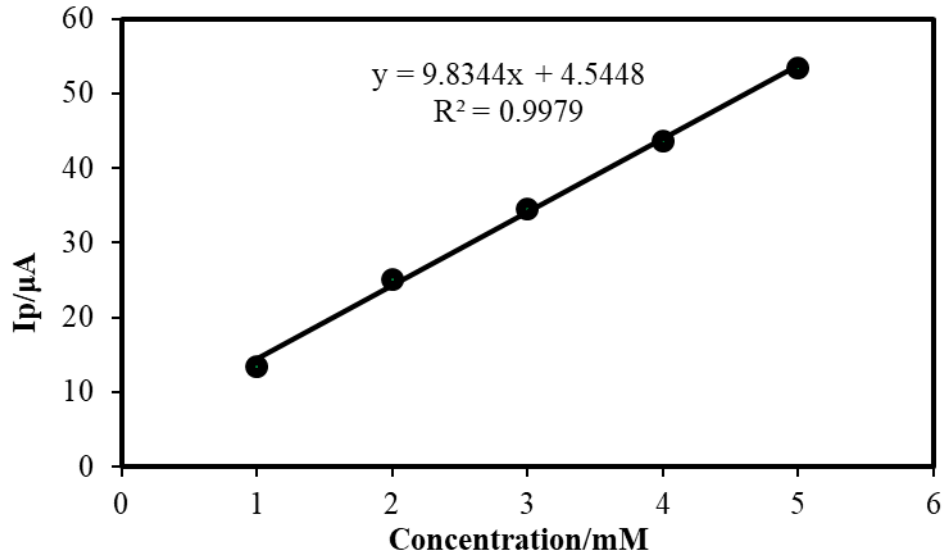

Fig. 4.73: Plots of peak currents (Ip) of VC vs concentrations (1-5 mM) at constant concentration of PA + CA (5 mM) in a ternary mixture of VC + PA + CA at APA modified WB electrode.

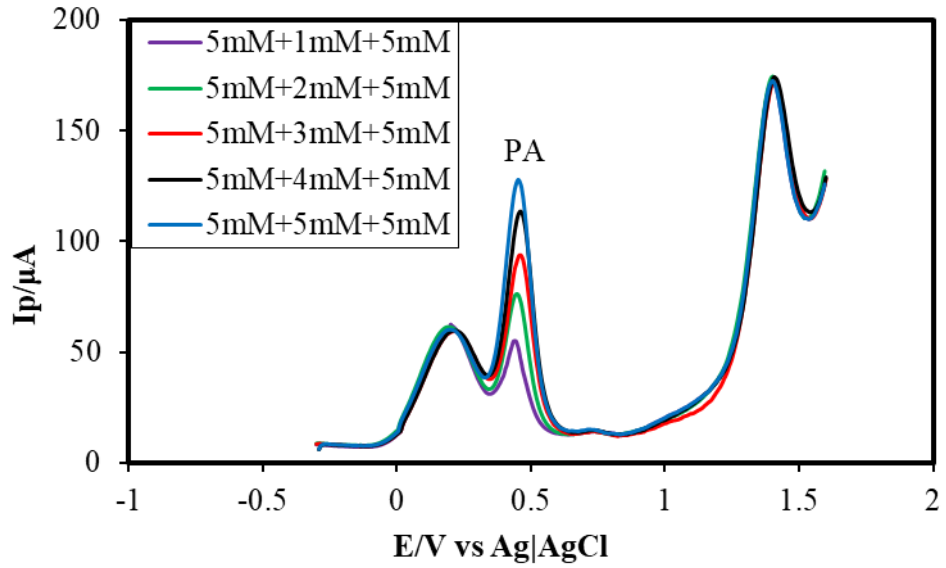

Fig. 4.74: DPV of different concentration of PA (1-5 mM) in constant VC + CA concentration (5 mM) ternary mixture in PBS (pH 7) at APA modified WB electrode at scan rate 0.1 V/s.

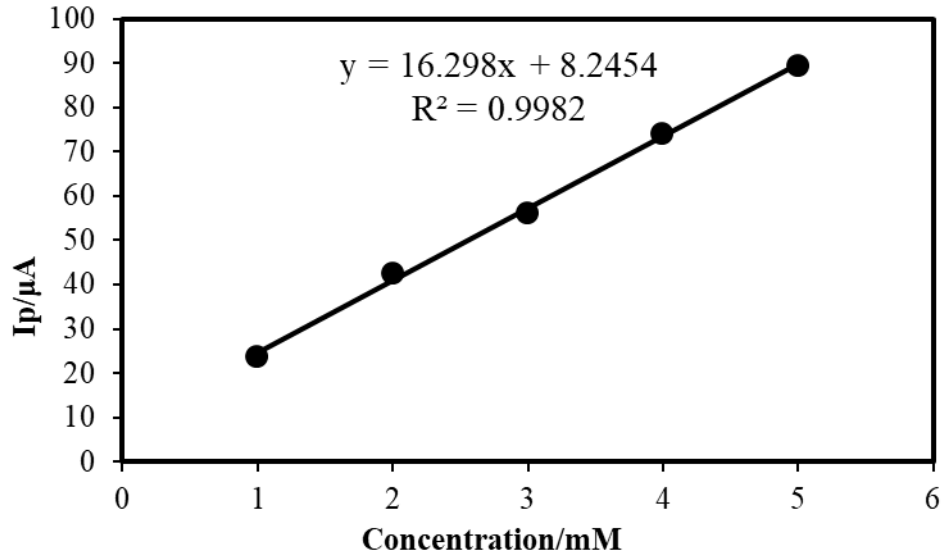

Fig. 4.75: Plots of peak currents (Ip) of PA vs concentrations (1-5 mM) at constant concentration of VC + CA (5 mM) in a ternary mixture of VC + PA + CA at APA modified WB electrode.

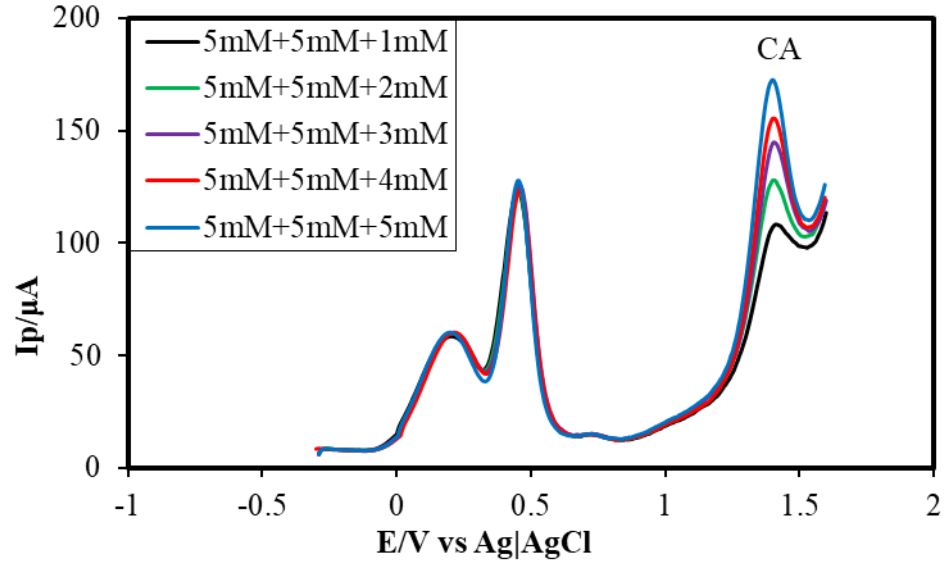

Fig. 4.76: DPV of different concentration of CA (1-5 mM) in constant VC + PA concentration (5 mM) ternary mixture in PBS (pH 7) at APA modified WB electrode at scan rate 0.1V/s.

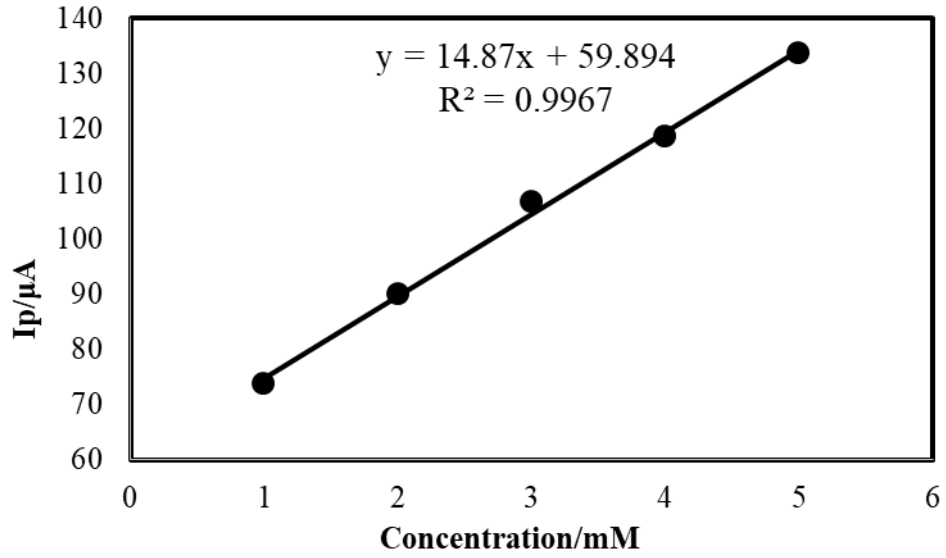

Fig. 4.77: Plots of peak currents (Ip) of CA vs concentrations (1-5 mM) at constant concentration of VC + PA (5 mM) in a ternary mixture of VC + PA + CA at APA modified WB electrode.

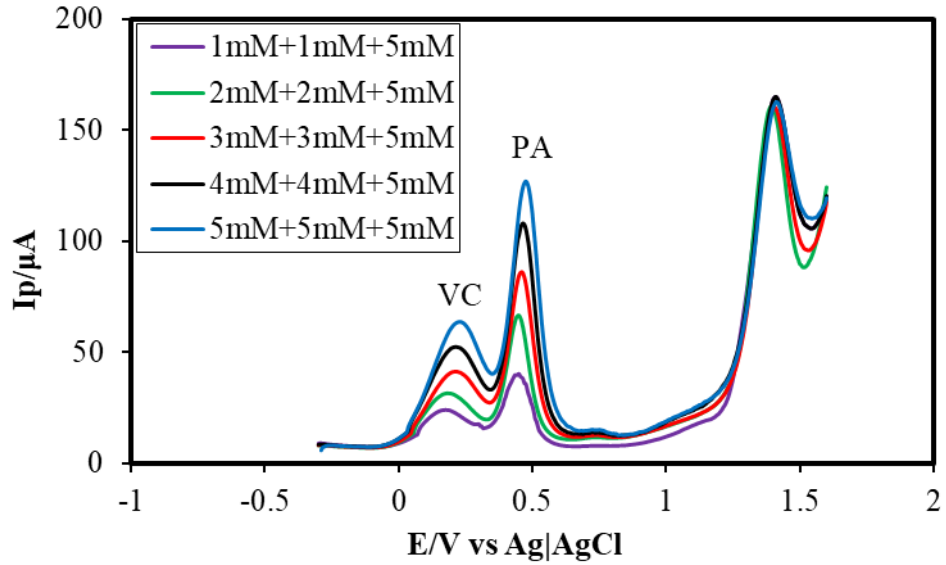

Fig. 4.78: DPV of different concentration of VC + PA (1-5 mM) in constant CA concentration (5 mM) ternary mixture in PBS (pH 7) at APA modified WB electrode at scan rate 0.1 V/s.

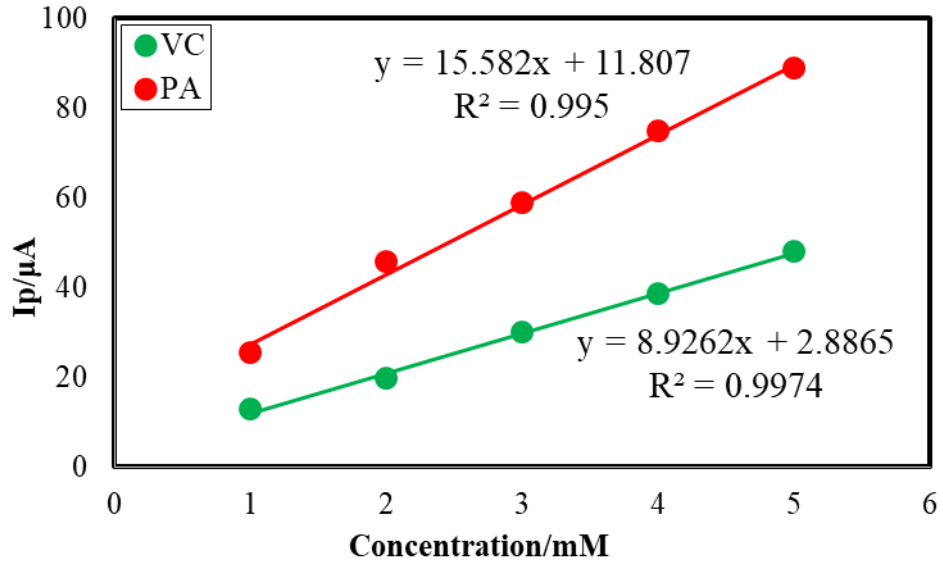

Fig. 4.79: Plots of peak currents (Ip) of VC and PA vs concentrations (1-5 mM) at constant concentration of CA (5 mM) in a ternary mixture of VC + PA + CA at APA modified WB electrode.

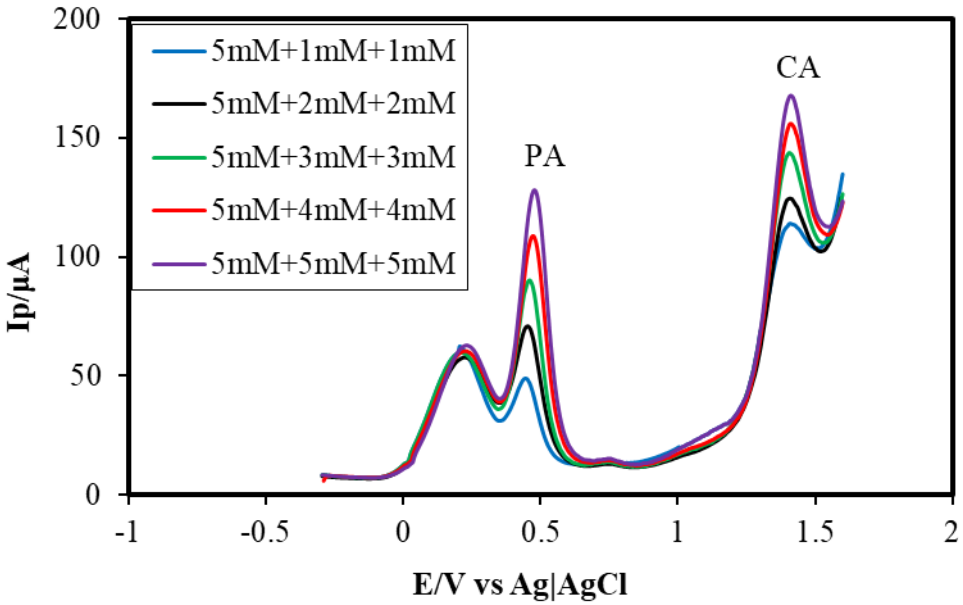

Fig. 4.80: DPV of different concentration of PA + CA (1-5 mM) in constant VC concentration (5 mM) ternary mixture in PBS (pH 7) at APA modified WB electrode at scan rate 0.1V/s.

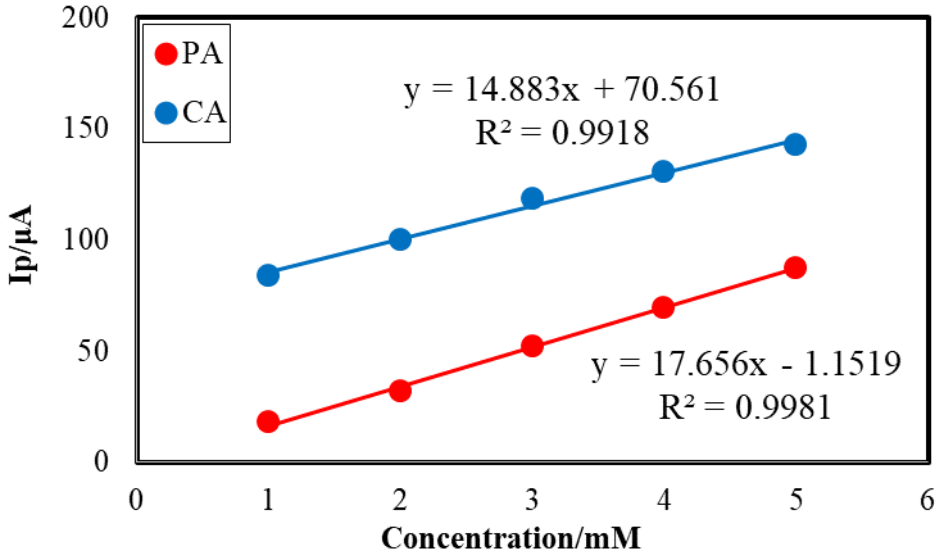

Fig. 4.81: Plots of peak currents (Ip) of PA and CA vs concentrations (1-5 mM) at constant concentration of VC (5 mM) in a ternary mixture of VC + PA + CA at APA modified WB electrode.

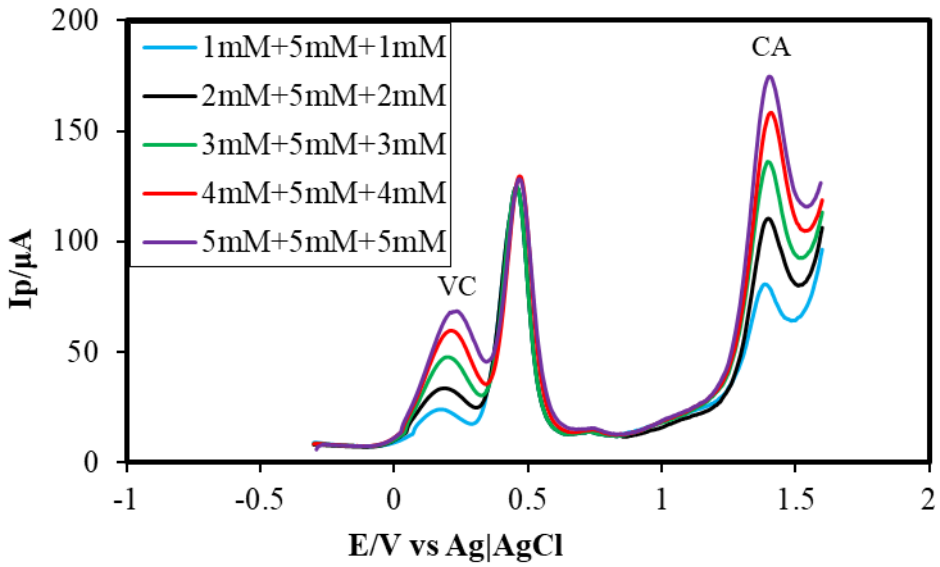

Fig. 4.82: DPV of different concentration of VC + CA (1-5 mM) in constant PA concentration (5 mM) ternary mixture in PBS (pH 7) at APA modified WB electrode at scan rate 0.1V/s.

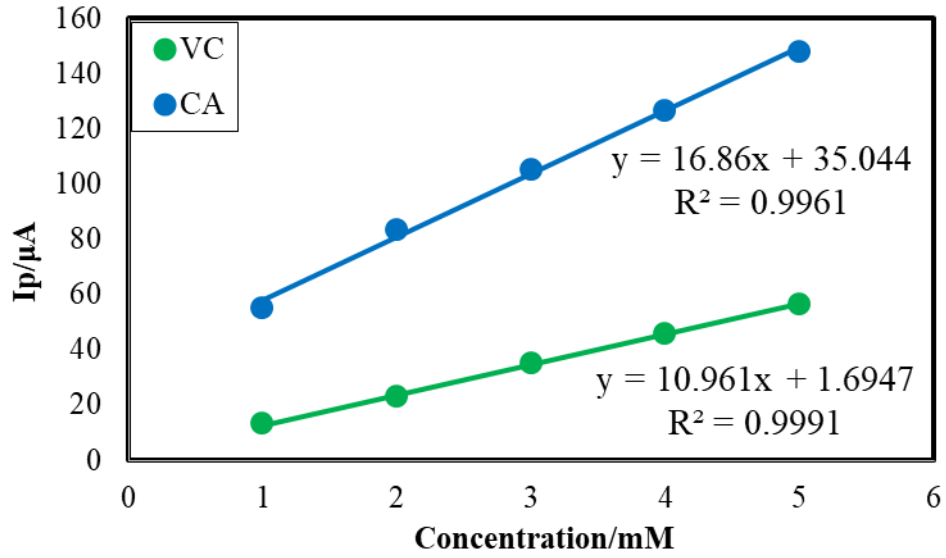

Fig. 4.83: Plots of peak currents (Ip) of VC and CA vs concentrations (1-5 mM) at constant concentration of PA (5 mM) in a ternary mixture of VC + PA + CA at APA modified WB electrode.

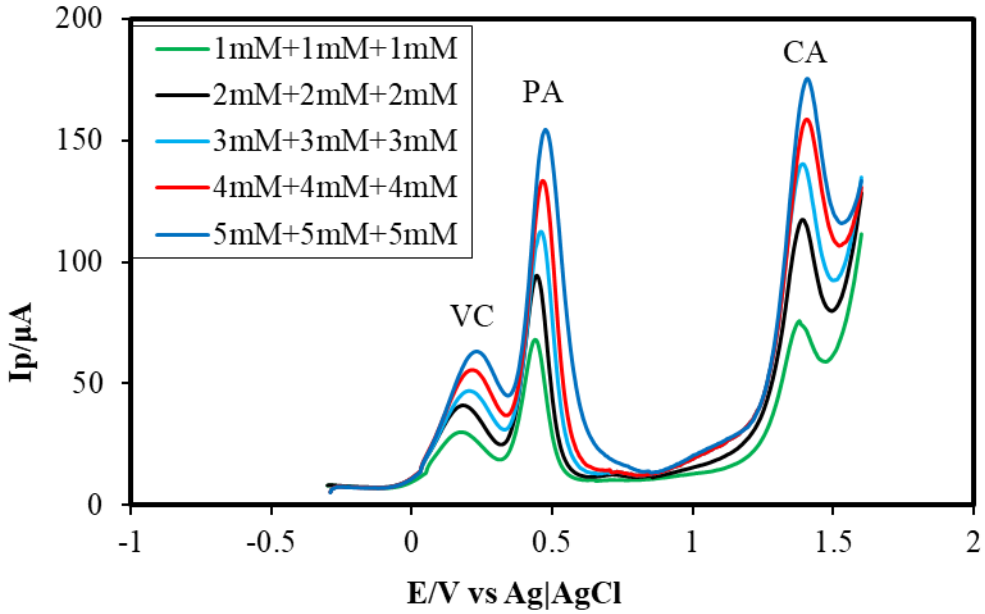

Fig. 4.84: DPV of different concentrations of the ternary mixture of VC + PA + CA (1-5 mM) in PBS (pH 7) at APA modified WB electrode at scan rate 0.1 V/s.

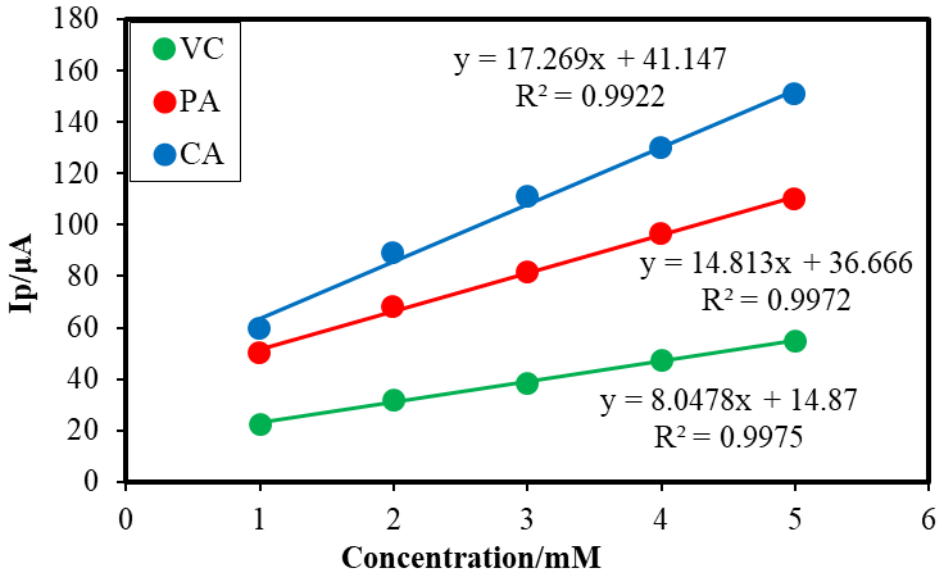

Fig. 4.85: Plots of peak currents (Ip) of VC, PA and CA vs concentrations (1-5 mM) in a ternary mixture of VC + PA + CA at APA modified WB electrode.

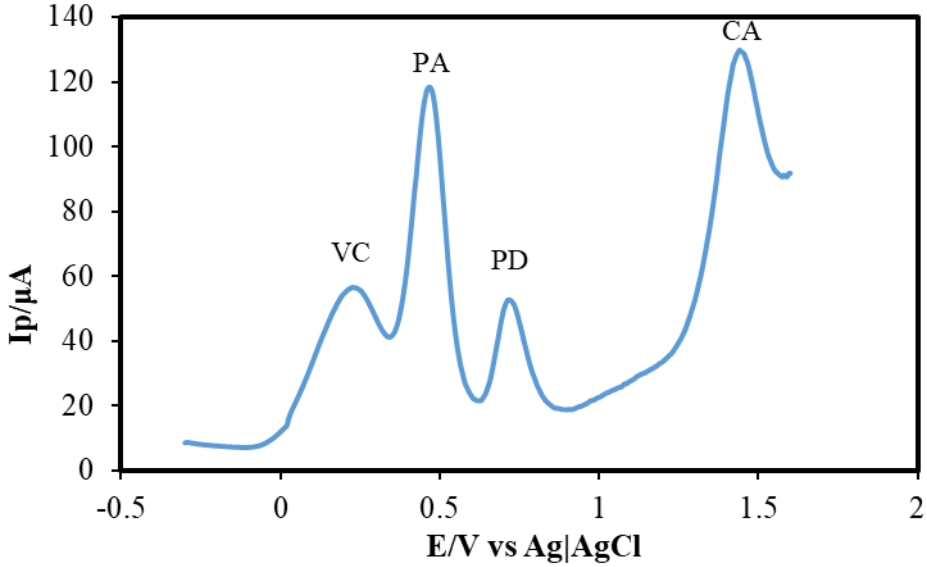

Fig. 4.86: DPV of the ternary solution of VC, PA and CA in presence of lysine, arginine, glycine, thiamine (vitamin B1), nicotinamide (vitamion B3), pyridoxine (PD) (vitamin B6) and glucose in PBS (pH 7) at APA modified WB electrode.

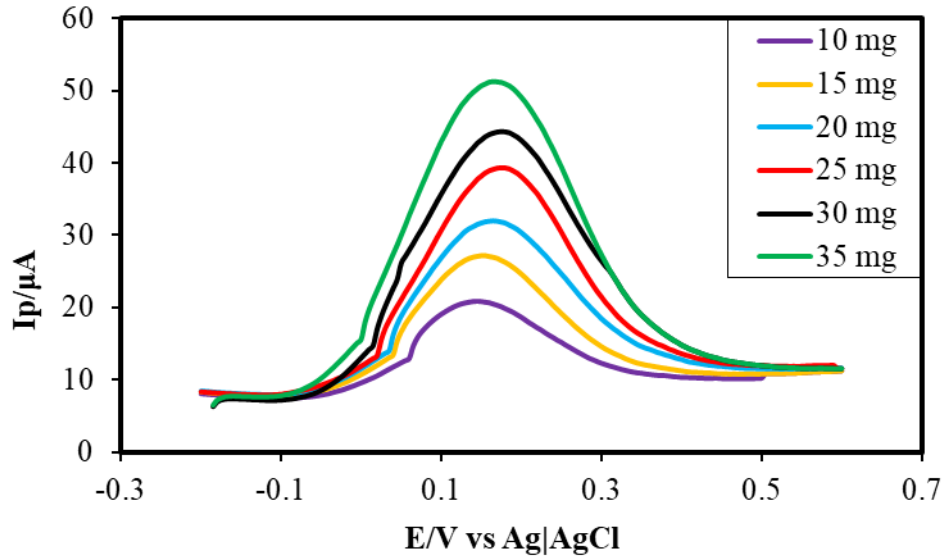

Fig. 4.87: DPVs of different amount of standard VC in 30 mL PBS (pH 7) solution at APA modified WB electrode.

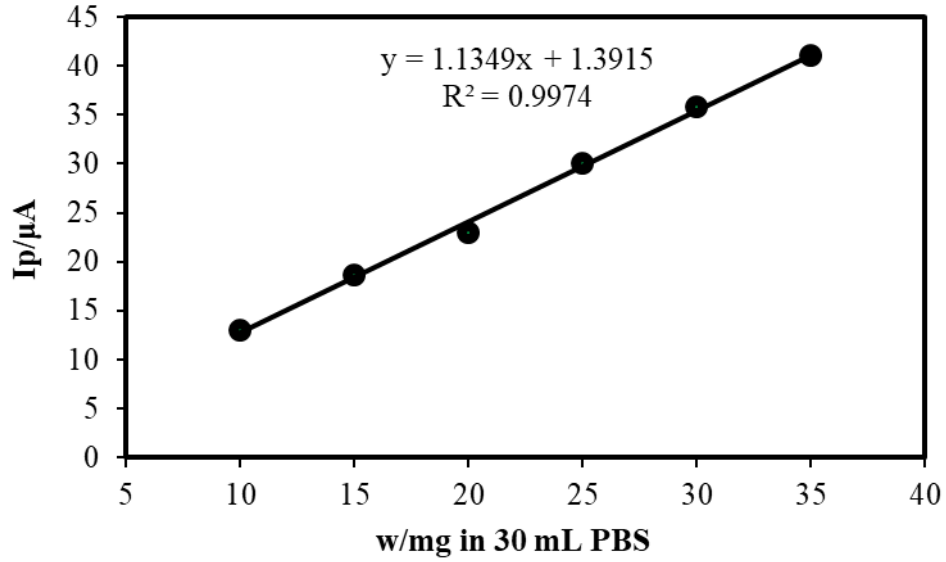

Fig. 4.88: Calibration curve of VC vs different amount (mg) in 30 mL PBS (pH 7).

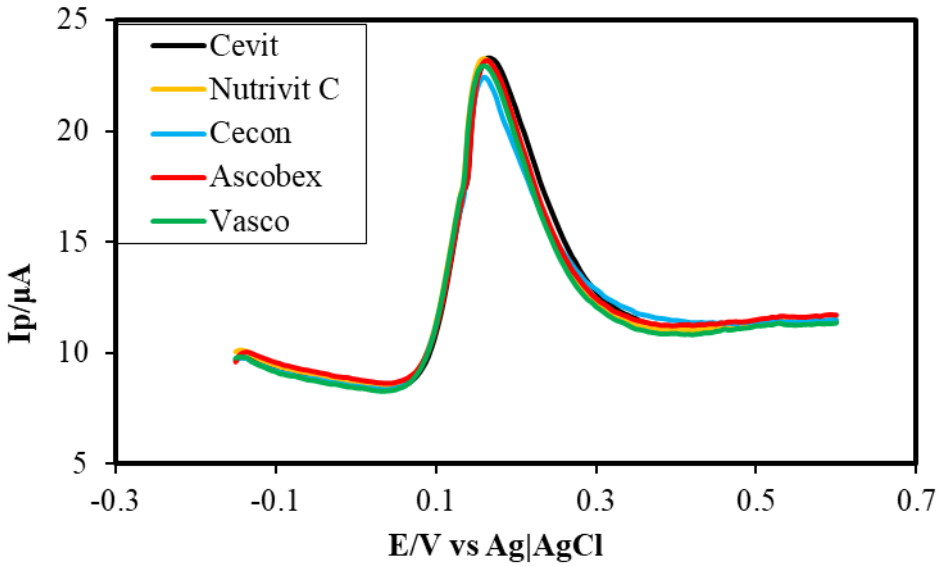

Fig. 4.89: DPVs of VC in Nutrivit C (gold line), Cecon (light blue line), Cevit (black line), Vasco (green line) and Ascobex (red line) tablets in PBS at APA modified WB electrode.

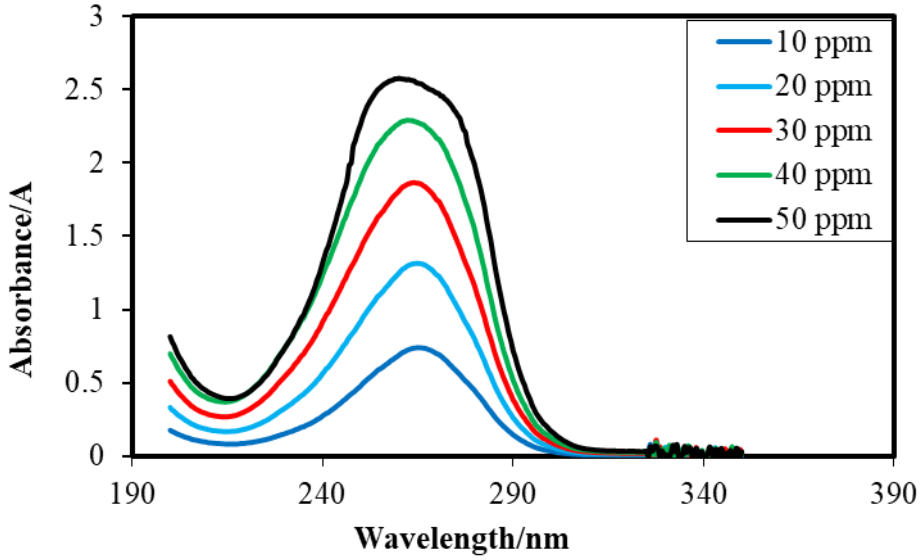

Fig. 4.90: UV-Visible spectra of the different concentration (10-50 ppm) of standard VC.

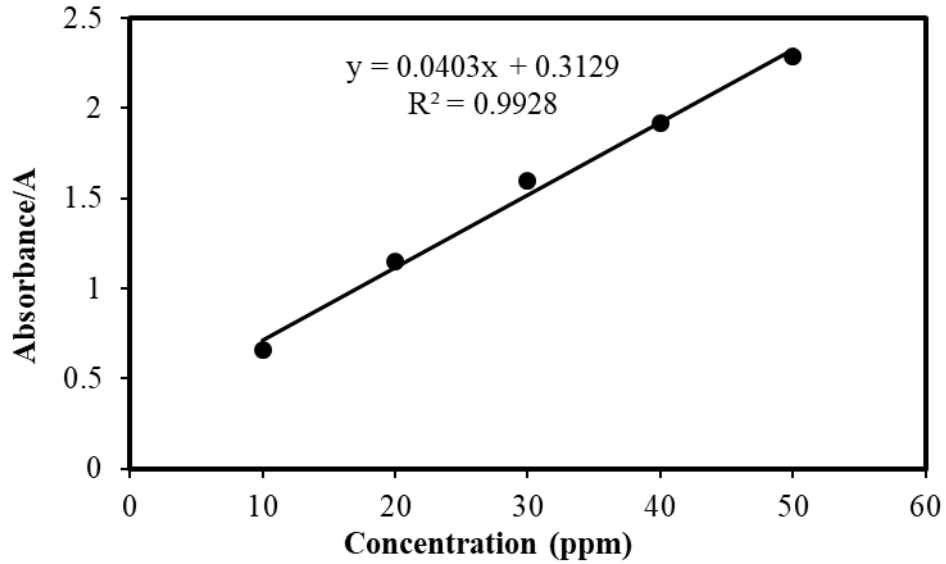

Figure 4.91: Calibration curve of standard VC with response to different concentrations (10-50 ppm) in water.

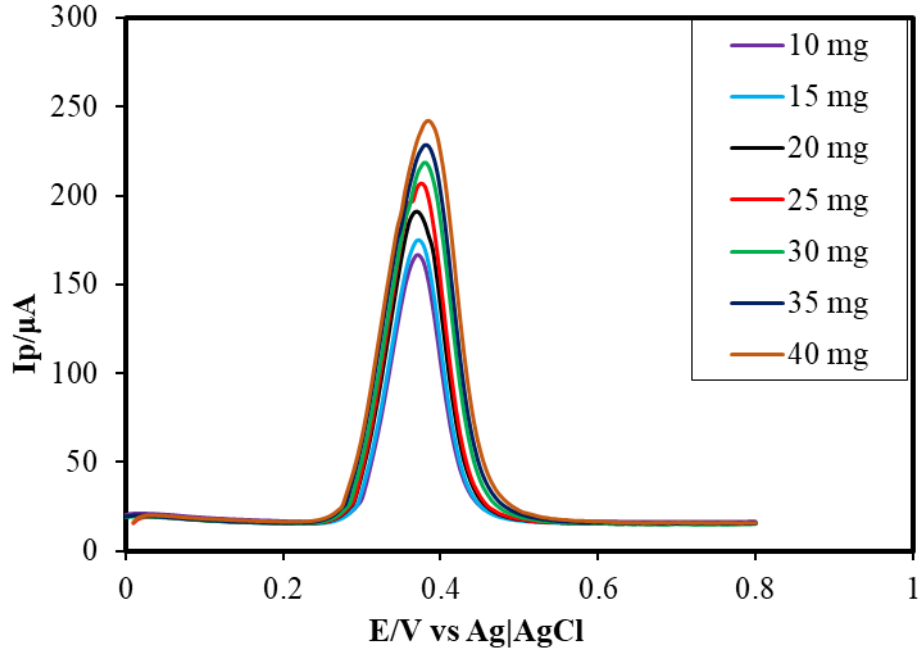

Fig. 4.92: Differential pulse voltammogram (DPV) of different amount (10-40 mg) of standard PA in 50 mL PBS (pH 7) at APA modified WB electrode.

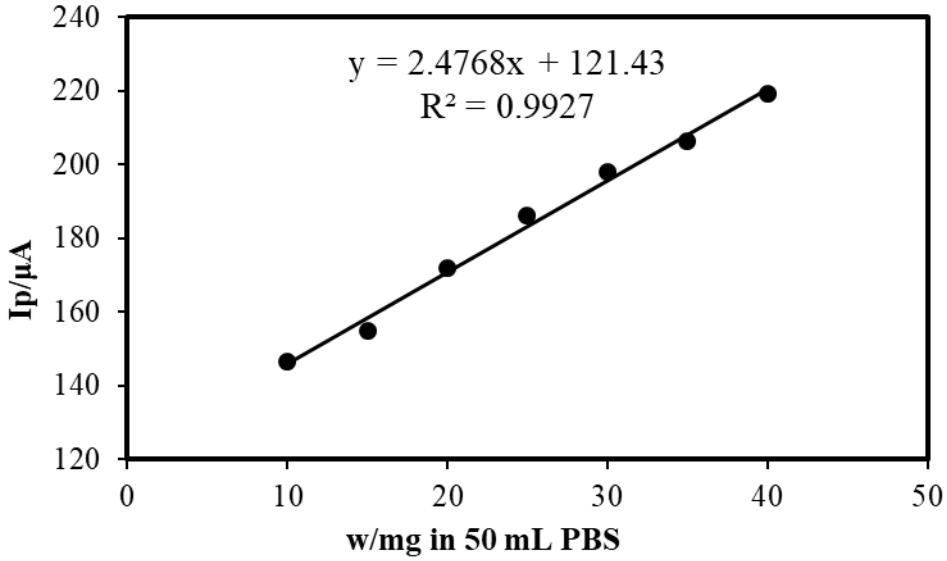

Fig. 4.93: Calibration curve of PA with response to different amount (05-35 mg) in 50 mL PBS (pH 7).

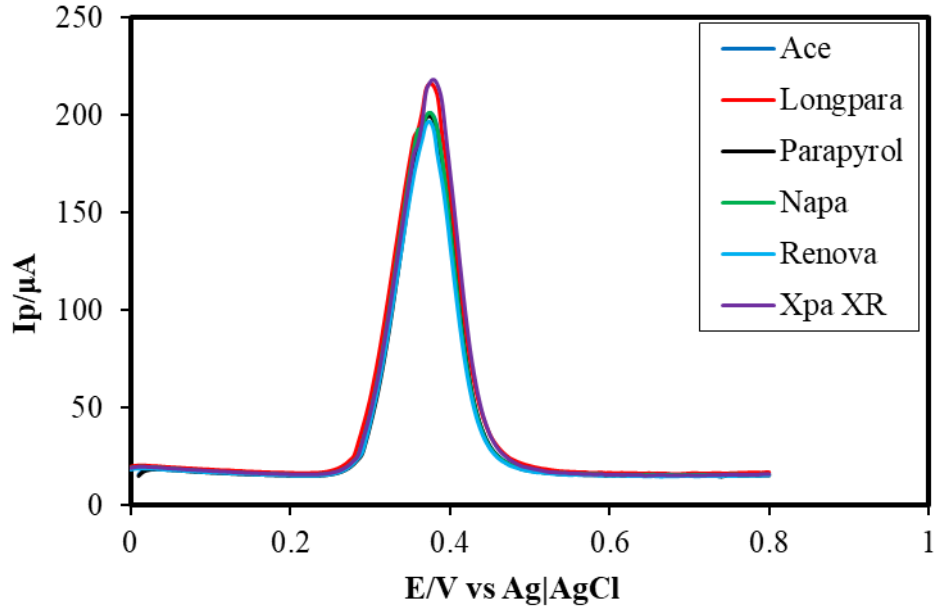

Fig. 4.94: DPVs of PA in Napa (green line), Ace (blue line), Xpa XR (violet line), Renova (light blue line), Parapyrol (black line) and Longpara (red line) tablets in PBS at APA modified WB electrode.

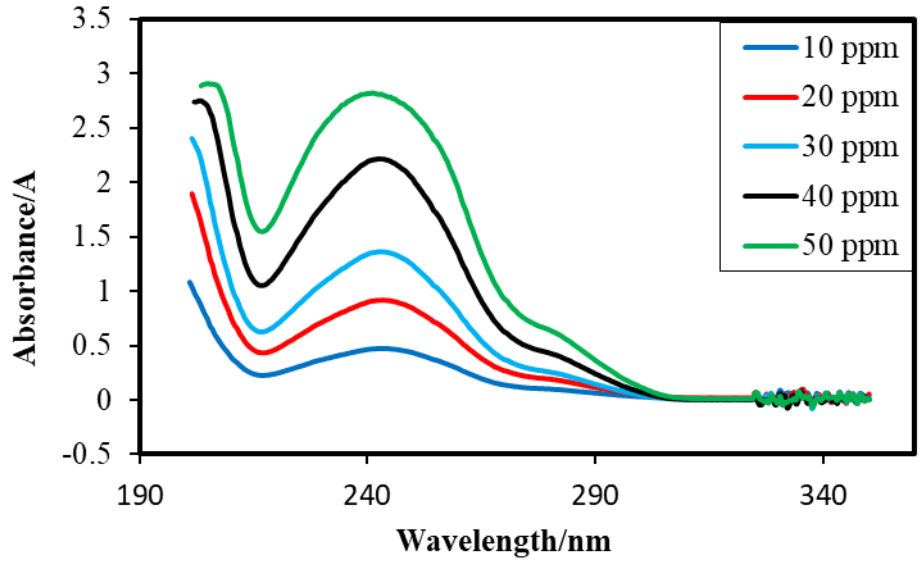

Figure 4.95: UV-Vis spectra of different concentrations (10-50 ppm) of standard PA in water.

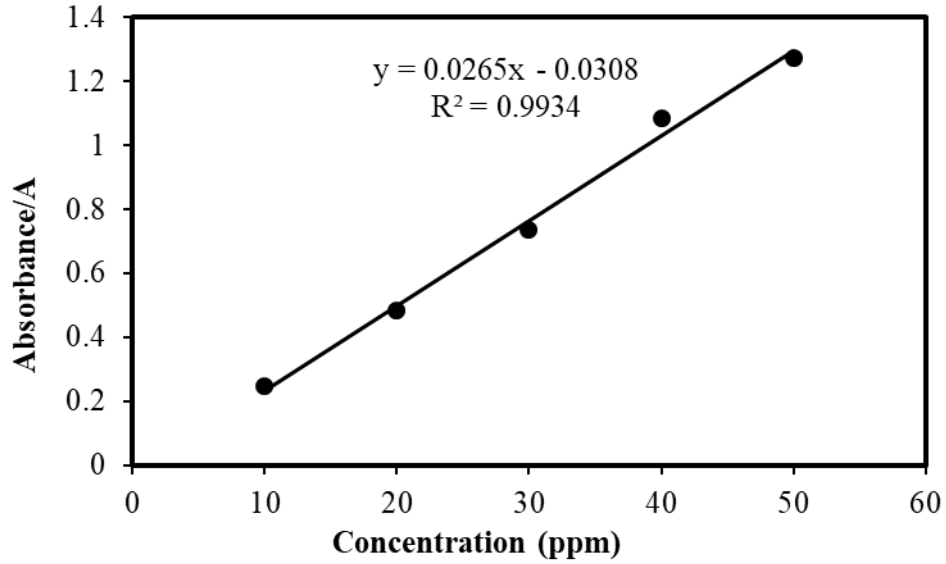

Figure 4.96: Calibration curve of standard PA with response to different concentrations (10-50 ppm) in water.

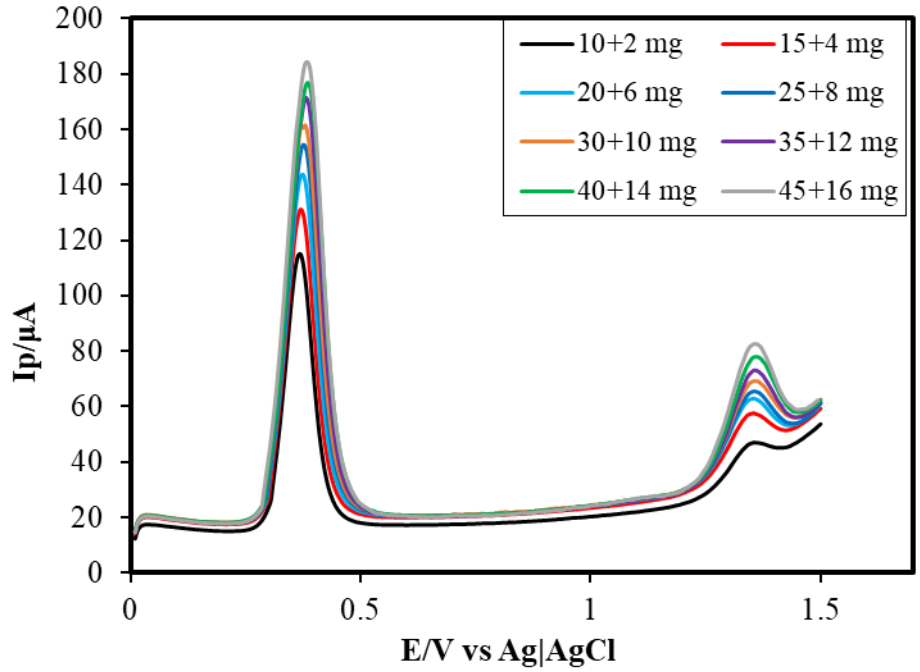

Fig. 4.97: DPVs of different amount of standard PA + CA in 50 mL PBS (pH 7) solution at APA modified WB electrode.

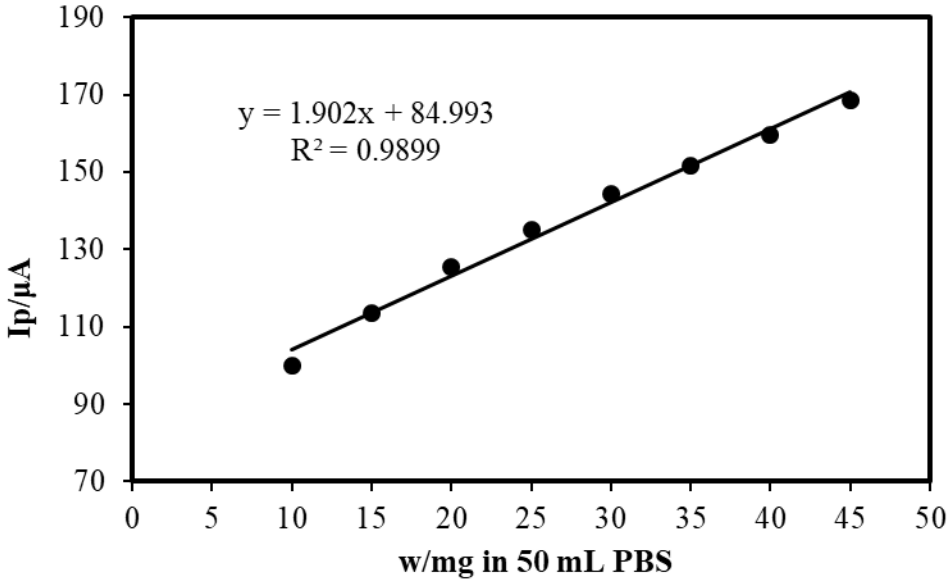

Fig. 4.98: Calibration curve of PA with response to different amount (mg) of binary mixture of PA + CA in 50 mL PBS (pH 7).

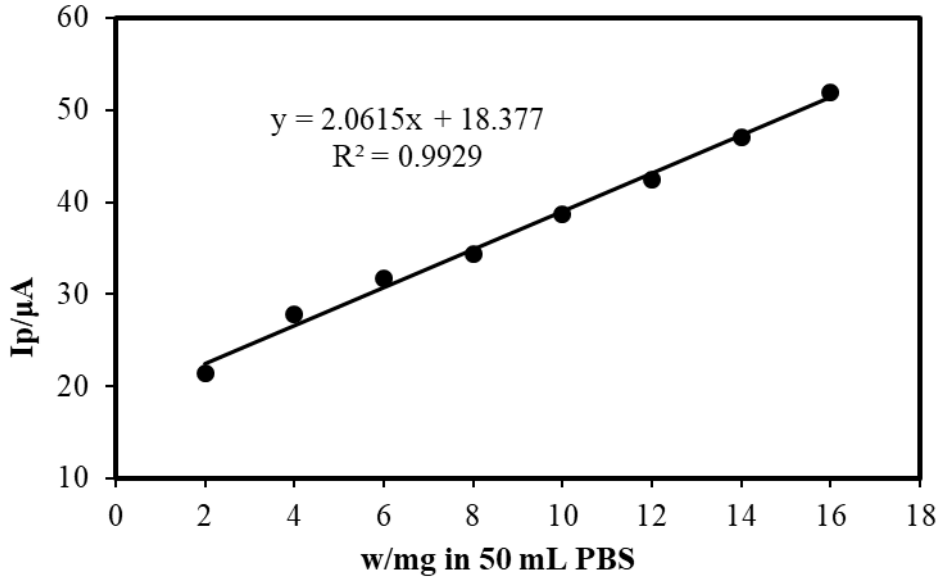

Fig. 4.99: Calibration curve of CA with response to different amount (mg) of binary mixture of PA + CA in 50 mL PBS (pH 7).

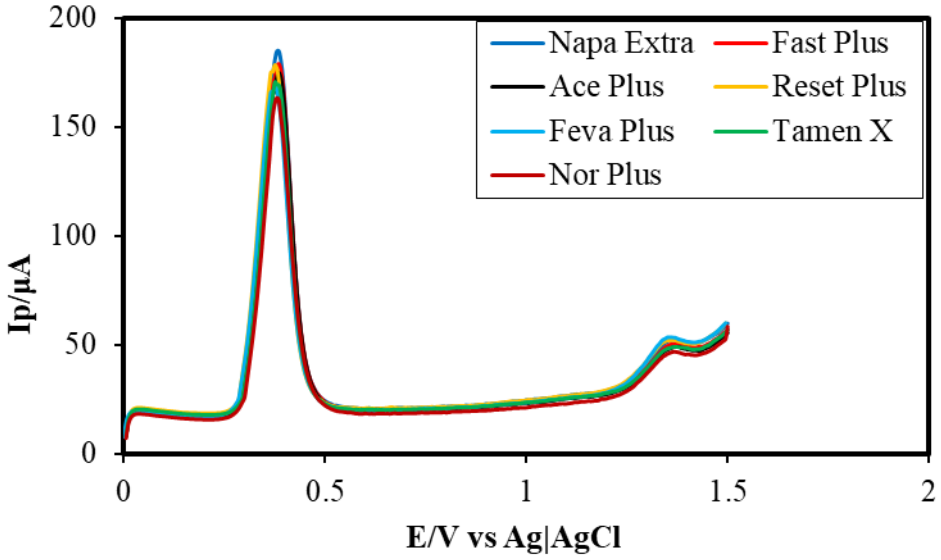

Fig. 4.100: DPVs of PA + CA in Fast plus (blue line), Napa extra (red line), Ace plus (black line), Reset plus (gold line), Feva Plus (light blue line), Tamen X (green line) and Nor Plus (dark line) tablets in PBS at APA modified WB electrode.

CHAPTER V

Conclusions

Vitamin C (VC), Paracetamol (PA) and Caffeine (CA) are very important drugs for the treatment of common diseases such as cold, fever, headache etc. They are co-exists in tablets and some cold remedy powders. Simultaneous detection and quantitative determination of these three drugs have been carried out in this work. Cyclic voltammetry (CV) and Differential pulse voltammetry (DPV) techniques were used for the detection and UV-Vis spectroscopic method was used for the validation of the quantitative determination.

A single and sensitive electrochemical sensor based on APA modified WB electrode was developed for the determination of VC, PA and CA. The APA modified WB electrode has been found to have sensing capability for simultaneous detection of VC, PA and CA.

The detection was mostly favorable at pH 7. The sensitivity that the APA modified WB electrode shows is better than that of bare WB electrode with considerable detection limit. In simultaneous detection, the limit of detection (LoD) for VC, PA and CA are 0.2 µmol L^{-1}, 0.16 µmol L^{-1} and 0.33 µmol L^{-1} respectively at APA modified WB electrode. The sensitivity for VC, PA and CA are 54.4 µA/mM/cm^2, 99.9 µA/mM/cm^2 and 151.7 µA/mM/cm^2 respectively.

APA modified WB electrode displays a very good recovery value with minimum standard deviations. It has been successfully used to determine the amount of VC, PA and CA in their relevant tablets of some different pharmaceutical companies of Bangladesh. The modified electrode sensor values are consistent with spectroscopic measurement value. Moreover, APA modified WB electrode is low cost, simple, rapid to fabricate and good selectivity in the presence of interfering species.

APA modified WB electrode sensor is recommended to the pharmaceutical industries for the determination of VC, PA and CA. This sensor can effectively determine the above mentioned drugs in a single moment. It can save testing time and testing reagents to reduce the testing cost of the pharmaceutical tablets.

REFERENCES

1. N. Perez, 2009, "Electrochemistry and Corrosion Science", Vol. 27, Kluwer Academic publishers, New York.
2. A.J. Bard, I. Rubinstein (eds.), 2004, "Electroanalytical chemistry", Vol. 22, pp. 310, Marcel Dekker, New York.
3. P. T. Kissenger and W. R. Heineman, 1984, "Laboratory Techniques in Electroanalytical Chemistry", Vol. 43, Marcel Dekker, New York.
4. J. Wang, 1988, "Electroanalytical Techniques in Clinical Chemistry and Laboratory Medicine", Vol. 110, VCH Publishers, New York.
5. Gutés, A., Cespedes, F., Valle, M. D., Louthander, D., Krantz-Rülcker, C. and Winquist, F., 2006, "A flow injection voltammetric electronic tongue applied to paper mill industrial waters", Sensors and Actuators B: Chemical, Vol. 115, pp. 390-395.
6. Ramírez, E. A., Molina, P. G., Zón, M. A. and Fernández, H., 2005, "Development of an Electroanalytical Method for the Quantification of Zearalenone (ZEA) in Maize Samples", Electroanalysis, Vol. 17, pp. 1635-1640.
7. Süzen, S., Demírcígíl, B. T., Buyukbingol, E. and Özkan, S. A., 2003, "Electroanalytical evaluation and determination of 5-(3′-indolyl)-2-thiohydantoin derivatives by voltammetric studies: possible relevance to *in vitro*metabolism", New Journal of Chemistry, Vol. 27, pp. 1007-1011.
8. Carlsson, A., Krantz-Rülcker, C. and Winquist,F., 2001, "An electronic tongue as a tool for wet-end monitoring", Nordic Pulp & Paper Research Journal, Vol. 16, pp. 319-326.
9. Ivarsson, P., Johansson, M., Höjer, N., Krantz-Rülcker, C., Winquist, F. and Lundström, I., 2005, "Supervision of rinses in a washing machine by a voltammetric electronic tongue", Sensors and Actuators B: Chemical, Vol. 108, pp. 851-857.
10. Krantz-Rülcker, C., Stenberg, M., Winquist, F. and Lundström, I., 2001, "Electronic tongues for environmental monitoring based on sensor arrays and pattern recognition: a review", Analytica Chimica Acta, Vol. 426, pp. 217-226.
11. Yogeswaran, U. and Chen, S. M., 2008, "Recent Trends in the Application of Carbon Nanotubes– Polymer Composite Modified Electrodes for Biosensors: A Review", Analytical Letters, Vol. 41, pp. 210-243.

12. A. J. Bard and L. R. Faulkner, 1980, “Electrochemical Methods, Fundamentals and Applications”, John wiley & sons, inc., New York.
13. D. A. Skoog, D. M. West, F. J. Holler and S. R. Crouch, 2007, “Principles of Instrumental Analysis”, Thomson Brooks/Cole Publishing, Belmont, CA.
14. C. M. A. Brett and A. M. O. Brett, 1998, “Electroanalysis”, Oxford University Press, Oxford.
15. R. Kellner, J. M. Mermet, M. Otto, M. Valcarcel and H. M. Widmer, 2004, “Analytical Chemistry”, Wiley- VCH, Weinheim.
16. D. A. Skoog, D. M. West and F. J. Holler, 1992, “Fundamentals of Analytical Chemistry, Saunders College Publishing, Fort Worth.
17. Stradiotto, N. R., Yamanaka, H. and Zanoni, M. V. B., 2003, “Electrochemical sensors: A powerful tool in analytical chemistry”, Journal of the Brazilian Chemical Society, Vol. 14, pp. 159-173.
18. Janata, J., 2001, “Centennial retrospective on chemical sensors”, Analytical Chemistry, Vol. 73, pp. 150A-153A.
19. R. W. Cattrall, 1997, “Chemical Sensors”, Oxford Chemistry Premiers, New York.
20. Qu, W., Wu, K. and Hu, S., 2004, “Voltammetric determination of pyridoxine (vitamin B6) by use of a chemically-modified glassy carbon electrode”, Journal of Pharmaceutical and Biomedical Analysis, Vol. 36, pp. 631-635.
21. Mousty, C., 2010, “Biosensing applications of clay-modified electrodes: a review”, Analytical and Bioanalytical Chemistry, Vol. 396, pp. 315-325.
22. Hyde, C. M., Nekrassova, O., Dai, X., Compton, R. G., 2004, “Fabrication, Characterisation and Voltammetric Studies of Gold Amalgam Nanoparticle Modified Electrodes”, Chemical Physics and physical Chemistry, Vol. 5, pp. 1405-1410.
23. Manisankar, P., Sundari, P. A. and Sasikumar, R., 2009, “Square-wave stripping voltammetric determination of some organic pollutants using modified electrodes”, International Journal of Environmental Analytical Chemistry, Vol. 89, pp. 245-260.
24. Wang, S. M., Su, W. Y., and Cheng, S. H., 2010, A simultaneous and Sensitive Determination of Hydroquinone and Catechol at Anodically Pretreated Screen-Printed Carbon Electrodes”, International Journal of Electrochemical Science, Vol. 5, pp. 1649 - 1664.

25. Diab, N., Oni, J. and Schuhmann, W., 2005, “Electrochemical nitric oxide sensor preparation: A comparison of two electrochemical methods of electrode surface modification”, Bioelectrochemistry, Vol. 66, pp. 105-110.
26. Deng, C., Li, M., Xie, Q., Liu, M., Tan, Y., Xu, X. and Yao, S., 2006, “Electrochemical quartz crystal impedance study on immobilization of glucose oxidase in a polymer grown from dopamine oxidation at an Au electrode for glucose sensing”, Electrochimica Acta, Vol. 557, pp. 1-9.
27. Pyun, S. and Bae, J. S., 1997, “Electrochemical lithium intercalation into vanadium pentoxide xerogel film electrode”, Journal of Power Sources, Vol. 68, pp. 669-673.
28. Sivakumar, C., Nian, J. N. and Teng, H., 2005, “Poly(o-toluidine) for carbon fabric electrode modification to enhance the electrochemical capacitance and conductivity”, Journal of Power Sources, Vol. 144, pp. 295-301.
29. Munoz, E., Heras, M. A., Colina, A. I., Ruiz, V. and Lo’pez-Palacios, J., 2007, “Electropolymerization of aniline on polyaniline-modified electrodes under hydrodynamic conditions”, Electrochimica Acta, Vol. 52, pp. 4778-4783.
30. Murray, R. W., 1980, “Chemically modified electrodes”, Accounts of Chemical Research, Vol. 13, pp. 135-141.
31. Qi, H. L. and Zhanh, C. X., 2005, “Simultaneous determination of hydroquinone and catechol at a glassy carbon electrode modified with multiwall carbon nanotubes”, Electroanalysis, vol. 17, pp. 832-838.
32. Juan, L. and Xiaoli, Z., 2012, “Fabrication of Poly(Aspartic Acid)-Nanogold Modified
Electrode and Its Application for Simultaneous Determination of Dopamine, Ascorbic Acid, and Uric Acid”, American Journal of Analytical Chemistry, Vol. 3, pp. 195-203.
33. Duvall, S. H. and McCreery, R. L., 1999, “Control of Catechol and. Hydroquinone Electron-Transfer Kinetics on Native and. Modified Glassy Carbon Electrodes,” Analytical Chemistry, Vol. 71, pp. 4594–4602.
34. Pascali, G., Watts, P., Salvadori, P.A., 2013, “Microfluidics in radiopharmaceutical Chemistry”, Nucl. Med. Biol. Vol. 40, pp. 776–787.
35. Liu, W. Z., Wang, X. G., Wu, Q. S., Ding, Y. P., 2009, “A facile and fast electrochemical method for the simultaneous determination of *o*-dihydroxybenzene

and *p* dihydroxybenzene using a surfactant", Journal of Analytical Chemistry, Vol. 64, pp. 54-58.

36. Fernandes, D. M., Silva, N., Pereira, C., Moura, C., Magalhaes, J. M. C. S., Bachiller-Baeza, B., Rodriguez-Ramos, I., Guerrero-Ruiz, A., Delerue-Matos, C. and Freire, C., 2015, "MnFe2O4@CNT-N as novel electrochemical nanosensor for determination of caffeine, acetaminophen and ascorbic acid", Sensors and Actuators B: Chemical, Vol. 218, pp. 128-136.
37. Hu, I. F. and Kuwana, T., 1986, "Oxidative mechanism of ascorbic acid at glassy carbon electrodes", Analytical Chemistry, Vol. 58, pp. 3235–3239.
38. Zidan, M., Tee, T. W., Abdullah, A. H., Zainal, Z. and Kheng, G. J., 2011, "Electrochemical Oxidation of Paracetamol Mediated by Nanoparticles Bismuth Oxide Modified Glassy Carbon Electrode", International Journal of Electrochemical Science, Vol. 6, pp. 279 – 288.
39. Zhao, F., Wang, F., Zhao, W., Zhou, J., Liu, Y., Zou, L. and Ye, B., 2011, "Voltammetric sensor for caffeine based on a glassy carbon electrode modified with Nafion and graphene oxide", Vol. 174, pp. 383-390.
40. Kutluay, A. and Aslanoglu, M., 2013, "Modification of electrodes using conductive porous layers to confer selectivity for the voltammetric detection of paracetamol in the presence of ascorbic acid, dopamine and uric acid", Sensors and Actuators B: Chemical, Vol. 185, pp. 398–404.
41. Zhao, H., Zhang, Y. Z. and Yuan, Z. B., 2002, "Determination of Dopamine in the Presence of Ascorbic Acid Using Poly (hippuric acid) Modified Glassy Carbon Electrode", Electroanalysis, Vol. 14, pp. 1031-1034.
42. Roy, P. R., saha, M. S., Okajima, T., Park, S. G., Fujishima, A. and Ohsaka, T., 2004, "Selective Detection of Dopamine and Its Metabolite, DOPAC, in the Presence of Ascorbic Acid Using Diamond Electrode Modified by the Polymer Film", Electroanalysis, Vol. 16, pp. 1777-1784.
43. Roy, P. R., Saha, M. S., Okajima, T. and Ohsaka, T., 2004, "Electrooxidation and Amperometric Detection of Ascorbic Acid at GC Electrode Modified by Electropolymerization of *N*,*N*-Dimethylaniline", Electroanalysis, Vol. 16, pp. 289-297.
44. Roy, R. R., Okajima, T. and Ohsaka, T., 2004, J. Electroanal. Chem., Vol. 75, pp. 561.

45. IUPAC Recommendation, 1997, Pure and Appl. Chem., Vol. 69, pp. 132.
46. Afkhami-Ardekani, M. and Shojaoddiny-Ardekani, A., 2007, 'Effect of vitamin C on blood glucose, serum lipids & serum insulin in type 2 diabetes patients", Indian Journal of Medical Research, Vol. 126, pp. 471-474.
47. Antoon, A. Y., Donovan, D. K., Burn Injuries. In: Behrman RE, Kliegman RM, Jenson HB. 2000, eds. Nelson Textbook of Pediatrics. Philadelphia, Pa: W.B. Saunders Company; pp.287-294.
48. Audera, C., Patulny, R. V., Sander, B. H. and Douglas, R. M., 2001, "Mega-dose vitamin C in treatment of the common cold: a randomised controlled trial", Medical Journal of Australia, Vol. 175, pp. 359-362.
49. "Ascorbic Acid". The American Society of Health-System Pharmacists. Retrieved 8 December 2016.
50. Afkhami, A., Khoshsafar, H., Bagheri, H. and Madrakian, T., 2014, "Preparation of NiFe2O4/graphene nanocomposite and its application as a modifier for the fabrication of an electrochemical sensor for the simultaneous determination of tramadol and acetaminophen", Analytica Chimica Acta, Vol. 831, pp. 50-59.
51. Bertolini, A., Ferrari, A., Ottani, A., Guerzoni, S., Tacchi, R. and Leone, S., 2006, "Paracetamol: new vistas of an old drug", CNS Drug Reviews, Vol. 12, pp. 250 – 75.
52. Viswanathan, A. N., Feskanich, D., Schernhammer, E. S. and Hankinson, S. E., 2008, "Aspirin, NSAID, and Acetaminophen Use and the Risk of Endometrial Cancer", Cancer Research, Vol. 68, pp. 2507 – 13.
53. Altinoz, M. A. and Korkmaz, R., 2004, "NF-kappaB, macrophage migration inhibitory factor and cyclooxygenase-inhibitions as likely mechanisms behind the acetaminophen- and NSAID-prevention of the ovarian cancer", Neoplasma, Vol. 51, pp.239 – 247.
54. K., Salerno and M., Evelyn, 2007, Pharmacology for health professionals.
55. Sin, B., Wai, M., Tatunchak, T. and Motov, S. M., 2016, "The use of intravenous acetaminophen for acute pain in the emergency department", Academic Emergency Medicine, Vol. 23, pp. 543–53.
56. Maurizio, D. M. and Alberto, C., 2015, "Recent Advances in Pediatric Use of Oral Paracetamol in Fever and Pain Management", Pain and Therapy, Vol. 4, pp. 149–168.
57. Jeevagan A. J. and John, S. A., 2012, "Electrochemical determination of caffeine in the presence of paracetamol using a self-assembled monolayer of non-peripheral

amine substituted copper(II) phthalocyanine", Electrochimica Acta, Vol. 77, pp. 137–142.

58. Hochhauser D. and Daniel H., 2014, Cancer and its Management, Wiley-Blackwell.
59. Mitchell, D. C., Knight, C. A., Hockenberry, J., Teplansky, R., Hartman, T. J., 2014, "Beverage caffeine intakes in the U.S.", Food and Chemical Toxicology, Vol. 63, pp. 136 –142.
60. Nehlig, A., Daval, L. and Debry, G., 1992, "Caffeine and the central nervous system: mechanisms of action, biochemical, metabolic and psychostimulant effects", Brain Research. Brain Research Reviews, Vol. 17, pp. 139–70.
61. Donald Voet, Judith G Voet, Charlotte W Pratt, "Fundamentals of biochemistry : life at the molecular level", ISBN 9781118918401. OCLC 910538334.
62. Dunn, M. S. and Smart, B. W., 1950, "DL-Aspartic Acid", Organic Syntheses, Vol. 4, pp. 55-57.
63. Piatkowski, M., Radwan-Pragłowska, J. and Raclavský, K., 2015, "Application of Poly (aspartic acid) and its Derivatives in Medicine and Pharmacy", Asian Journal of Applied Sciences, Vol. 3, pp. 718- 734.
64. Sochor, J., Dobes, J., Krystofova, O., Ruttkay-Nedecky, B., Babula, P., Pohanka, M., Jurikova, T., Zitka, O., Adam, V., Klejdus, B. and Kizek, R., 2013, "Electrochemistry as a Tool for Studying Antioxidant Properties", International Journal of Electrochemical Science, Vol. 8, pp. 8464 – 8489.
65. Vestergaard, M., Kerman, K. and Tamiya, E., 2005, "An electrochemical approach for detecting copper-chelating properties of flavonoids using disposable pencil graphite electrodes: possible implications in copper-mediated illnesses", Analytica Chimica Acta, Vol. 538, pp. 273-281.
66. http://www.drhuang.com/science/chemistry/electrochemistry/polar.doc.htm.
67. D.A. Skoog, F.J. Holler and T.A. Nieman, 2007, "Principles of Instrumental Analysis", Thomson Brooks/ Cole, 6th Ed., pp. 349-351.
68. Brad, A. J., and Faulkner, L. R., 2001, Electrochemical methods: Fundamentals and Applications, 2nd ed., John Wiley & Sons, Hobokon, Nj.
69. Skoog, D. A., Holler, F. J. and Neiman, T. A., 2007, Principles of Instrumental Analysis, 6th edn, Thomson Brooks/Cole., pp. 169-173.

70. Vega, E., Sola, N., 2001, “Quantitative analysis of metronidazole in intravenous admixture with ciprofloxacin by first derivative spectrophotometry”, Journal of biomedical, Vol. 25, pp. 525-530.
71. P.T. Kissinger and W.R. Heineman, 1996, “Laboratory Techniques in Electroanalytical Chemistry”, Marcel Dekker, Inc.
72. Shippy, S. and Lu, M., 2007, Cyclic voltammetry: An example of voltaic methods, http://www.chem.uic.edu/chem421/cv.PDF (accessssed April 18, 2010), pp. 1-5.
73. J. N. Miller and J. C. Miller, 2000, “Statistics and Chemometrics for analytical chemistry, 4th edition, Prentice Hall, Harlow.
74. Fritz Scholz (21 December 2013), Electroanalytical Methods: Guide to Experiments and Applications, Springer, pp. 109, ISBN 978-3-662-04757-6.
75. Laborda, E., González, J. and Molina, A., 2014, "Recent advances on the theory of pulse techniques: A mini review", Electrochemistry Communications, Vol, 43, pp. 25-30.
76. Khoshhesab, Z. M., 2015, “Simultaneous electrochemical determination of acetaminophen, caffeine and ascorbic acid using a new electrochemical sensor based on CuO–graphene nanocomposite”, Royal Society of Chemistry Advances, Vol. 5, pp. 95140-95148.
77. Tefera, M., Geto, A., Tessema, M. and Admassie, S., 2016 “Simultaneous determination of caffeine and paracetamol by square wave voltammetry at poly(4-amino-3-hydroxynaphthalene sulfonic acid)-modified glassy carbon electrode”, Journal of Electroanalytical Chemistry, Vol. 210, pp. 156-162.
78. Chitravathi, S. and Munichandraiah, N., 2016, “Voltammetric determination of paracetamol, tramadol and caffeine using poly(Nile blue) modified glassy carbon electrode”, Journal of Electroanalytical Chemistry, Vol. 764, pp. 93-103.
79. Sadok, I., Tyszczuk-Rotko, K. and Nosal-Wiercińska, A., 2016, “Bismuth particles Nafion covered boron-doped diamond electrode for simultaneous and individual voltammetric assays of paracetamol and caffeine”, Sensors and Actuators B: Chemical, Vol. 235, pp. 263-272.
80. Pramod, K., Kalambate, Srivastava, A. K., 2016, “Simultaneous voltammetric determination of paracetamol, cetirizine and phenylephrine using a multiwalled carbon nanotube-platinum nanoparticles nanocomposite modified carbon paste electrode”, Sensors and Actuators B: Chemical, Vol. 233, pp. 237-248.

81. Pramod, K., Kalambate, Sanghavi, B. J., Karna, S. P. and Srivastava, A. K., 2015 "Simultaneous voltammetric determination of paracetamol and domperidone based on a graphene/platinum nanoparticles/nafion composite modified glassy carbon electrode", Sensors and Actuators B: Chemical, Vol. 213, pp. 285-294.

82. Bouabi, Y. E., Farahi, A., Labjar, N., Hajjaji, S. E., Bakasse, M. and Mhammedi, M. A. E., 2016, "Square wave voltammetric determination of paracetamol at chitosan modified carbon paste electrode: Application in natural water samples, commercial tablets and human urines", Materials Science and Engineering: C, Vol. 58, pp. 70-77.

83. Bouabi, Y. E., Farahi, A., Achak, M., Zeroual, M., Hnini, K., Houssame, S. E., Bakasse, M., Bouzidi, A. and Mhammedi, M.A.E., 2016, "Electrocatalytic effect of fluoroapatite in reducing paracetamol at carbon paste electrode: Analytical application", Journal of the Taiwan Institute of Chemical Engineers, Vol. 66, pp. 33-42.

84. Daneshvar, L., Rounaghi, G., Eshaghi, Z., Chamsaz, M. and Tarahomi, S., 2016, "Electrochemical determination of carbamazepin in the presence of paracetamol using a carbon ionic liquid paste electrode modified with a three-dimensional graphene/MWCNT hybrid composite film", Journal of Molecular Liquids, Vol. 215, pp. 316-322.

85. Majidi, M. R., Pournaghi-Azar, M. H. and Baj, R. F. B., 2016, "Graphene nanoplatelets like structures formed on ionic liquid modified carbon-ceramic electrode: As a sensing platform for simultaneous determination of dopamine and acetaminophen", Journal of Molecular Liquids, Vol. 220, pp. 778-787.

86. Afrasiabi M. and Kianipour S., 2015, "Simultaneous Determination of Ascorbic Acid, Uric Acid and Acetaminophen on a Glassy Carbon Electrode Coated with a Novel Single Walled Carbon Nanotubes/ Chitosan/ MCM-41 Composite", Anal. Bioanal. Electrochem., Vol. 7, pp. 331-343.

87. Karimi-Maleh, H., Moazampour, M., Ahmar, H., Beitollahi, H. and Ensafi, A. A., 2014, "A sensitive nanocomposite-based electrochemical sensor for voltammetric simultaneous determination of isoproterenol, acetaminophen and tryptophan", Measurement, Vol. 51, pp. 91-99.

88. Mazloum-Ardakani, M., Beitollahi, H., Amini, M. K., Mirkhalaf, F., and Mirjalili, B., 2011, "A highly sensitive nanostructure-based electrochemical sensor for

electrocatalytic determination of norepinephrine in the presence of acetaminophen and tryptophan", Biosensors and Bioelectronics, Vol. 26, pp. 2102-2106.

89. Liu, B., Ouyang, X., Ding, Y., Luo, L., Xu, D. and Ning, Y., 2016, "Electrochemical preparation of nickel and copper oxides-decorated graphene composite for simultaneous determination of dopamine, acetaminophen and tryptophan", Talanta, Vol. 146, pp. 114-121.
90. Tavana, T., Khalilzadeh, M. A., Karimi-Maleh, H., Ensafi, A. A., Beitollahi, H., and Zareyee, D., 2012, "Sensitive voltammetric determination of epinephrine in the presence of acetaminophen at a novel ionic liquid modified carbon nanotubes paste electrode", Journal of Molecular Liquids, Vol. 168, pp. 69-74.
91. Keyvanfard, M., Shakeri, R., Hassan Karimi-Maleh, H. and Alizad, K., 2013, "Highly selective and sensitive voltammetric sensor based on modified multiwall carbon nanotube paste electrode for simultaneous determination of ascorbic acid, acetaminophen and tryptophan", Materials Science and Engineering: C, Vol. 33, pp. 811-816.
92. Mazloum-Ardakani, M., Sheikh-Mohseni, M. A., Abdollahi-Alibeik, M. and Benvidi, A., 2012, "Electrochemical sensor for simultaneous determination of norepinephrine, paracetamol and folic acid by a nanostructured mesoporous material", Sensors and Actuators B: Chemical, Vol. 171–172, pp. 380-386.
93. Beitollahi, H., Mohadesi, A., Mohammadi, S., Pahlavan, A., Karimi-Maleh, H. and Akbari, A., 2012, "New voltammetric strategy for determination of dopamine in the presence of high concentrations of acetaminophen, folic acid and N-acetylcysteine", Journal of Molecular Liquids, Vol. 169, pp. 130-135.
94. Beitollahi, H., Mohadesi, A., Mohammadi, S. and Akbari, A., 2012, "Electrochemical behavior of a carbon paste electrode modified with 5-amino-3′,4′-dimethyl-biphenyl-2-ol/carbon nanotube and its application for simultaneous determination of isoproterenol, acetaminophen and N-acetylcysteine", Electrochimica Acta, Vol. 68, pp. 220-226.
95. Taei, M. and Jamshidi, M. S., 2017, "A voltammetric sensor for simultaneous determination of ascorbic acid, noradrenaline, acetaminophen and tryptophan", Microchemical Journal, Vol. 130, pp. 108-115.

96. Adhikari, B., Govindhan, M. and Chen, A., 2015, "Sensitive Detection of Acetaminophen with Graphene-Based Electrochemical Sensor", Electrochimica Acta, Vol. 162, pp. 198-204.
97. Amiri-Aref, M., Raoof, J. B. and Ojani, R., 2014, "A highly sensitive electrochemical sensor for simultaneous voltammetric determination of noradrenaline, acetaminophen, xanthine and caffeine based on a flavonoid nanostructured modified glassy carbon electrode", Sensors and Actuators B: Chemical, Vol. 192, pp. 634-641.
98. Afkhami, A., Khoshsafar, H., Bagheri, H. and Madrakian, T., 2014, "Preparation of $NiFe_2O_4$/graphene nanocomposite and its application as a modifier for the fabrication of an electrochemical sensor for the simultaneous determination of tramadol and acetaminophen", Analytica Chimica Acta, Vol. 831, pp. 50-59.
99. Beitollahi, H., Raoof, J. and Hosseinzadeh, R., 2011, "Fabrication of a nanostructure-based electrochemical sensor for simultaneous determination of N-acetylcysteine and acetaminophen", Talanta, Vol. 85, pp. 2128-2134.
100. Liu, X., Shangguan, E., Li, J., Ning, S., Guo, L. and Li, Q., 2017, "A novel electrochemical sensor based on FeS anchored reduced graphene oxide nanosheets for simultaneous determination of dopamine and acetaminophen", Materials Science and Engineering: C, Vol. 70, pp. 628-636.
101. Taei, M. and Ramazani, G., 2014, "Simultaneous determination of norepinephrine, acetaminophen and tyrosine by differential pulse voltammetry using Au-nanoparticles/poly(2-amino-2-hydroxymethyl-propane-1,3-diol) film modified glassy carbon electrode", Colloids and Surfaces B: Biointerfaces, Vol. 123, pp. 23-32.
102. Haghshenas, E., Madrakian, T. and Afkhami, A., 2015, "A novel electrochemical sensor based on magneto Au nanoparticles/carbon paste electrode for voltammetric determination of acetaminophen in real samples" Materials Science and Engineering: C, Vol. 57, pp. 205-214.
103. Beitollahi, H. and Mohammadi, S., 2013, "Voltammetric determination of ascorbic acid in the presence of acetaminophen and tryptophan using an improved carbon nanotube paste electrode" Chinese Journal of Catalysis, Vol. 34, pp. 1098-1104.
104. Ensafi, A. A., Ahmadi, N., Rezaei, B. and Abarghoui, M. M., 2015, "A new electrochemical sensor for the simultaneous determination of acetaminophen and

codeine based on porous silicon/palladium nanostructure", Talanta, Vol. 134, pp. 745-753.

105. Chen, X., Zhu, J., Xi, Q. and Yang, W., 2012, "A high performance electrochemical sensor for acetaminophen based on single-walled carbon nanotube–graphene nanosheet hybrid films", Sensors and Actuators B: Chemical, Vol. 161, pp. 648-654.
106. Li, H., Wang, Y.,Ye, D., Luo, J., Su, B., Zhang, S. and Kong, J., 2014, "An electrochemical sensor for simultaneous determination of ascorbic acid, dopamine, uric acid and tryptophan based on MWNTs bridged mesocellular graphene foam nanocomposite", Talanta, Vol. 127, pp. 255-261.
107. Mazloum-Ardakani, M., Sheikh-Mohseni, M. A., Beitollahi, H., Benvidi, A. and Naeimi, H., 2010, "Electrochemical determination of vitamin C in the presence of uric acid by a novel TiO_2 nanoparticles modified carbon paste electrode", Chinese Chemical Letters, Vol. 21, pp. 1471-1474.
108. Tadayon, F., Vahed, S. and Bagheri, H., 2016, "Au-Pd/reduced graphene oxide composite as a new sensing layer for electrochemical determination of ascorbic acid, acetaminophen and tyrosine", Materials Science and Engineering: C, Vol. 68, pp. 805-813.
109. Karikalan, N., Karthik, R., Chen, S., Velmurugan, M. and Karuppiah, C., 2016, "Electrochemical properties of the acetaminophen on the screen printed carbon electrode towards the high performance practical sensor applications", Journal of Colloid and Interface Science, Vol. 483, pp. 109-117.
110. Song, J., Yang, J., Zeng, J., Tan, J. and Zhang, L., 2011, "Graphite oxide film-modified electrode as an electrochemical sensor for acetaminophen", Sensors and Actuators B: Chemical, Vol. 155, pp. 220-225.
111. Jena, B. R., Babu, S. M., Pradhan, D. P. and Swain, S., 2017, "UPLC Analytical Method Development and Validation for the Simultaneous Estimation of Paracetamol and Caffeine Capsules Dosages Form," Pharmaceutical Regulatory Affairs, Vol. 6, pp. 1-9.
112. Jeevagan, A. J. and John, S. A., 2012, "Electrochemical determination of caffeine in the presence of paracetamol using a self-assembled monolayer of non-peripheral amine substituted copper (II) phthalocyanine," Electrochimica Acta, Vol. 77, pp.137-142.

113 Shoup, D. and Szabo, A., 1982, “Chronoamperometric current at finite disk electrodes”, Journal of Electroanalytical Chemistry, Vol. 140, pp. 237.

114. Ikeuchi, H. and Kanakubo, M., 2000, “Determination of diffusion coefficients of the electrode reaction products by the double potential step chronoamperometry at small disk electrodes”, Journal of Electroanalytical Chemistry, Vol. 493, pp. 93-99.

115. Shahin Ara Mitu, 2017, M.Sc Thesis, Dept. of Chemistry, KUET.

116. F.M. Hawkridgein, P.T. Kissinger and W.R. Heieman, 1996, “Laboratory Techniques in Electroanalytical chemistry”, Marcel Dekker Inc., New York, 2nd Ed.

117. E. J. Laviron, 1979, “Electroanalitycal Chemistry”, Vol. 101, pp. 19-26.

118. J. A., Plambeck, 1982, Electroanalytical Chemistry, Basic Principles and Application, Wiley Interscience Pub., USA.

119. E.R. Brown, R.F. Larg, A. Weissberger and B. (Eds.) Rossiter, 1971, Physical Methods of chemistry, Wiley-Inter science, New York, Vol.1-Part IIA.

120. M. Whitfield, and D. Jagner, 1981, Marine electrochemistry: A practical introduction, John Wiley &Sons Inc.

121. Palash Kumar Dhar, 2016, M.Sc Thesis, Dept. of Chemistry, KUET.

122. Bulbul Chowdhury, 2018, M.Sc Thesis, Dept. of Chemistry, KUET.

123. Allmand, A., and Harold Johann Thomas. Ellingham. "Chapter 4: The Electrolysis Bath." The Principles of Applied Electrochemistry,. New York: Longmans, Green, 1924.

124. Richard S. Kelly, Analytical Electrochemistry: The Basic Concepts.

125. A. Balamurugan and S. M. Chen, Chapter-I: Introduction and Overview of Cyclic Voltammetry and Its Theoretical Considerations, pp. 1-43.

126. Skoog, D. A., Holler, F. J. and Neiman, T. A., 2007, Principles of Instrumental Analysis, 6th Ed., Thomson Brooks/Cole., pp. 169-173.

127. Bland, J. M. and Altman, D. G., 1996, "Statistics notes: measurement error". British Medical Journal, vol. 312, pp.1654.

128. Ensafi, A. A., Taei, M. and Khayamian T., 2009, “ A differential pulse voltammetric method for simultaneous determination of ascorbic acid, dopamine, and uric acid using poly (3-(5-chloro-2-hydroxyphenylazo)-4,5-dihydroxynaphthalene-2,7-disulfonic acid) film modified glassy carbon electrode, Journal of Electroanalytical Chemistry, vol. 633, pp. 212-220.

129. F.M. Hawkridgein, P.T. Kissinger and W.R. Heieman, 1996, “Laboratory Techniques in Electroanalytical chemistry”, Marcel Dekker Inc., New York, 2nd Ed.
130. Li, J. and Zhang, X., 2012, “Fabrication of Poly(Aspartic Acid)-Nanogold Modified Electrode and Its Application for Simultaneous Determination of Dopamine, Ascorbic Acid and Uric Acid,” American Journal of Analytical Chemistry, Vol. 3, pp. 195-203.
131. Zidan, M., Tee, T. W., Abdullah, A. H., Zainal, Z. and Kheng, G. J., 2011, “Electrochemical Oxidation of Paracetamol Mediated by Nanoparticles Bismuth Oxide Modified Glassy Carbon Electrode,” International Journal of Electrochemical Science, Vol. 6, pp. 279-288.
132. Tadesse, Y., Tadese, A., Saini, R. C. and Pal, R., 2013, “Cyclic Voltammetric Investigation of Caffeine at Anthraquinone Modified Carbon Paste Electrode,” International Journal of Electrochemistry, Vol. 2013, pp. 1-7.